UNIVERSITY OF CALIFORNIA, SAN DIEGO

Green Fluorescent Protein Based Indicators of Dynamic Redox Changes and Reactive Oxygen Species

A dissertation submitted in partial satisfaction of the

requirements for the degree Doctor of Philosophy

in

Chemistry

by

Colette Dooley

Committee in charge:

Professor Roger Y. Tsien, Chair
Professor Marjorie Caserio
Professor Susan S.Taylor
Professor Robert H.Tukey
Professor Anthony Wynshaw-Boris

2006

The dissertation of Colette Dooley is approved, and it is acceptable in quality and form for publication on microfilm:

_____

_____

_____

_____

_____

Chair

University of California, San Diego

2006

Dedication

This work is dedicated to the memory of my father:
Patrick Anthony Dooley
And in gratitude to my mother:
Christina Dooley

Table of Contents

List of Figures and Tables

Acknowledgements

I wish to thank Roger and all in the Tsien lab for their help and cooperation while I worked on this thesis. Particularly Paul, Christina, Rene and Qing to went above and beyond the call of duty to assist me. I thank my husband Greg for reading my first draft while at the 72nd parallel. I thank my committee members for reading and giving me their comments on this tome. My heartfelt thanks to those who gave generously the products of their own work so I could undertake this study; George Hanson, Timothy Dore, Alexander Sorkin, Peter Copeland and Peter Newburger.

Chapter One in full, is a reprint as it appears in THE JOURNAL OF BIOLOGICAL CHEMISTRY Vol. 279, No. 21, Issue of May 21, pp. 22284–22293, 2004 © 2004 by The American Society for Biochemistry and Molecular Biology, Inc. Printed in U.S.A. The dissertation author was the primary investigator and single author of this paper.

This work was supported by grants from the Superfund Basic Research Program (ES10337), National Institutes of Health (NS27177), Department of Energy (DE-FG03-01ER63276), and the Howard Hughes Medical Institute. The DNA Sequencing Shared Resource at the University of California-San Diego Cancer Center is funded in part by National Institutes of Health, NCI Cancer Support Grant 2P30CA23100-18.

Vita

1983-1987	B.Sc. Zoology, University College Dublin, Ireland
1987-1990	Teaching Assistant, Zoology Department University College Dublin, Ireland
1992	M.Sc. Zoology, University College Dublin, Ireland
1990-1993	Research Assistant, Department of Neuroendocrinology, Torrey Pines Institute for Molecular Studies, San Diego, CA
1994-2000	Senior Scientist, Department of Neuroendocrinology, Torrey Pines Institute for Molecular Studies, San Diego, CA
2000-2002	Teaching Assistant Department of Chemistry and Biochemistry, University of California, San Diego
2004	Ph.D., Biochemistry,University of California, San Diego

PUBLICATIONS

1. Dooley,C.T., Dore,T.M., Hanson,G.T., Jackson,W.C., Remington,S.J., Tsien, R.Y. (2004) Imaging dynamic redox changes in mammalian cells with green fluorescent protein indicators. *J. Biol. Chem* 279 22284-22293.
2. Houghten,R.A. Dooley,C.T., Appel,J.A. (2004) De novo identification of highly fluorescent kappa opioid ligands from a rhodamine labeled tetrapeptide positional scanning library. Bioorg Med Chem Lett. 14 1947-1951.
3. Dooley, C.T. and Houghten R.A. (2000) New opioid peptides, peptidomimetics and heterocyclic compounds from combinatorial libraries. *Biopolymers-Peptide Science* 51, 379-390.
4. Dooley, C.T. and Houghten R.A. (2000) Orphanin FQ/Nociceptin Receptor Binding Studies *Peptides* 21, 949-960.
5. Pinilla, C., Appel, J.R., Blondelle, S.E., Dooley, C.T.,Eichler, J., Nefzi, A., Ostresh, J.M., Martin, R., Wilson, D.B., and Houghten, R.A. (2000) Synthesis and screening of positional scanning synthetic combinatorial libraries. In: Combinatorial chemistry - a practical approach (Fenniri, H., Ed.), Oxford University Press, Oxford, pp. 51-74.

6. Houghten, R. A., Pinilla, C., Appel, J. R., Blondelle, S. E., Dooley, C. T., Eichler, J., Nefzi, A., and Ostresh, J. M. (1999). Mixture-based synthetic combinatorial libraries. *J. Med. Chem.* 42, 3743-3778.
7. Houghten, R. A., Blondelle, S. E., Dooley, C. T., Meyer, J.-P., Ostresh, J. M., and Nefzi, A. (1999). Preparation of heterocyclic positional scanning combinatorial libraries from peptides. In '*Peptide Science - Present and Future.'* (Ed Y. Shimonishi.) pp. 123-127. (Kluwer Academic Publishers: The Netherlands.)
8. Dooley, C. T., Ny, P., Bidlack, J. M., and Houghten, R. A. (1998). Selective ligands for the μ, δ and κ opioid receptors identified from a single tetrapeptide positional scanning combinatorial library. *Journal of Biological Chemistry* 273, 18848-18856.
9. Dooley, C. T. and Houghten, R. A. (1998). Synthesis and screening of positional scanning combinatorial libraries. In '*Methods in Molecular Biology: Combinatorial Peptide Library Protocols.* Vol. 87.' (Ed S. Cabilly.) pp. 13-24. (Humana Press, Inc.: New Jersey.)
10. Eichler, J., Blondelle, S. E., Dooley, C. T., and Houghten, R. A. (1998). Scaffolded peptide combinatorial libraries for the design of proteinmimetics. In *'Peptides 96: Proceedings of the 24th European Peptide Symposium.*' (Ed R. Epton.) pp. 361-362. (Mayflower Scientific,Ltd.: Kingswinford.)
11. Houghten, R. A, Dooley, C. T., Giulianotti, M. A., Hamashin, V. T., Schoner, C., Ostresh, J. M., and Nefzi, A. (1998) Solid Phase synthesis of Heterocyclic Positional Scanning combinatorial Libraries. Epton, R. *Proc. 5th Intl. Symposium[Innovation and Perspectives in Solid Phase synthesis and Combinatorial libraries*], 11-14. Birmingham,UK, Mayflower Worldwide Ltd. Peptides, Proteins and Nucleic acids.
12. Nefzi, A., Dooley, C. T., Ostresh, J. M., and Houghten, R. A. (1998). Combinatorial chemistry: from peptides and peptidomimetics to small organic and heterocyclic compounds. *Bioorganic & Medicinal Chemistry Letters* 8, 2273-2278.
13. Dooley, C. T., Spaeth, C. G., Craymer, K., Adapa, I. D., Brandt, S. R., Houghten, R., and Toll, L. (1997). Binding and in vitro activities of peptides with high affinity for the Nociceptin/Orphanin FQ receptor, ORL1. *Journal of Pharmacology and Experimental Therapeutics* 283, 735-741.
14. Dörner, B., Ostresh, J. M., Blondelle, S. E., Dooley, C. T., and Houghten, R. A. (1997). Peptidomimetic synthetic combinatorial libraries. In 'Advances in Amino Acid Mimetics and Peptidomimetics. Vol. 1.' (Ed A. Abell.) pp. 109-125. (JAI Press: Greenwich, CT.)
15 .Dooley, C. T. and Houghten, R. A. (1996). Orphanin FQ: receptor binding and analog structure activity relationships in rat brain. *Life Sciences* 59, PL23-PL29.
16. Dooley, C. T., Bower, A. N., and Houghten, R. A. (1996). Identification of mu-selective tetrapeptides using a positional scanning combinatorial library containing L-, D- and unnatural amino acids. In '*Peptides: Chemistry, Structure and Biology (Proceedings of the Fourteenth American Peptide Symposium).*' (Eds P. T. P. Kaumaya and R. S. Hodges.) (ESCOM: Leiden.)

17. Dörner, B., Blondelle, S. E., Pinilla, C., Appel, J., Dooley, C. T., Eichler, J., Ostresh, J. M., Pérez- Payá, E., and Houghten, R. A. (1996). Soluble synthetic combinatorial libraries: The use of molecular diversities for drug discovery. In *'Combinatorial libraries. Synthesis, Screening and Application Potential.*' (Ed R. Cortese.) pp. 1-25. (Walter de Gruyter & Co.: New York.)
18. Griffith, M. C., Dooley, C. T., Houghten, R. A., and Kiely, J. S. (1996). Solid-phase synthesis, characterization, and screening of a 43,000-compound tetrahydroisoquinoline combinatorial library. In *'Molecular Diversity and Combinatorial Chemistry: Libraries and Drug Discovery.*' (Eds I. M. Chaiken and K. D. Janda.) pp. 50-57. (American Chemical Society: Washington, DC.)
19. Houghten, R. A., Blondelle, S. E., Dooley, C. T., Dörner, B., Eichler, J., and Ostresh, J. M. (1996). Libraries from libraries: Generation and comparison of screening profiles. *Molecular Diversity* 2, 41-45.
20. Houghten, R. A., Dooley, C. T., and Ostresh, J. M. (1996). The use of soluble polyamine combinatorial libraries for the identification of potent opioid receptor active compounds. In '*Peptide:chemistry, structure and biology*.' (Eds P. T. P. Kaumaya and R. S. Hodges.) pp. 278- 280. (Mayflower Scientific Ltd.: England.)
21. Kiely, J. S., Dörner, B., Ostresh, J. M., Dooley, C. T., and Houghten, R. A. (1996). Rapidly Expanding Molecular Diversity: Libraries from Libraries. In *'High Throughput Screening: The Discovery of Bioactive Substances.*' (Ed M. R. Pavia.) (Marcel-Dekker)
22. Pinilla, C., Appel, J., Dooley, C. T., Blondelle, S. E., Eichler, J., Dörner, B., Ostresh, J. M., and Houghten, R. A. (1996). The versatility of nonsupport-bound combinatorial libraries. In '*Combinatorial peptide and nonpeptide libraries.'* (Ed G. Jung.) pp. 139-171. (Verlag Chemie: Wienheim.)
23. Pinilla, C., Appel, J. R., Blondelle, S. E., Dooley, C. T., Dörner, B., Eichler, J., Ostresh, J. M., and Houghten, R. A. (1996). Synthetic combinatorial libraries screened in solution. In '*Peptides: Chemistry, Structure and Biology. Proceedings of the Fourteenth American Peptide Symposium.'* (Eds P. T. P. Kaumaya and R. S. Hodges.) pp. 884-886. (Mayflower Scientific Ltd: Kingswinford, UK.)
24. Dooley, C. T., Kaplan, R. A., Chung, N. N., Schiller, P. W., Bidlack, J. M., and Houghten, R. A. (1995). Six highly active mu-selective opioid peptides identified from two synthetic combinatorial libraries. *Peptide Research* 8, 124-137.
25. Dooley, C. T. and Houghten, R. A. (1995). A comparison of combinatorial library approaches for the study of opioid compounds. *Perspectives in Drug Discovery and Design* 2, 287-304.
26. Dooley, C. T. and Houghten, R. A. (1995). Identification of mu-selective polyamine antagonists from a synthetic combinatorial library. *Analgesia* 1, 400-404.
27. Dooley, C. T., Hope, S. K., and Houghten, R. A. (1995). Identification of tetrameric opioid peptides from a combinatorial library composed of L-, D- and non-proteinogenic amino acids. In *'Peptides 94: Proceedings of the 23rd European Peptide Symposium.*' (Ed H. L. S. Maia.) pp. 805-806. (ESCOM: Leiden.)

28. Blondelle, S. E., Pérez-Payá, E. , Dooley, C. T., Pinilla, C., and Houghten, R. A. (1995). Soluble combinatorial libraries of organic, peptidomimetic and peptide diversities. *Trends Anal.Chem.* 14, 83-92.
29. Eichler, J., Appel, J. R., Blondelle, S. E., Dooley, C. T., Dörner, B., Ostresh, J. M., Pérez-Payá, E., Pinilla, C., and Houghten, R. A. (1995). Peptide, peptidomimetic and organic synthetic combinatorial libraries. *Med.Res.Rev.* 15, 481-496.
30. Pinilla, C., Appel, J., Blondelle, S. E., Dooley, C. T., Dörner, B., Eichler, J., Ostresh, J. M., and Houghten, R. A. (1995). A review of the utility of peptide combinatorial libraries. *Biopolymers (Peptide Science)* 37, 221-240.
31. Dooley, C. T., Chung, N. N., Wilkes, B. C., Schiller, P. W., Bidlack, J. M., Pasternak, G. W., and Houghten, R. A. (1994). An all D-amino acid opioid peptide with central analgesic activity from a combinatorial library. *Science* 266, 2019-2022.
32. Dooley, C. T., Hope, S., and Houghten, R. A. (1994). Rapid identification of novel opioid peptides from an N-acetylated synthetic combinatorial library. *Regulatory Peptides* 54, 87-88.
33. Dooley, C. T. and Houghten, R. A. (1994). New, potent N-acetylated all D-amino acid opioid peptides. In 'Peptides: Chemistry, Structure and Biology. *Proceedings of the 13th American Peptide Symposium.'* (Eds R. S. Hodges and J. A. Smith.) pp. 984-985. (ESCOM: Leiden.)
34. Houghten, R. A., Appel, J. R., Blondelle, S. E., Cuervo, J. H., Dooley, C. T., Eichler, J., and Pinilla, C. (1994). Optimal peptide length determination using synthetic peptide combinatorial libraries. In *'Peptides: Chemistry, Structure and Biology. Proceedings of the 13th American Peptide Symposium.*' (Eds R. S. Hodges and J. A. Smith.) pp. 971-974. (ESCOM: Leiden.)
35. Pinilla, C., Appel, J. R., Blondelle, S. E., Dooley, C. T., Eichler, J., Ostresh, J. M., and Houghten, R. A. (1994). Versatility of positional scanning synthetic combinatorial libraries for the identification of individual compounds. *Drug Development Res* 33, 133-145.
36. Dooley, C. T., Chung, N. N., Schiller, P. W., and Houghten, R. A. (1993). Acetalins: Opioid receptor antagonists determined through the use of synthetic peptide combinatorial libraries. *PNAS* 90, 10811- 10815.
37. Dooley, C. T. and Houghten, R. A. (1993). The use of positional scanning synthetic peptide combinatorial libraries for the rapid determination of opioid receptor ligands. *Life Sci.* 52, 1509- 1517.
38. Dooley, C. T., Prochera, A. M., and Houghten, R. A. (1993). A priori determination of peptide ligands for opiate receptors using synthetic peptide combinatorial libraries. In *'Peptides 1992: Proceedings of the 22nd European Peptide Symposium.*' (Eds C. H. Schneider and A. N. Eberle.) pp. 649-650. (ESCOM Science Publishers B.V.: Leiden.)
39. Houghten, R. A. and Dooley, C. T. (1993). Novel N-acetylated opioid peptides determined through the use of synthetic peptide combinatorial libraries. In *'Peptide Chemistry 1992: Proceedings of the 2nd Japan Symposium on Peptide Chemistry.'* (Ed N. Yanaihara.) pp. 11-13. (ESCOM Science Publishers B.V.: Leiden.)

40. Houghten, R. A. and Dooley, C. T. (1993). Synthetic peptide combinatorial libraries may be used to determine peptide ligands for opiate receptors. In *'NIDA Research Monograph Series*. Vol. 134.' pp. 66-74. (NIH: Rockville, MO.)
41. Houghten, R. A. and Dooley, C. T. (1993). The use of synthetic peptide combinatorial libraries for the determination of peptide ligands in radio-receptor assays: opioid peptides. *Bioorganic & Medicinal Chemistry Letters* 3, 405-412.
42. Houghten, R. A., Cuervo, J. H., Pinilla, C., Appel, J. R., Dooley, C. T., and Blondelle, S. E. (1992). The use of a peptide library composed of 34 012 224 hexamers for basic research and drug discovery. In *'Peptides, Proceedings of the Twelfth American Peptide Symposium.'* (Eds J. A. Smith and J. E. Rivier.) pp. 560-561. (ESCOM Science Publishers B.V.: Leiden.)
43. Houghten, R. A., Appel, J. R., Blondelle, S. E., Cuervo, J. H., Dooley, C. T., and Pinilla, C. (1992). The use of synthetic peptide combinatorial libraries for the identification of bioactive peptides. *Biotechniques* 13, 412-421.
44. Houghten, R. A., Appel, J. R., Blondelle, S. E., Cuervo, J. H., Dooley, C. T., and Pinilla, C. (1992). The use of synthetic peptide combinatorial libraries for the identification of bioactive peptides. *Peptide Research* 5, 351-358.
45. Houghten, R. A., Pinilla, C., Blondelle, S. E., Appel, J. R., Dooley, C. T., and Cuervo, J. H. (1991). Generation and use of synthetic peptide combinatorial libraries for basic research and drug discovery. *Nature* 354, 84-86.

ABSTRACT OF THE DISSERTATION

Green Fluorescent Protein Based Indicators of Dynamic Redox Changes and Reactive Oxygen Species

by

Colette Dooley

Doctor of Philosophy in Chemistry

University of California, San Diego, 2006

Professor Roger Y. Tsien, Chair

Alterations in the redox equilibrium are precipitated by changing either the glutathione/glutathione-disulfide ratio (GSH/GSSG) and/or the reduced/oxidized thioredoxin ratio. Redox-sensitive green fluorescent proteins (GFP) allow real time visualization of the oxidation state of the indicator while canceling out the amount of indicator and the absolute optical sensitivity. Because the indicator is genetically encoded, it can be targeted to specific proteins or organelles of interest and expressed in a wide variety of cells and organisms. We evaluated roGFP1 and roGFP2 with physiologically or toxicologically relevant oxidants both *in vitro* and in living mammalian cells. Furthermore, we investigated the response of the redox probes under physiological redox changes during superoxide bursts in macrophage

cells, hyperoxic and hypoxic conditions, and in responses to H_2O_2-stimulating agents, *e.g.* epidermal growth factor and lysophosphatidic acid. Placing positive charges near cysteine residues increases sensitivity to oxidation by H_2O_2. We designed a series of roGFP variants with outward-facing lysine residues placed in close proximity to the key cysteine residues. The double lysine mutant RoGFP2-F223KA206K (roGFP2-FA) was used in three distinct applications for roGFPs; expression in primary neurons; the evaluation for sensitivity to environmental toxicants; and finally the potential for clamping roGFP2-FA in a particular redox state following equilibration using formaldehyde was investigated. Sensitivity of selenocysteine to oxidation was harnessed to further optimize roGFPs. By employing the 3'UTR of gluthathione peroxidase and an opal codon at each of the cysteine residues of roGFP we were able to create seleno-GFPs, which have a greater sensitivity to oxidation. A rational approach was taken for the discovery of the green fluorescent protein based singlet oxygen sensors (SOS-GFP). There was a strong response to singlet oxygen in particularly for mutations expressing histidines at positions 147 and 204. These double histidine mutants were evaluated for specificity and sensitivity to singlet oxygen. The most reactive/sensitive mutations were then used in biological settings to sense singlet oxygen generated from a nearby source.

Introduction

Reactive oxygen species (ROS) include superoxide anion ($O_2^{\bullet -}$), hydroxyl radical ($OH^{\bullet}$), hydrogen peroxide (H_2O_2), singlet oxygen ($^1O_2$) and nitric oxide ($NO^{\bullet}$). Pathologies of ROS are seen in inflammation and immune responses, aging, cardiovascular disorders and neurodegenerative diseases. They may be produced in the cell by agonists like cytokines and growth factors, or as a stress response induced by chemicals drugs, radiation or infectious agents (see [1-4] for reviews). Oxidative stress is the imbalance between oxidant exposure and antioxidant protection. Severe stress leads to impaired cell function, activation of repair mechanisms and ultimately apoptosis or necrosis. Normal levels of ROS play a role in regulating cell signaling and gene expression.

ROS production can most broadly be classified as those derived from mitochondrial oxygen consumption and those that are mitochondrial independent. Superoxide is generated enzymatically by oxidoreductases; NADPH oxidase cytochrome P450, xanthine oxidase, as side products of mitochondrial electron transport, and metal catalyzed oxidation of metabolites e.g. arachidonic acid cholesterol and amino acids. Superoxide can be converted non-enzymatically to H_2O_2 and singlet oxygen [2,5]. The major source of H_2O_2 in cells is from the dismutation of superoxide by superoxide dismutases. In the presence of reduced metals H_2O_2 is converted to a hydroxyl radical which is short-lived but can cause considerable damage to nuclear and mitochondrial DNA, lipids, carbohydrates and proteins [6]. Singlet oxygen is also highly reactive it is produced by NADPH oxidases, and lactoperoxidase, most notably in human eosinophils [5,7]. Lastly nitric oxide is produced from arginine by nitric oxygen synthase.

Stimulated ROS production by NADPH oxidase was first described in phagocytes and is known as “the respiratory burst”. Superoxide is the predominant ROS formed, which is then dismuted to H_2O_2, but singlet oxygen production has also been detected [8]. Recently new NADPH-oxidases not specific to phagocytes have been identified, this growing family of proteins are referred to as NOX [9].

In redox signaling there are only small oxidative perturbations. Superoxide and hydrogen peroxide act as second messengers to modulate cell function. NFκ-B was the first eukaryotic transcription factor found to respond to oxidative stress [10], but both insulin and nerve growth factor also stimulate endogenous H_2O_2 production. Transcription activation by ROS is not surprisingly found for genes that express proteins for oxidative repair, such as AP-1 [11] and HIF-1 [2].

Protection mechanisms against ROS induced oxidative stress include; enzymes such as superoxide dismutase (SOD), catalase, peroxiredoxins and glutathione peroxidase; small thiols such as glutathione and thioredoxin and their corresponding reductases; and antioxidants such as tocopherol (vitamin E) and ascorbate (vitamin C) [1]. Alterations in the redox equilibrium are reflected in changes of the glutathione/glutathione-disulfide ratio (GSH/GSSG) and the reduced/oxidized thioredoxin ratio. Indeed, the GSH/GSSG ratio is used as an indicator of cellular redox state [12].

Methods used to detect ROS have included: the use of antioxidants to inhibit ROS accumulation, over-expression or inhibition of enzymes involved in ROS removal and compounds that interact directly with ROS such as spin trapping agents. Historically small molecule indicators of ROS were specific; lucigenin for superoxide or coelenterazine for H_2O_2, somewhat specific; xanthene based dyes

HPF and APF [13] or non-specific; dichlorofluorescien. Most modern fluorescent probes for detection of ROS are derived from fluorescien, rhodamine or ethidium, and are somewhat targetable; fluorescien (cytoplasm), rhodamine (mitochondria) or ethidium (nucleus). These aromatic compounds are made cell permeant by esterification of hydrophilic groups. They are usually colorless and convert to the fluorescent form following oxidation. Disadvantages of these probes range from non-specificity to auto-oxidation e.g. dichlorofluorescien is easily auto-oxidized it will spontaneously fluorescence upon exposure to light.

Green fluorescent protein (GFP) based indicators for ROS have been described. Redox-sensitive GFP (roGFP) [14] has a ratiometric response and (rxYFP) [15] responds with a fluorescent intensity change. Both allow real-time visualization of the oxidation state of the indicator. A genetically encoded indicator for hydrogen peroxide (HyPer) has recently been described which is a fusion of circularly permuted YFP in the regulatory domain of OxyR [16]. Unlike the former sensors the sensitive site is buried within the indicator. A GFP capable of producing ROS has also been described; the photosensitizer (Killer red) can be used in chromophore-assisted light inactivation (CALI) [17] or photodynamic therapy.

Since redox indicators are genetically encoded, they can be targeted to specific proteins or organelles and expressed in a wide variety of cells or organisms. We first evaluated the behavior of the roGFPs *in vitro* and in cells. We then undertook optimization of their kinetics. Thiols are often limited by the need to deprotonate before they can oxidize. By placing positive charges near the cysteine residues we increased sensitivity to oxidation by H_2O_2. By further increasing the sensitivity of roGFPs we hoped to overcome the cells reductive

machinery enough to detect small or localized redox changes. Selenocysteine, a naturally encoded but rare amino acid has a lower pKa than cysteine and is more sensitive to oxidation. Protein expression of selenocysteine is a relatively new field of study, and expression of the amino acid requires several accessory structures and proteins. Although not widely practiced, selenocysteine has been successfully expressed in a mammalian protein that would not naturally contain the amino acid [18]. We explored the possibility of using selenocysteine's sensitivity to oxidation to optimize roGFP. In spite of gaining increased sensitivity to oxidation, we found it difficult to detect redox signaling. We hypothesized that the reductive capabilities of the cell were difficult to overcome and thereby irreversible ROS sensors might be of greater use and proceeded to develop irreversible ROS indicators based on the natural oxidative reactions of amino acid side chains. We have successfully generated an irreversible ROS indicator; the probe is in fact highly specific for singlet oxygen.

A. References

1. Rojkind M, Dominguez-Rosales JA, Nieto N, Greenwel P. Role of hydrogen peroxide and oxidative stress in healing responses. Cell Mol Life Sci 2002;59:1872-1891.

2. Droge W. Free radicals in the physiological control of cell function. Physiol Rev 2002;82:47-95.

3. Forman HJ, Torres M. Redox signaling in macrophages. Mol Aspects Med 2001;22:189-216.

4. Negre-Salvayre A, Auge N, Duval C, Robbesyn F, Thiers JC, Nazzal D, Benoist H, Salvayre R. Detection of intracellular reactive oxygen species in cultured cells using fluorescent probes. Methods Enzymol 2002;352:62-71.

5. Steinbeck MJ, Khan AU, Karnovsky MJ. Extracellular production of singlet oxygen by stimulated macrophages quantified using 9,10-diphenylanthracene and perylene in a polystyrene film. J Biol Chem 1993;268:15649-15654.

6. Barzilai A, Rotman G, Shiloh Y. ATM deficiency and oxidative stress: a new dimension of defective response to DNA damage. DNA Repair 2002;1:3-25.

7. Kanofsky JR. Singlet oxygen production by biological systems. Chem Biol Interact 1989;70:1-28.

8. Cao Y, Koo YE, Koo SM, Kopelman R. Ratiometric singlet oxygen nano-optodes and their use for monitoring photodynamic therapy nanoplatforms. Photochem Photobiol 2005;81:1489-1498.

9. Suh YA, Arnold RS, Lassegue B, Shi J, Xu X, Sorescu D, Chung AB, Griendling KK, Lambeth JD. Cell transformation by the superoxide-generating oxidase Mox1. Nature 1999;401:79-82.

10. Schreck R, Rieber P, Baeuerle PA. Reactive oxygen intermediates as apparently widely used messengers in the activation of the NF-kappa B transcription factor and HIV-1. EMBO J 1991;10:2247-2258.

11. Toone WM, Morgan BA, Jones N. Redox control of AP-1-like factors in yeast and beyond. Oncogene 2001;20:2336-2346.

12. Schafer FQ, Buettner GR. Redox environment of the cell as viewed through the redox state of the glutathione disulfide/glutathione couple. Free Radic Biol Med 2001;30:1191-1212.

13. Setsukinai K, Urano Y, Kakinuma K, Majima HJ, Nagano T. Development of novel fluorescence probes that can reliably detect reactive oxygen species and distinguish specific species. J Biol Chem 2003;278:3170-3175.

14. Hanson GT, Aggeler R, Oglesbee D, Capaldi RA, Tsien RY, Remington SJ. Investigating mitochondrial redox potential with redox-sensitive green fluorescent protein indicators. J Biol Chem 2004;279:13044-13053.

15. Ostergaard H, Henriksen A, Hansen FG, Winther JR. Shedding light on disulfide bond formation: engineering a redox switch in green fluorescent protein. EMBO J 2001;20:5853-5862.

16. Belousov VV, Fradkov AF, Lukyanov KA, Staroverov DB, Shakhbazov KS, Terskikh AV, Lukyanov S. Genetically encoded fluorescent indicator for intracellular hydrogen peroxide. Nat Methods 2006;3:281-286.

17. Bulina ME, Chudakov DM, Britanova OV, Yanushevich YG, Staroverov DB, Chepurnykh TV, Merzlyak EM, Shkrob MA, Lukyanov S, Lukyanov KA. A genetically encoded photosensitizer. Nat Biotechnol 2006;24:95-99.

18. Shen Q, Chu FF, Newburger PE. Sequences in the 3'-untranslated region of the human cellular glutathione peroxidase gene are necessary and sufficient for selenocysteine incorporation at the UGA codon. J Biol Chem 1993;268:11463-11469.

Chapter One

Imaging Dynamic Redox Changes in Mammalian Cells with Green Fluorescent Protein Indicators

A. Introduction

Cells have elaborate homeostatic mechanisms to regulate the thiol-disulfide redox status of their internal compartments. Most thiol groups within the cytoplasm are normally reduced. Very few are present as disulfides. It has been speculated that the cytoplasm is reducing because many metabolic reactions evolved before oxygen became abundant in the atmosphere (1). Modest alterations in the thiol-disulfide equilibrium could have major consequences in the cell, including defective protein folding or enzyme activity (because many enzymes have a cysteine in their active site). When excess oxidation overwhelms the reductive capabilities of the cell, death results. Despite the dangers of excessive oxidation, cells sometimes use redox adjustments as signaling events, such as in the activation of transcription factors (NF-κB and AP-1), caspases, protein tyrosine phosphatases, or GTPases (Ras). Thus, changes in the redox equilibrium influence a host of cell functions, including but not limited to growth, stress responses, differentiation, metabolism, cell cycle, communication, migration, gene transcription, ion channels, and immune responses (for reviews see Refs. 2–6). Alterations in the redox equilibrium are reflected in changes of the glutathione/glutathione-disulfide ratio (GSH/GSSG) and the reduced/oxidized thioredoxin ratio. Glutathione is found in high concentrations in cells (5–10 mM) and is considered to be the major player in maintaining intracellular redox equilibrium. Ratios of GSH to GSSG are reported to range from 100 to 300:1 (7, 8),

but these measurements have been problematic because they require destruction of the tissue, during which great care must be taken not to allow further oxidation. The major source of error is the determination of GSSG concentration, because this species is at low abundance yet is measured only after complete removal of GSH to prevent oxidation. The spatial and temporal resolution of such destructive assays is very poor.

Redox-sensitive green fluorescent proteins (GFP)1 described recently (9) allow real-time visualization of the oxidation state of the indicator. The indicators examined in this work are GFP mutants with two surface-exposed cysteine placed at positions 147 and 204 on adjacent β-strands close to the chromophore. Disulfide formation between the cysteine residues promotes protonation of the chromophore and increases the excitation spectrum peak near 400 nm at the expense of the peak near 490 nm. The ratios of fluorescence from excitation at 400 and 490 nm indicate the extent of oxidation and thus the redox potential while canceling out the amount of indicator and the absolute optical sensitivity. Because the indicator is genetically encoded, it can be targeted to specific proteins or organelles of interest and expressed in a wide variety of cells and organisms. Here we evaluate roGFP1 (GFP with mutations C48S, S147C, and Q204C) and roGFP2 (the same plus S65T) with physiologically or toxicologically relevant oxidants both *in vitro* and in living mammalian cells. The probes expressed in cell cytoplasm responded as expected to a variety of oxidants. Although lower concentrations of hydrogen peroxide were required to oxidize cytosolic roGFPs than oxidize the same proteins *in vitro*, attempts to detect growth factor-stimulated production of hydrogen peroxide were not

successful. However, the probes could detect superoxide generated during the oxidative burst of HL60 cells.

B. Methods

Aldrithiol, diamide, hydrogen peroxide, buthionine sulfoximine, 3-amino-1,2,4-triazole, apocynin (acetovanillone), and 4-(2-aminoethyl)-benzenesulfonyl fluoride were obtained from Aldrich. Oxidized and reduced lipoate, oxidized and reduced glutathione, menadione, diphenylene iodonium chloride, BCNU (1,3-bis-(2-chloroethyl)-1-nitrosourea) (carmustine), and apocynin were obtained from Sigma. 2,3-Dimethoxy- 1,4-naphthoquinone (DMNQ) and DTT were obtained from Calbiochem. Bis(2-mercaptoethyl)sulfone (BMES) was from USB Corp. Its cyclic disulfide was prepared by oxidation with a stoichiometric quantity of iodine (10) followed by recrystallization from hexane. HL60 cells were obtained from American Type Culture Collection.

***In Vitro* Studies**—roGFPs were subcloned into pRSETB (Invitrogen) using BamHI and EcoRI restriction sites. The plasmid encodes a fusion protein of the insert and an N-terminal extension containing a $(His)_6$ tag, enabling purification by nickel affinity chromatography. The construct was expressed in the JM109 strain of Escherichia coli. Isolated protein was reduced daily by mixing concentrated protein (50–200 μM) with 10mM DTT and diluting to the required concentration. When necessary, DTT was removed from the solution using Centri-spin 20 columns (Princeton Separations Inc.). Reactions were carried out in 125mM KCl, 75 mM HEPES, and 1 mM EDTA, pH 7.3, which had been degassed by repetitive evacuation and nitrogen bubbling. Excitation scans (350–500 nm, 2.5-nm bandwidth) were run in 100-μl volumes in 96-

well plates (sealed when required) on a Safire spectrofluorometer (Tecan), collecting emission at 530 nm, 7.5-nm bandwidth.

Redox Titration Using Fluorescence Spectroscopy— Redox probes were titrated in degassed HEPES buffer containing 1 μM protein and 10 mM lipoate or BMES as redox buffers. Concentrations of oxidized and reduced forms were reciprocally varied from 0:10 to 10:0 mM in 1 mM increments. The eleven solutions comprising each titration series were incubated at 25 or 30 °C for 1 h while sealed under a nitrogen atmosphere before measuring fluorescence excitation spectra. The redox potential of the redox probes using BMES or lipoate as redox buffers were obtained by first applying the following formula to each of the incrementing concentrations in the titration: Y = (Rn - Rmin)/(Rmax - Rn), where Rn = ratio at a particular concentration of redox buffer, Rmin = ratio in 10 mM reduced redox buffer, and Rmax = ratio in 10 mM oxidized redox buffer. From a plot of log Y versus log ([oxidized redox buffer]/[reduced redox buffer]), the buffer ratio (A) required to achieve 50% of the ratio change can be determined from the intercept where log Y = 0. Keq was derived from log Keq = log(F490 red)/(F490 ox)) - log A. The redox potential (E') was then calculated from the Nernst equation shown in Equation 1,

$$E' = E'_0 - (RT/nF)\ln Keq \qquad \text{(Eq. 1)}$$

where E'_0 is the redox potential of the redox buffers (lipoate =290 mV (11); BMES =295 mV (see below)), R is the gas constant (8.313 J/mol/K), T is temperature (K), n = 2 is the number of electrons exchanged, and F is Faraday's constant (96490 J/mol/volt).

Redox Potential of BMES Using NMR Spectroscopy—Solution A initially containing 10 mM dihydrolipoate and 10 mM oxidized BMES and solution B initially containing 10 mM oxidized lipoate and 10 mM reduced BMES were separately prepared in deoxygenated sodium phosphate buffer (10 mM, pD 7.4) in D_2O. NMR spectra were recorded on a Varian 200-MHz spectrometer at 283 K. The spectra of solutions A and B taken following a 1-h incubation after preparation were essentially identical, showing that equilibrium had been attained. Peaks specific to each of the reagents both oxidized and reduced were found: oxidized lipoate (3.2 ppm); dihydrolipoate (2.65 ppm); oxidized BMES (3.85 ppm); and reduced BMES (3.4 ppm). To determine the equilibrium constant (Keq) between lipoic acid and BMES, Keq = [BMES red] ω [lipoate ox] / ([BMES ox] ω [lipoate red]), we used the integrals under the peaks, Keq = (integral @ 3.4 ppm) ω (integral @ 3.2 ppm) / ((integral @ 3.85 ppm) ω (integral @ 2.65 ppm)). Inserting the value Keq = 1.46 into the Nernst equation (using a value of -290 mV for lipoate standard (11)), the redox potential of BMES in D2O was determined to be -295 mV.

Superoxide Production by Xanthine Oxidase—Reactivity to superoxide was determined by incubating 1 μM roGFP with 25 milliunits of xanthine oxidase (which had been centrifuged to remove ammonium sulfate) and 50 μM xanthine in 150 μl of 50 mM Tris buffer, pH 7.4. Imaging in Cells—roGFPs were expressed in HeLa, P388D1, or HL60 cells using modified pEFGP-N1 as expression vector and Lipofectin as transfection reagent. After 24–72 h of incubation at 37 °C in culture medium, the cells were washed twice with Hanks' balanced salt solution buffer. Cells were imaged on a Zeiss Axiovert microscope with a cooled CCD camera (Photometrics, Tucson, AZ) controlled by Metafluor 2.75 software (Universal Imaging, West Chester, PA).

Dual excitation ratio imaging used excitation filters 400DF15 and 480DF30 for roGFP1 and 400DF15 and 495DF10 for roGFP2 altered by a filter changer (Lambda 10-2, Sutter Instruments, San Rafael, CA). A 505DRLP dichroic mirror and an emission filter, 535DF25, were used for both probes. Fluorescence images were background-corrected by manual selection of background regions. Exposure time was 200–1000 ms, and images were taken every minute.

Fluorescence-activated Cell Sorter Analysis—Ratios for HL60 cells were obtained on a FACS Vantage SE with DIVA option (BD Biosciences). Cells were excited using laser lines at 407 nm (50 milliwatts) and 488 nm (150 milliwatts). Emission filters were 510/21 for both excitation wavelengths. HL60 cells were grown in the presence of 1.3% Me_2SO in IMDM plus 10% fetal bovine serum, 1% penicillin-streptomycin for 5–7 days. The cell suspension (1 ω 10^7 cells) was washed twice in IMDM without fetal bovine serum and resuspended in 1 ml of IMDM for electroporation. DNA (50–75 μg) was added to the solution and incubated at room temperature for 10 min. The cells were electroporated using a Cell-Porator electroporation system I (Invitrogen) using a 310-V pulse and 1180-microfarad capacitance. Cells were grown in IMDM (10% fetal bovine serum) for 2 days before oxidation experiments. Cells were washed and suspended in Hanks' balanced salt solution, and aliquots of cells were incubated in 50 μM PMA or 100 μM aldrithiol. For inhibition studies, cells were preincubated for 30 min in either 500 μM 4-(2-aminoethyl)benzenesulfonyl fluoride (AEBSF) or 200 μM apocynin.

Gene Cloning—Five mutations of amino acids neighboring Cys-14 and Cys-204 of roGFP1 and roGFP2 were incorporated using a QuikChange kit (Stratagene). They included N149K, A206K, F223K, N149K with A206K, and F223K with A206K. The

mutated constructs in pRSETB (Invitrogen) were expressed using JM109 bacteria and purified as described above. For expression in mammalian cells, the constructs were subcloned into pcDNA3 (Invitrogen) using BamHI and EcoRI restriction sites.

For membrane targeting, a sequence for myristoylation and palmi-toylation was appended to the N terminus of roGFP1 and roGFP2. The signal sequence, MGCINSKRKDNLND, was derived from Lyn, a tyrosine kinase protein belonging to the Src family. The following primers: forward primer (5'-GCGGATCCTAAGCTTCGAGCCACCATGGGCTGCATCAACAGCAAGCGCAAGGACAACCTGAACG-3') and reverse primer (5'-GTTTCAGGTTCAGGGGGAGGTGTGGGAGG-3') were used to subclone the sequence into pEGFP-N1 (Clontech). For nuclear localization, the sequence PKKKRKVEDA was added to the C terminus of the redox probes using PCR to subclone the construct in pEGFP-N1. For mitochondrial localization, the redox probes were transferred to pECFPmito (Clontech) using BamHI and NotI restriction to swap the cyan fluorescent protein and roGFP sequences.

C. Results

Confirmation of Redox Potential—Preliminary experiments showed that roGFP1 and roGFP2 in the cytosol of mammalian cells were largely reduced, so it was important to characterize the behavior of reduced roGFP1 and roGFP2 *in vitro*. The proteins were expressed in E. coli, purified, and were freshly reduced each experimental day. Experiments were carried out in deoxygenated buffers unless stated otherwise (see "Materials and Methods"). Hanson et al. (9) measured the midpoint redox potentials (E'_0) of roGFP1 and roGFP2 to be -288 and -272 mV, respectively, using DTT (E'_0 = -330 mV) as the calibrating redox buffer. The large difference between E'_0 values for the roGFPs versus DTT means that roGFP is half-

reduced with very small ratios of [DTT] to [DTT_{ox}]. It would be desirable to confirm the E'_0 values for roGFPs using redox buffers with E'_0s more closely matched to those of roGFPs. We chose dihydrolipoic acid (thioctic acid) and BMES because they form internal disulfides upon oxidation, similar to DTT and roGFPs. Therefore, roGFPs should react with these buffers with a 1:1 stoichiometry. Furthermore, both of these buffers are small molecules, which should cross cell membranes, possibly allowing *in situ* calibration of intracellular roGFPs. Titrations of the protein in redox buffers of increasing ratios of reduced to oxidized states were performed (Figure. 1.1) from which the midpoint potentials of the redox proteins were calculated. Initially, we found distinct redox potentials when using lipoate or BMES as standard solutions; however, the values for roGFP1 and roGFP2 differed by the identical values. Because E'0 for BMES (-313 mV) (12) had only been determined in 1:1 methanol-water, we used NMR spectroscopy to determine the value for BMES in a purely aqueous solution relative to the dihydrolipoate/lipoate couple. When the resulting value E'_0 = -295 $\pm$ 1 mV was used to determine E'_0 for the roGFPs, we obtained close agreement between the values obtained in the two standard buffers. These values, E'_0 = -294 and -287 mV for roGFP1 and roGFP2, respectively, are somewhat more negative than the redox potentials reported by Hanson et al. (9) based on DTT as standard, -288 and -272 mV, although the ordering of roGFP1 as more reducing than roGFP2 is preserved.

Oxidation of Redox Probes *in Vitro*—Because roGFPs were largely reduced inside cells until membrane-permeant oxidants were added, we characterized the *in vitro* dose-response relationships of roGFPs to those same oxidants. roGFPs are easily oxidized upon storage *in vitro*, so they were freshly reduced prior to most experiments

and characterized in degassed buffers and sealed reactions. Figure. 1.2 shows the extent of roGFP oxidation by varying concentrations of oxidants after 30 min and 24 h of reaction. Aldrithiol (2,2-dipyridyl disulfide) and diamide (1,1-azobis(N,N-dimethylformamide)) were very reactive and completely oxidized roGFPs in <30 min at all of the concentrations tested (0.008–1 mM). Two other disulfides, GSSG and the oxidized form of BMES, required longer reaction times and higher concentrations to oxidize roGFPs, even partially. Hydrogen peroxide was not very effective *in vitro* until given at nearly millimolar concentrations for >30 min. We also tested two naphthoquinones commonly used to stimulate redox cycling in live cells. Menadione, 2-methyl-1,4-naphthoquinone, caused an initial increase in emission ratio consistent with oxidation, but prolonged incubations gave anomalous ratios and large decreases in fluorescence emission at all of the excitation wavelengths. Mass spectral analysis of the proteins after menadione exposure revealed the addition of 344 Da, consistent with the addition of 2 molecules of menadione to the proteins. Arylation of cysteines by menadione has been reported previously (13, 14). GSH reacts with menadione to give the thioether as well as hydrogen peroxide and superoxide (15). DMNQ (16), reported to elicit redox cycling without arylating thiols, did not cause fluorescence quenching but only partially oxidized roGFPs even after 24 h. Surprisingly, a given oxidant concentration and exposure time generally caused more oxidation of roGFP2 than those of roGFP1, even though roGFP1 is thermodynamically a stronger reductant (i.e. has a more negative E'_0) than roGFP2.

Oxidation of Redox Probes in HeLa Cells—When roGFPs were transiently expressed in HeLa cells, expression was observed throughout the cytosol and nucleus and ratios were comparable for all of the areas of the cell. Oxidants such as

aldrithiol increased the excitation ratio (400/480 nm for roGFP1, 400/495 nm for roGFP2) over a few minutes in a spatially uniform manner (Figure. 1.3). Upon washing out the oxidant, the cells slowly reduced the roGFPs. Administering DTT usually accelerated this reaction. To calibrate these ratios, we attempted to use saturating doses of membrane-permeant reductants and oxidants to establish minimum and maximum ratios in situ. However, we generally could not achieve ratios as extreme as those from fully reduced or oxidized protein in microdroplets of buffer observed with the same imaging system (Figure. 1.4). Based on the *in vitro* ratios, roGFP1 in unperturbed HeLa cells was 16% oxidized, implying a basal redox potential of -315 mV. After the addition of 4 mM DTT or 0.5 mM aldrithiol (concentrations determined to cause maximal effects), the extent of roGFP1 oxidation changed to 6.5 and 72%, respectively. Unperturbed cells maintained roGFP2 5% oxidized, after which DTT reduced the ratio to 0% and aldrithiol oxidized the protein to a slightly greater ratio than obtainable in droplets of buffer on the microscope stage. Thus, roGFP2 reports a basal redox potential of -325 mV, reasonably consistent with the value seen by roGFP1.

Cells transiently expressing roGFPs were treated with 0.1 mM of the oxidants tested *in vitro* with the exception of GSSG, which does not cross cell membranes. Similar results were observed for both roGFP1 and roGFP2 (Figure. 1.5). The rank order of oxidant efficacies, aldrithiol, diamide > H_2O_2, menadione, DMNQ > oxidized BMES, and lipoate was similar to that *in vitro*, but 0.1 mM hydrogen peroxide or the quinones produced robust increases in ratio in cells within 10 min, whereas even 1 mM concentrations were not capable of full oxidation *in vitro*. Although oxidized BMES and lipoate were ineffective at 0.1 mM, at 5 mM they did cause considerable

oxidation. However, this maximal effect was still somewhat less than that produced by 0.1 mM aldrithiol, so we concluded that redox buffers made from BMES and lipoate would probably not clamp intracellular redox potentials robustly enough to serve as standards for *in situ* calibration.

To determine the roles of glutathione and catalase in maintaining cellular redox status under basal and H_2O_2-challenged conditions, cells were pretreated with buthionine sulfoximine (BSO), an inhibitor of GSH synthesis, or aminotriazole, a catalase inhibitor (Figure. 1.6). GSH depletion by BSO resulted in a small but significant ($p < 0.05$) increase in the resting excitation ratio of the probe and an even greater extent of oxidation due to (100 μM) hydrogen peroxide ($p < 0.005$). Pretreatment with BSO for 2,5,or 24 h showed similar results. Pre-incubation with aminotriazole did not significantly change the basal excitation ratio (i.e. had no effect on the basal oxidation state) but was almost as effective as BSO at enhancing the response to 100μM hydrogen peroxide. Identification of the reductase responsible for reducing the roGFPs in the cell was inconclusive, but reduction is most likely enzyme-dependent because it is observed immediately after removal of oxidant when there is little glutathione available for reduction. Unfortunately, the inhibitors of the NADPH reductases are selective rather than specific. We observed that inhibition of reduction following a 1-h preincubation with 100 μM cisplatin (thioredoxin reductase inhibitor (17)) and 200 μM 5-methoxyindole-2-carboxylic acid (dihydrolipoamide dehydrogenase inhibitor (18)) both prevented cells from reducing roGFPs after brief exposure to aldrithiol (Figure. 1.7). BCNU (carmustine) interacts with the roGFPs directly and could not be used for inhibition studies.

A possible explanation for H_2O_2 and the quinones being much more potent in cells than *in vitro* is that in cells they can generate reactive oxygen species (ROS) such as superoxide, $O2^{\rho}$-, which might react more rapidly with the roGFPs. The superoxide generated *in vitro* by reaction of xanthine with xanthine oxidase was able to oxidize roGFPs to a modest extent (Figure. 1.8) but was greater than air oxidation observed in the control. However, the identical superoxide-generating system placed outside roGFP-expressing cells caused a much larger and faster response, even though superoxide would have to diffuse across the plasma membrane to reach the roGFP. Therefore, the effect of superoxide itself seems to be amplified inside cells. We considered the possibility that hydroxyl radicals generated from H_2O_2 by Fenton chemistry might be the kinetically reactive oxidants, but the addition of Fe(II) to H_2O_2 and roGFPs *in vitro* destroyed the protein fluorescence rather than accelerate the normal change in emission ratio. Another hypothesis might be that glutathione peroxidase or related enzymes either catalyze H_2O_2 reaction with roGFPs or generate enough GSSG to oxidize the roGFPs by thiol-disulfide exchange. However, commercially available glutathione peroxidase failed to accelerate H_2O_2 reaction *in vitro* with roGFPs with or without added GSH. Therefore, the basis for the enhanced H_2O_2 response in cells remains unclear.

Redox Responses during Physiological Stimulation—Can roGFPs detect redox changes under physiological conditions and not just direct nonphysiological oxidants and reductants as tested above? The simplest challenge was to vary the partial pressure of O_2 from 0 to 1 atm, corresponding to pO_2 values ranging from anoxic to hyperoxic. Media bubbled with pure N_2 or O_2 were passed over roGFP-expressing HeLa, HEK293, PC12, or P388D1 cells in a closed perfusion chamber, but neither

treatment caused any detectable change in the excitation ratios compared with air-saturated medium, even when the cells had been pretreated with BSO (reducing GSH levels) or aminotriazole (inhibiting catalase). Thus, cytosolic roGFPs (and presumably the intracellular redox potential) seem to be very well buffered against simple changes in pO_2, in contrast to their sensitivity to H_2O_2, superoxide, and quinones.

One of the most dramatic oxidative events in mammalian cells is the oxidative burst in immune cells, which plays a major role in destroying pathogens (4). Therefore, we expressed roGFPs in HL60 cells induced to differentiate into monocytes by incubation in 1.3% Me_2SO for 7 days (19) and then stimulated with PMA to activate protein kinase C. Observation of time courses by microscopy was difficult because of poor transfection efficiency by electroporation (30%), incomplete transformation by Me_2SO, and nonadherence of the cells. However, we were able to obtain the ratios by flow cytometry (FACSVantage SE, BD Biosciences). Upon application of 20 μM PMA, the roGFPs indicated substantial oxidation within 10–15 min (Figure.1.9). Diphenyleneiodonium could not be used to inhibit NADPH oxidase (20), because preincubation with this compound prevented oxidation of the roGFPs by aldrithiol. This effect was not observed *in vitro*. Inhibition of the PMA-induced oxidation was observed with AEBSF (21) and apocynin (22), two other inhibitors of NADPH oxidase.

Localization of roGFP2 to Plasma Membranes—Endogenous production of H_2O_2 has also been implicated in growth factor responses such as in NR6 cells treated with epidermal growth factor (EGF) (23) or HeLa cells stimulated with lysophosphatidic acid (LPA) (24). The concentrations of H_2O_2 and other ROS attained during such

signaling are still unknown but presumably much less than those used to kill pathogens during oxidative bursts. We were unable to detect any oxidation of the probe following the addition of EGF to NR6 cells expressing EGF receptor or LPA to HeLa cells. As a positive control, flow cytometry with dichlorodihydrofluorescein diacetate (data not shown) verified the previously reported increase in oxidation of this traditional probe to the dichlorofluorescein product (23). Presumably, the dye is more sensitive than the proteins because oxidation of the dye is irreversible so that it qualitatively integrates even significant localized and transient production of ROS. By contrast, roGFPs are reversible indicators that should track the overall redox equilibrium of the cell, which may well be constant.

One possible explanation for the different responses of the roGFP versus dichlorofluorescein to growth factors was that the dye was integrating localized increases in oxidant potential, whereas the overall redox potential of the entire cell, recorded using roGFPs, remained constant. Therefore, we tested whether redox responses were highly localized near the growth factor receptors on the plasma membrane (Figure. 1.10). We targeted roGFP2 to the plasma membrane using a N-terminal myristoylation and palmitoylation signal from Lyn, a tyrosine kinase protein belonging to the Src family. Following transfection into NR6 and HeLa cells, the redox probe was indeed localized to the plasma membrane. Responses to aldrithiol and to DTT were noticeably faster than those of untargeted roGFP2. However, the membrane-targeted protein remained unreactive to stimulation by EGF or LPA. Targeting the roGFPs to the mitochondria and the nucleus did not result in any significant difference in activity to roGFP expressed in the cytosol.

Increasing the Sensitivity of roGFPs to H_2O_2—Responses of the current roGFPs generally take minutes or longer, which may be too slow to detect some signaling events. Redox kinetics of thiols are often limited by the need to deprotonate the thiol before it can oxidize. Placing positive charges near cysteine residues increases sensitivity to oxidation by H_2O_2 (25), presumably by facilitating deprotonation. Therefore, we designed a series of roGFP variants with outward-facing lysine residues placed in close proximity to the key cysteine residues. Asn-149, Ala-206, and Phe-223 were individually replaced with lysine. Two double mutants were also prepared in which both positions 149 and 223 or positions 206 and 223 were replaced with lysine. Mutated proteins were isolated and tested *in vitro*. All exhibited greater sensitivity to oxidation by H_2O_2 (Figure. 1.11A). Five of the mutated proteins were transfected into HeLa cells, but only F223K and F223K/A206K showed a larger response to H_2O_2 than those of the parent roGFP2 (Figure. 1.11B). These two mutants were tested for responses to EGF stimulation, but oxidation of the mutated roGFPs was still not detected.

D. Discussion

GFP-based probes of redox potential offer many advantages over previous methods for assessing redox status. Genetic encoding means that the probes can be introduced into any cell or organism that can express recombinant cDNA, that the proteins can be targeted to specific subcellular locations or tissue distributions, and that reagent distribution costs are minimized. Continuous nondestructive monitoring of redox potential with a reversible indicator is far easier and higher in spatial and temporal resolution than traditional discontinuous sampling using destructive assays of thiol and disulfide contents. A similar redox probe based on yellow fluorescent

protein (YFP) has been reported previously (26), but this probe gives only an intensity change, not a ratiometric response. In each case, disulfide formation favors protonation of the chromophore, which typically quenches YFPs completely but shifts excitation maxima of GFPs to ~400 nm as observed here. Ratiometric output is valuable not only for all of the usual reasons of indifference to variable expression levels, such as cell thickness, lamp intensities, detector sensitivities, and photobleaching, but also to distinguish genuine redox changes from artifacts such as arylation of the probe as observed here with menadione and roGFP1. By the standards of other GFP based indicators, roGFPs give fairly large changes in ratio from maximally reduced to maximally oxidized, up to 6-fold *in vitro* and up to ~3-fold in cytosol of viable mammalian cells.

Quantitative calibration of redox potentials reported by roGFPs posed some unexpected problems. We felt that roGFPs should be re-titrated in redox buffers whose midpoint potential E'_0 was a better match for the proteins than that of DTT. Eventually, we succeeded with dihydrolipoate and bis(mercaptoethyl) sulfone, although the E'_0 of the latter had to be redetermined in a fully aqueous medium. The resulting estimates of E'_0 = -294 and -287 mV for roGFP1 and roGFP2, respectively, are only slightly more negative than the independently measured values of Hanson et al. (9) based on DTT, -288 and -272 mV, respectively (9). For future work, we suggest consensus average values of -291 and -280 mV for roGFP1 and roGFP2, respectively (9). Thus, the roGFPs require significantly stronger reducing conditions than rxYFP whose E'_0 was reported to be -261 mV (26). Østergaard et al. (26) reported that rxYFP was 50% oxidized when expressed in bacteria.

Oxidation of the probes by a panel of common oxidants was studied *in vitro* to determine relative oxidation rates before examination *in vivo*. Strong oxidants such as aldrithiol and diamide fully oxidized the probes in minutes. Hydrogen peroxide was also found to be a weak oxidant. Even 1 mM concentrations did not fully oxidize the protein even after a 24-h incubation. Prolonged exposure to menadione caused a reduction in fluorescence when excited at either peak, and it was found to arylate the cysteine thiols of the redox probes as it has been found to do with other proteins (13). However, the dimethoxy analogue DMNQ caused only modest oxidation after 24 h *in vitro*.

When expressed in the cytoplasm of HeLa cells, roGFP1 and roGFP2 were either 84 or 95% reduced, implying a basal redox potential of -315 and -325 mV, respectively, at pH 7.0. The apparent redox potential of the mitochondrial matrix is even more negative, approximately -360 mV (9), because the pH of that compartment is almost 8. These values measured with roGFPs suggest that the cytosol and mitochondria are much more reducing than predicted from measurements of intracellular GSH and GSSG (-200 to -240 mV) (27, 28). The discrepancy persists even during glucose deprivation, which has been reported to make cells less reducing. Therefore, we suspect that the various redox couples in the cell are not in equilibrium with each other. Instead, the NADPH, dihydrolipoamide, and thioredoxin redox couples may have to be poised substantially more negatively than the GSH/GSSG redox pair in order to drive substantial net flow of electrons to GSSG. Although reduced roGFPs react with GSSG *in vitro*, albeit slowly (Figure. 2), oxidized roGFPs are difficult or impossible to reduce with GSH *in vitro*. This unreactivity is probably because the E'_0 values are so far apart that the slightest contamination of

GSH with GSSG is enough to make the reaction thermodynamically unfavorable at millimolar concentrations of GSH. roGFPs do react readily and reversibly with more strongly reducing couples such as dihydrolipoate/lipoate, so they will primarily reflect the potential of the most strongly reducing redox buffers in the cell.

Application of exogenous membrane-permeant oxidants to cells initiated a change in ratio of the roGFP probes. Although the extent of the ratio and the time required to reach a plateau differed among the oxidants, the reactivity closely followed that seen in experiments *in vitro*. The major exception was hydrogen peroxide, which was found to react at 100 μM concentrations in the cells, whereas millimolar concentrations were required *in vitro*. Thus, we wished to determine whether the redox probes would be sensitive to direct oxidation by other ROS agents such as superoxide and we found that xanthine oxidase + xanthine (as an external source for superoxide (29)) caused oxidation of the roGFPs both extracellularly and intracellularly.

Although air slowly oxidizes unprotected reduced roGFPs *in vitro*, shifting from air to 100% O_2 failed to change the resting ratio of roGFPs expressed in a number of cell lines including HeLa, HEK293, NR6, PC12, and P388D1. This may not simply be due to insensitivity of the probe because dihydrorhodamine 123 has also been found to be unresponsive to hyperoxic conditions (30). A 20-min exposure of cells to anoxia also did not affect the resting ratio. The ratio remained unchanged even under glucose-free media or serum starvation conditions known to sensitize cells to oxidative damage. It appears then that the cells possess a strong mechanism for preventing oxidation in the cytoplasm, which was not overcome in the duration of our experiments.

Phagocytes produce ROS such as superoxide as a primary response to bacterial invasion. These cells contain high quantities of NADPH oxidase, a complex capable of producing superoxide as a consequence of its enzymatic oxidation of NADPH to NADP. Phorbol myristic acid stimulates superoxide production in macrophages through the activation of protein kinase C. We used a human cell line HL60 prestimulated to differentiate to monocytes with Me_2SO cells (31). Stimulation of the human cell line HL60 prestimulated to differentiate to monocytes transfected with roGFPs with PMA caused an increase in the fluorescence ratio consistent with oxidation of the protein. The lysine replacement roGFP2 mutant F223K/A206K yielded the largest response to PMA treatment in accordance with its highest sensitivity to oxidation. When cells were pretreated with an inhibitor for NADPH oxidase, diphenylene iodonium, the oxidation induced by PMA was eradicated. We were concerned that diphenylene iodonium may inactivate the protein, because the addition of aldrithiol (which should directly oxidize the protein) after treatment with diphenylene iodonium did not induce oxidation. However, other inhibitors of NADPH oxidase such as apocynin and AEBSF, which act by different reaction mechanisms, also precluded the PMA-induced oxidation. Many studies have argued that ROS may act as a second messenger in signaling by growth factors such as platelet derived growth factor, EGF, and TNF and that H_2O_2 induces NF-κB (32) and AP-1 (33). It has been long recognized that high levels of ROS trigger apoptosis and necrosis. A more recent theory argues that differential GSH levels may discriminate between H_2O_2 acting as an oxidative stressor or a second messenger in growth factor regulation (34). Using roGFPs, we were unable to demonstrate any response of the redox probes to two growth factor stimuli reported to generate cellular H_2O_2: EGF in NR6

cells or LPA in HeLa cells. Targeting the probe to the plasma membrane or mutating the roGFPs to enhance sensitivity to H_2O_2 failed to uncover sensitivity to EGF in NR6 cells or by LPA in HeLa cells, even though the modified probes still reacted to exogenous oxidants. Meanwhile, we verified in parallel experiments that the classic ROS probe 2',7'-dichlorodihydrofluorescein diacetate in NR6 cells responded to EGF, although 2',7'-dichlorodihydrofluorescein diacetate has been reported to be vulnerable to autocatalytic oxidation or other artifacts (35, 36). Therefore, we doubt that the above growth factors cause significant acute global perturbations in thioldisulfide redox potential. If there is a chemically significant change in thiol-disulfide redox status, it would probably have to be highly compartmentalized.

Acknowledgments—

We thank Q. Xiong, L. Gross and P. Steinbach for technical assistance and C. Hauser for editorial assistance.

* This work was supported by grants from the Superfund Basic Research Program (ES10337), National Institutes of Health (NS27177), Department of Energy (DE-FG03-01ER63276), and the Howard Hughes Medical Institute. The DNA Sequencing Shared Resource at the University of California-San Diego Cancer Center is funded in part by National Institutes of Health, NCI Cancer Support Grant 2P30CA23100-18. The costs of publication of this article were defrayed in part by the payment of page charges. This article must therefore be hereby marked "advertisement" in accordance with 18 U.S.C. Section 1734 solely to indicate this fact.

§ Present address: Dept. of Chemistry, University of Georgia, 414 Chemistry Bldg., Athens, GA 30602-2556.

Present address: Invitrogen, 501 Charmany Dr., Madison, WI 53719-1236.

** To whom correspondence should be addressed. Tel.: 858-534-4891; Fax: 858-534-5270; E-mail: rtsien@ucsd.edu.

Chapter One in full, is a reprint as it appears in THE JOURNAL OF BIOLOGICAL CHEMISTRY Vol. 279, No. 21, Issue of May 21, pp. 22284–22293, 2004 © 2004 by The American Society for Biochemistry and Molecular Biology, Inc. Printed in U.S.A. The dissertation author was the primary investigator and single author of this paper.

The abbreviations used are: GFP, green fluorescent protein;AEBSF, 4-(2-aminoethyl)benzenesulfonyl fluoride; BMES, bis(2-mercaptoethyl) sulfone; BSO, buthionine sulfoximine; DMNQ, 2,3-dimethoxy-1,4-naphthoquinone; DTT, dithiothreitol; DTTox, trans-4,5-dihydroxy-1,2-dithiane; roGFP, redox-sensitive GFP; EGF, epidermal growth factor; IMDM, Iscove's modified Dulbecco's medium; PMA, phorbol 12-myristate 13-acetate; ROS, reactive oxygen species; LPA, lysophosphatidic acid.

THE JOURNAL OF BIOLOGICAL CHEMISTRY Vol. 279, No. 21, Issue of May 21, pp. 22284–22293, 2004

This paper is available on line at http://www.jbc.org

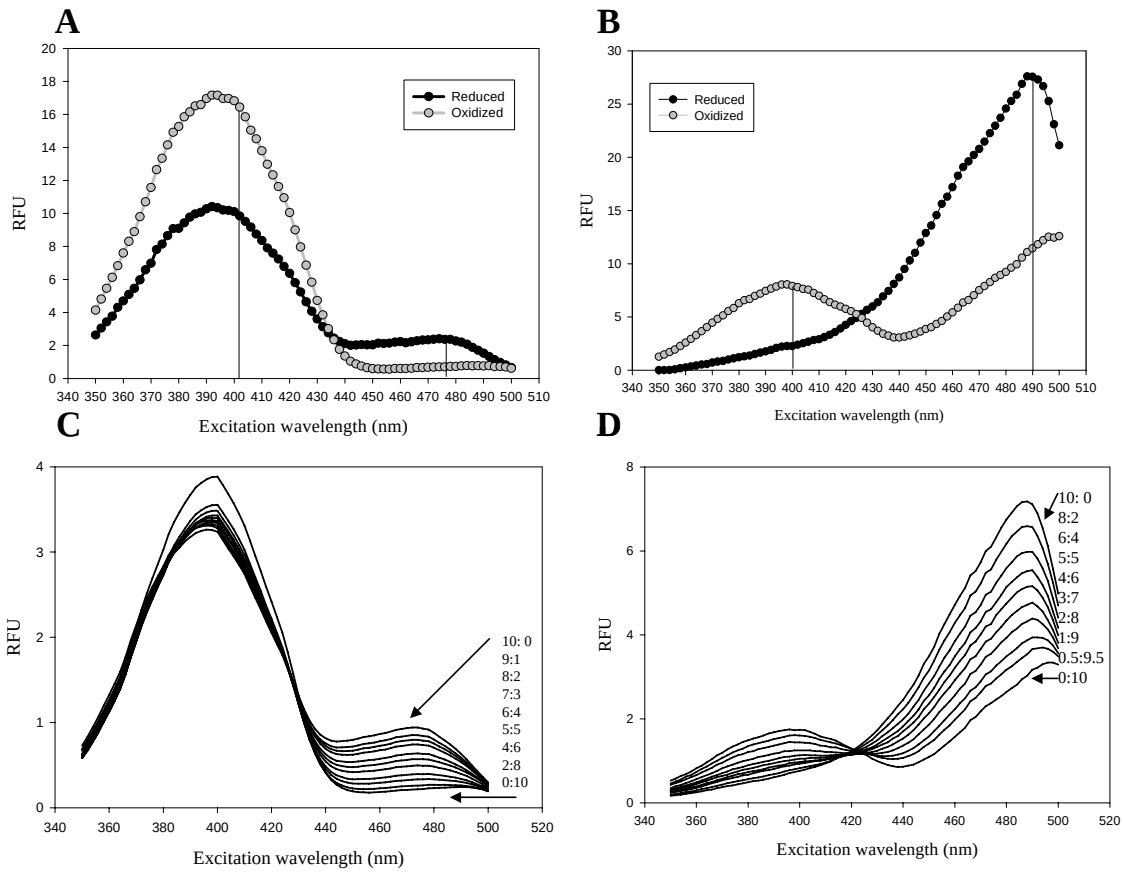

Figure 1.1. Excitation spectra and redox titration of roGFPs. Excitation spectra for fully oxidized and reduced roGFP1 (A) and roGFP2 (B). Emission was monitored at 515 nm. C, titration of roGFP1 (1 μM) with dihydrolipoate/ lipoate buffers (total 10 mM). D, titration of roGFP2 (1 μM) with reduced /oxidized BMES (total 10 mM). Conditions are as described under "Materials and Methods." Legends in C and D indicate the concentrations in millimolar of reduced:oxidized buffers, respectively. For clarity only the limiting spectra are connected by arrows to their buffer

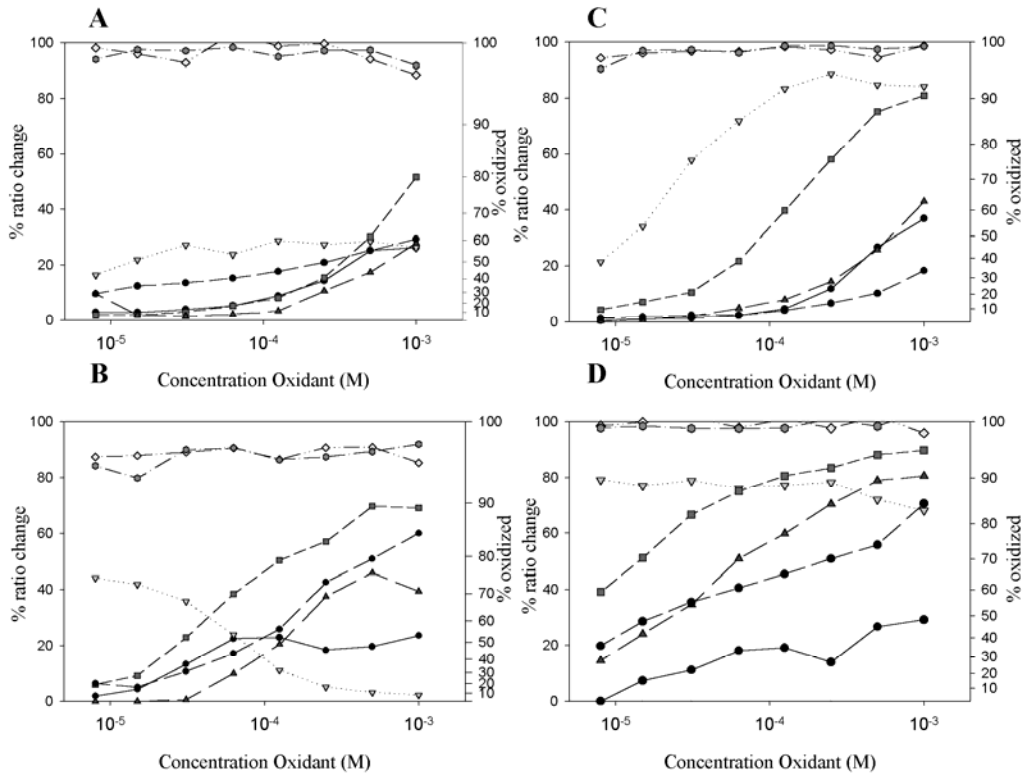

Figure. 1.2. Oxidation of the two roGFPs by common oxidants. A, roGFP1 following a 30-min incubation with oxidants. B, roGFP1 following 24-h exposure. C, roGFP2 following a 30-min incubation with oxidants. D, roGFP2 following 24-h exposure. Oxidation is expressed as a percentage of the fully reduced (0%) and fully oxidized (100%) proteins obtained under similar conditions. Excitation ratios were obtained from wavelengths of 400 and 472 nm for roGFP1 and 400 and 490 nm for roGFP2. Symbols:

.

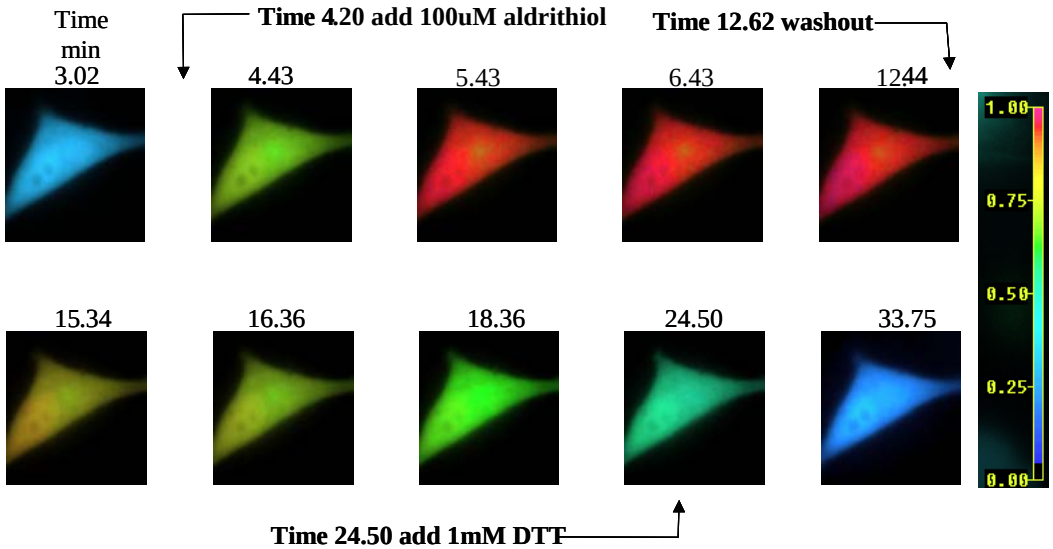

Figure 1.3. Oxidation upon addition of aldrithiol in HeLa cells expressing roGFP1. Images were taken using an emission wavelength of 535 nm and both 400-nm and 480-nm excitation wavelengths. The ratios of light emitted from 400- and 480-nm excitation were obtained at 1-min intervals, and images of the ratios obtained are shown in pseudocolor calibrated by the color scale at the far right. Times of addition and concentrations of reactants are indicated by arrows.

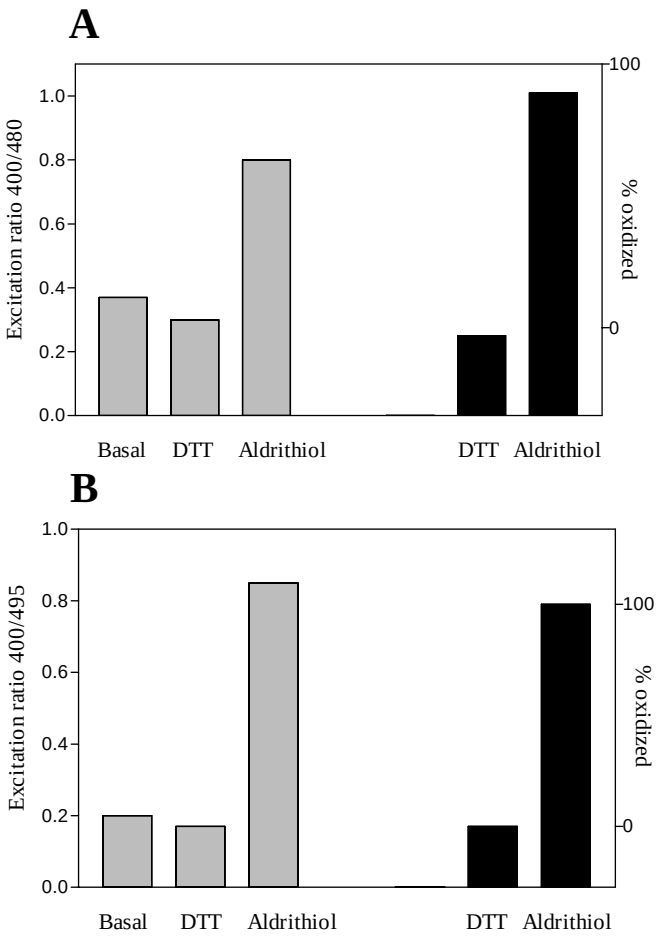

Figure 1.4. Dynamic range of roGFP ratios in cells versus protein microdroplets. roGFP1 and roGFP2 were expressed in HeLa cells. Ratio of fluorescence obtained at 400/480 (roGFP1) or 400/495 (roGFP2) maximum and minimum ratio was observed for protein microdroplets under the same conditions. Gray bars represent protein expressed in HeLa cells. Black bars represent free protein. A, roGFP1. B, roGFP2.

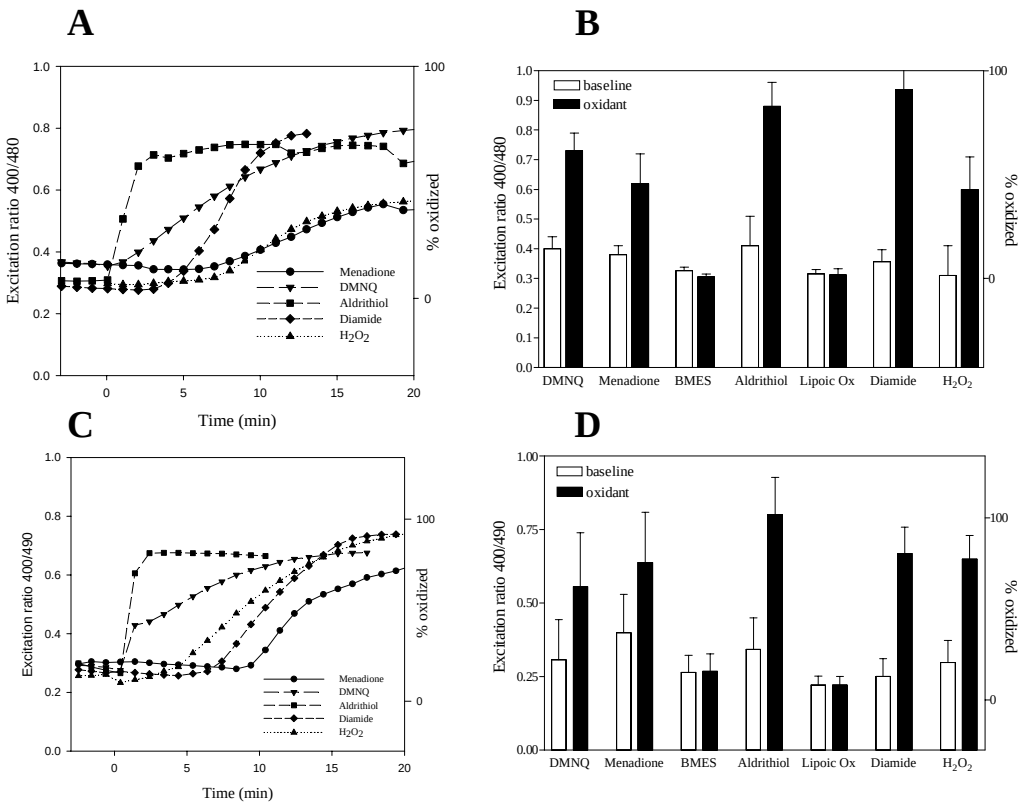

Figure.1.5. Oxidation of roGFPs expressed in HeLa cells upon stimulation with exogenous oxidants. Each oxidant was added to cells at a concentration of 100 μM. A, time course of oxidation of roGFP1. Oxidants were added at time zero, an average of three or more experiments. B, oxidation of roGFP1-averaged results from multiple experiments. Open bars, ratio observed before addition; solid bars, ratio observed when oxidation had reached a plateau. C, time course of oxidation for roGFP2. D, oxidation of roGFP2 averaged results from multiple experiments

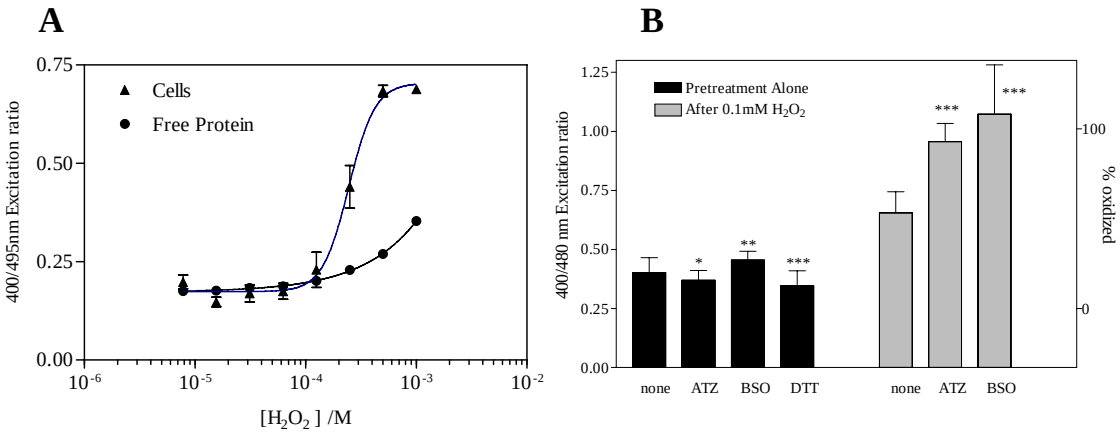

Figure. 1.6. Reactivity of roGFPs to hydrogen peroxide in HeLa cells. A, effective concentration for hydrogen peroxide induced oxidation in a HeLa cell line stably expressing roGFP2, and in vitro, the EC_{50} value obtained in HeLa cells was 213 ± 65 μM (n = 3). B, altering the GSH:GSSG ratio in the cell by pretreating cells with BSO (100 μM for 2 h) or aminotriazole (50 mM for 10 min) had small but significant effects on basal ratios, but those obtained after hydrogen peroxide treatment (100 μM) were greater (***, $p < 0.005$; **, $p < 0.05$; * $p < 0.5$) in HeLa cells transiently expressing roGFP1

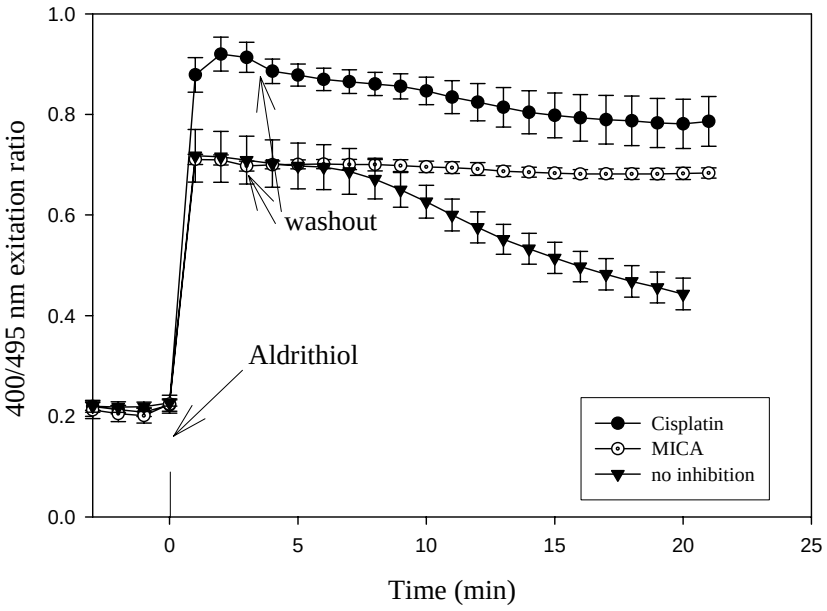

Figure. 1.7. Inhibition of cellular reduction of roGFP2. The reduction normally observed following oxidation with 100 μM aldrithiol was inhibited following a 1-h incubation with 200 μM 5-methoxyindole-2-carboxylic acid (MICA) or a 45-min incubation with 100 μM cisplatin.

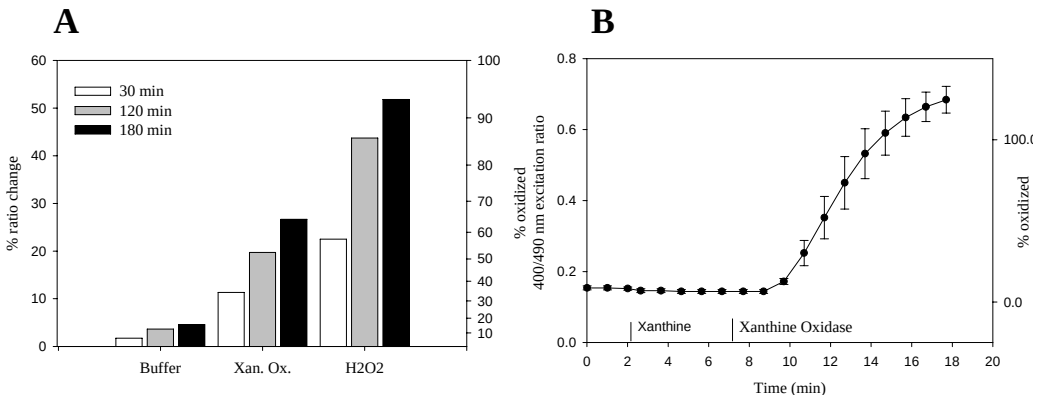

Figure 1.8. Superoxide-induced oxidation of roGFP2. A,oxidation of roGFP2 (0.75 μM) following incubation with xanthine oxidase (50 milliunits) and xanthine (50 μM) under aerobic conditions or co-incubated with 750 μM H_2O_2. B, oxidation of roGFP2 expressed in HeLa cells following extracellular production of superoxide by xanthine oxidase (36 milliunits) and xanthine (200 μM). roGFP1 gave similar results.

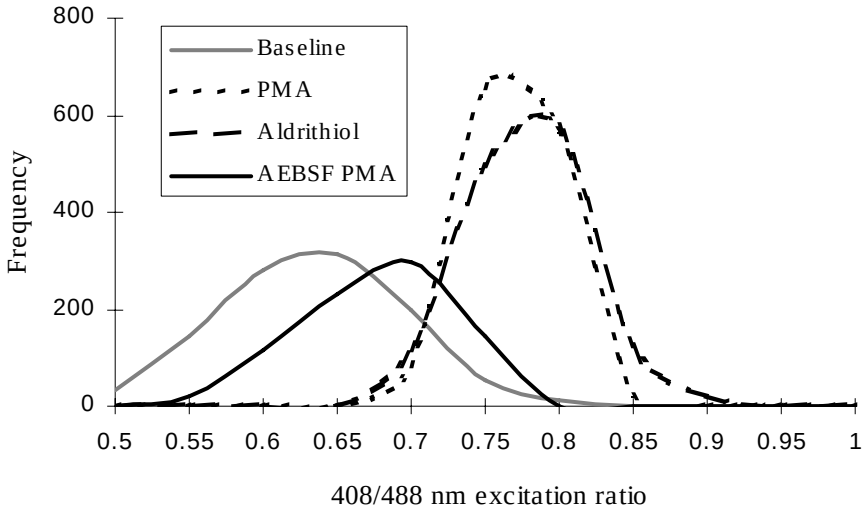

Figure 1.9. Detection of superoxide burst in differentiated HL60 cells. roGFP2 F223K/A206K was expressed in HL60 cells differentiated with 1.3% Me_2SO for 5 days. Histograms of excitation ratios are shown for unstimulated cells (gray line), cells stimulated with 50 μM PMA (dotted line), and cells treated with 100 μM aldrithiol (dashed line) and preincubated with AEBSF (500 μM) followed by 50 μM PMA (solid line). Similar results (not shown) were obtained with roGFP1.

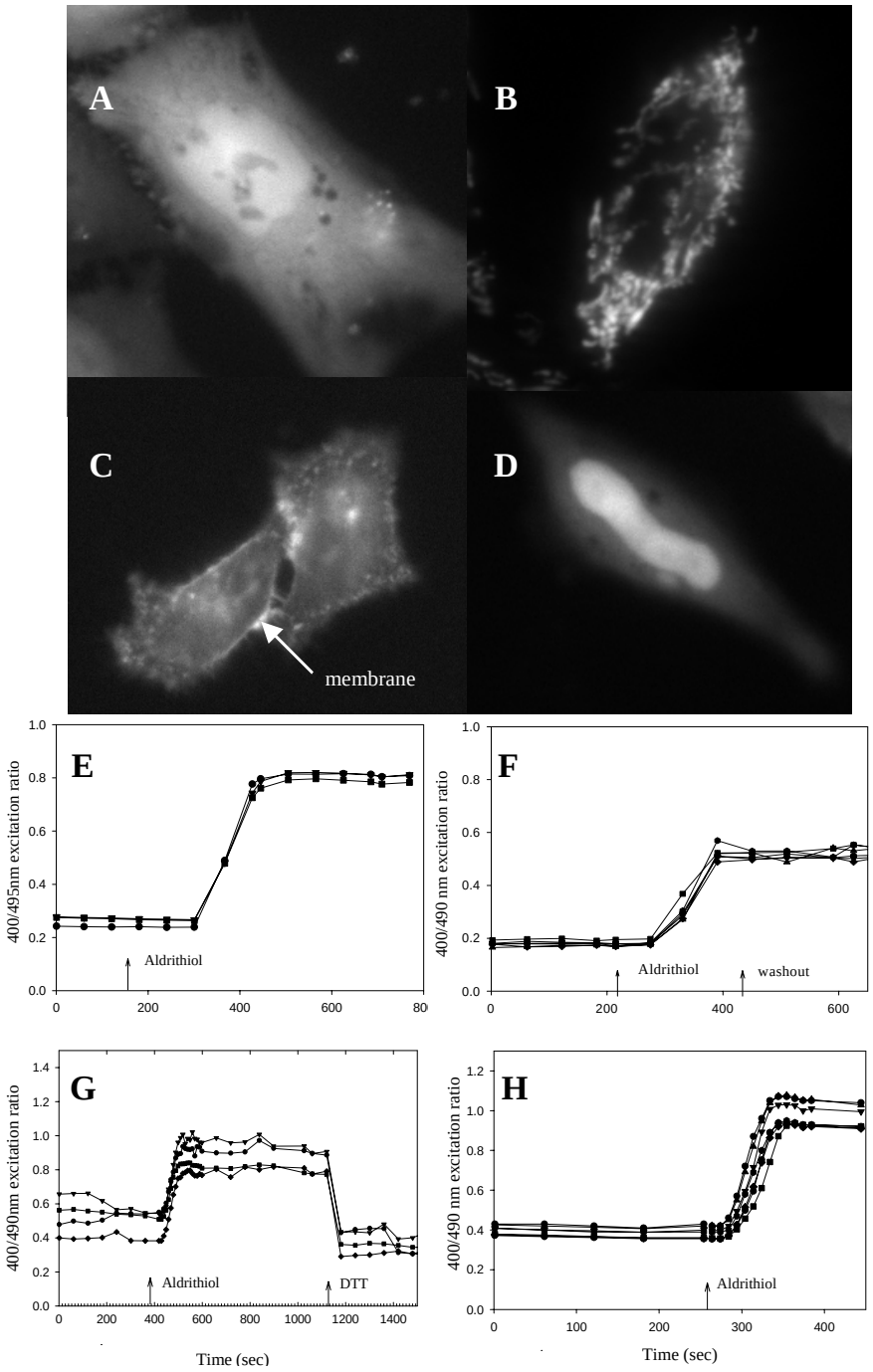

Figure 1.10. Targeting of the redox probes. Fluorescence of roGFP2 (495-nm emission) targeted to cytosol (A), mitochondria (B), plasma membrane (C), or fluorescence (D) of roGFP1 (400-nm emission) targeted to the nucleus. The constructs did not reveal significant differences in roGFP2 reactivity to aldrithiol (100 μM) in the cytosol (A and E) and mitochondria (B and F), at the plasma membrane (C and G), or roGFP1 in the nucleus (D and H). Each trace within panels E–H indicates a separate cell.

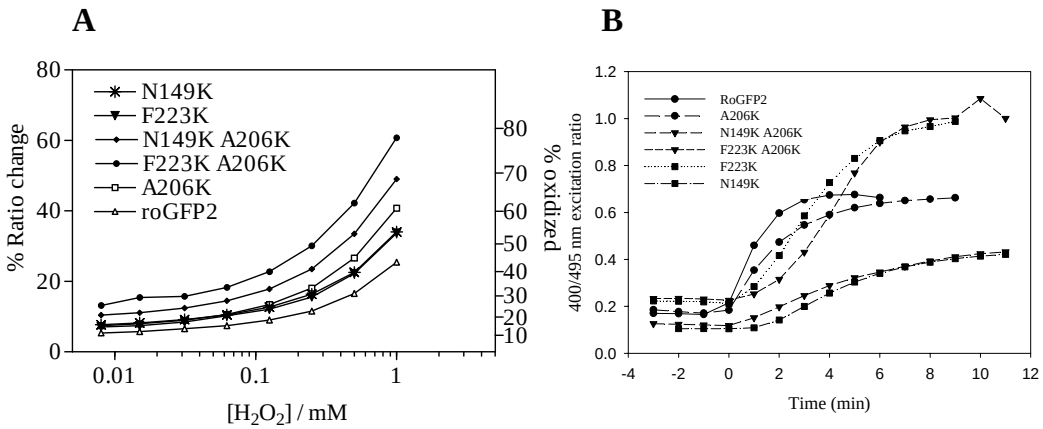

Figure 1.11. Responses of lysine mutants of roGFP2. A, reactivity of lysine mutants to H_2O_2 *in vitro* after 1 h. B, time course for response of roGFP2 lysine mutants in HeLa cells to 100 μM H_2O_2 added at time 0.

F. References

1. Krauth-Siegel, R. L., Jockers-Scherubl, M. C., Becker, K., and and Schirmer, R. H. (1989) Biochem. Soc. Trans. 17, 315–317

2. Forman, H. J., and Torres, M. (2002) Am. J. Respir. Crit. Care Med. 166, S4–S8

3. Forman, H. J., and Torres, M. (2001) Mol. Aspects Med. 22, 189–216

4. Droge, W. (2002) Physiol. Rev. 82, 47–95

5. Yanping, L., and David, D. G. (2002) Clin. Exp. Pharmacol. Physiol. 29, 305–311

6. Rojkind, M., Dominguez-Rosales, J. A., Nieto, N., and Greenwel, P. (2002) Cell. Mol. Life Sci. 59, 1872–1891

7. Hwang, C., Sinskey, A. J., and Lodish, H. F. (1992) Science 257, 1496–1502

8. Liu, S., Ansari, N. H., Wang, C., Wang, L., and Srivastava, S. K. (1996) Curr. Eye Res. 15, 726–732

9. Hanson, G. T., Aggeler, R., Oglesbee, D., Capaldi, R. A., Tsien, R. Y., and Remington, S. J. (2004) J. Biol. Chem. 279, 13044–13053

10. Goodrow, M. H., and Musker, W. K. (1981) Synthesis 457–459

11. Lamoureux, G. V., and Whitesides, G. M. (1993) J. Org. Chem. 58, 633–641

12. Lees, W. J., Singh, R., and Whitesides, G. M. (1991) J. Org. Chem. 56, 7328–7331

13. Di Monte, D., Ross, D., Bellomo, G., Eklow, L., and Orrenius, S. (1984) Arch. Biochem. Biophys. 235, 334–342

14. Mirabelli, F., Salis, A., Perotti, M., Taddei, F., Bellomo, G., and Orrenius, S. (1988) Biochem. Pharmacol. 37, 3423–3427

15. Ross, D., Thor, H., Orrenius, S., and Moldeus, P. (1985) Chem. Biol. Interact. 55, 177–184

16. Gant, T. W., Ramakrishna, D. N., Mason, R. P., and Cohen, G. M. (1988) Chem. Biol. Interact. 65, 157–173

17. Arner, E. S., Nakamura, H., Sasada, T., Yodoi, J., Holmgren, A., and Spyrou, G. (2001) Free Radic. Biol. Med. 31, 1170–1178

18. Haramaki, N., Han, D., Handelman, G. J., Tritschler, H. J., and Packer, L. (1997) Free Radic. Biol. Med. 22, 535–542

19. Collins, S. J. (1987) Blood 70, 1233–1244

20. Hampton, M. B., and Winterbourn, C. C. (1995) Free Radic. Biol. Med. 18, 633–639

21. Diatchuk, V., Lotan, O., Koshkin, V., Wikstroem, P., and Pick, E. (1997) J. Biol. Chem. 272, 13292–13301

22. Van den, W. E., Beukelman, C. J., Van den Berg, A. J., Kroes, B. H., Labadie, R. P., and Van Dijk, H. (2001) Eur. J. Pharmacol. 433, 225–230

23. Bae, Y. S., Kang, S. W., Seo, M. S., Baines, I. C., Tekle, E., Chock, P. B., and Rhee, S. G. (1997) J. Biol. Chem. 272, 217–221

24. Sekharam, M., Cunnick, J. M., and Wu, J. (2000) Biochem. J. 346, 751–758

25. Kim, J. R., Yoon, H. W., Kwon, K. S., Lee, S. R., and Rhee, S. G. (2000) Anal. Biochem. 283, 214–221

26. Østergaard, H., Henriksen, A., Hansen, F. G., and Winther, J. R. (2001) EMBO J. 20, 5853–5862

27. Hwang, C., Lodish, H. F., and Sinskey, A. J. (1995) Methods Enzymol. 251, 212–221

28. Schafer, F. Q., and Buettner, G. R. (2001) Free Radic. Biol. Med. 30, 1191–1212

29. Olson, J. S., Ballou, D. P., Palmer, G., and Massey, V. (1974) J. Biol. Chem. 249, 4363–4382

30. Royall, J. A., and Ischiropoulos, H. (1993) Arch. Biochem. Biophys. 302, 348–355

31. Collins, S. J., Ruscetti, F. W., Gallagher, R. E., and Gallo, R. C. (1979) J. Exp. Med. 149, 969–974

32. Schreck, R., Rieber, P., and Baeuerle, P. A. (1991) EMBO J. 10, 2247–2258

33. Karin, M., and Shaulian, E. (2001) IUBMB Life 52, 17–24

34. De Bleser, P. J., Xu, G., Rombouts, K., Rogiers, V., and Geerts, A. (1999) J. Biol. Chem. 274, 33881–33887

35. Rota, C., Fann, Y. C., and Mason, R. P. (1999) J. Biol. Chem. 274, 28161–28168

36. Liochev, S. I., and Fridovich, I. (1998) Free Radic. Biol. Med. 25, 926–928

Chapter Two

Biological Applications for Redox Sensitive Green Fluorescent Protein Mutant F223K A206K.

A. Introduction

Redox-sensitive green fluorescent proteins (GFP) allow real time visualization of the oxidation state of the indicator. The indicators examined in this work are GFP mutants with two surface-exposed cysteines placed at positions 147 and 204 on adjacent β-strands close to the chromophore. Disulfide formation between the cysteine residues promotes protonation of the chromophore and increases the excitation spectrum peak near 400 nm at the expense of the peak near 490 nm. Ratios of fluorescence from excitation at 400 and 490 nm indicate the extent of oxidation and thus the redox potential while canceling out the amount of indicator and the absolute optical sensitivity. Because the indicator is genetically encoded, it can be targeted to specific proteins or organelles of interest and expressed in a wide variety of cells and organisms. We evaluated roGFP1 (GFP with mutations C48S, S147C, and Q204C) and roGFP2 (the same plus S65T) with physiologically or toxicologically relevant oxidants both *in vitro* and in living mammalian cells. Responses of the current roGFPs generally take minutes or longer, which may be too slow to detect some signaling events. Redox kinetics of thiols are often limited by the need to deprotonate before they can oxidize. Placing positive charges near cysteine residues increases sensitivity to oxidation by H_2O_2 [1], presumably by facilitating deprotonation. Therefore, we designed a series of roGFP variants with outward-facing lysine residues placed in close proximity to the key cysteine residues. Asn-149, Ala-206,

and Phe-223 were individually replaced with lysine. Two double mutants were also prepared in which both positions 149 and 223 or positions 206 and 223 were replaced with lysine. Mutated proteins were isolated and tested *in vitro*. All exhibited greater sensitivity to oxidation by H_2O_2. Since we first reported the lysine mutants [2] there have been two new studies incorporating similar mutations to increase sensitivity to redox sensitive green and yellow fluorescent proteins [3,4].

In this chapter the double lysine mutant RoGFP2-F223KA206K (roGFP2-FA) is used in three distinct applications for roGFPs. 1) The protein was expressed in primary neurons to investigate the resting redox state of the neural cell body and reactions to redox stimuli. Neuronal cells treated with dopamine have been reported to increase glutathione disulfide concentrations, since hydrogen peroxide is a by-product of the metabolism of dopamine. Thus we examined the reaction of roGFP2-FA expressed in rat pheochromocytoma PC12 cell line to exogenous dopamine. 2) The redox indicator was evaluated for sensitivity to environmental toxicants. Toxicants known to produce reactive oxygen species were examined for their ability to influence the cytoplasmic redox equilibrium. 3) Finally the potential for clamping roGFP2-FA in a particular redox state following equilibration using formaldehyde was investigated.

B. Methods

Monitoring neural cytoplasmic redox state---Neurons were washed twice with Hanks' balanced salt solution buffer. All cells were imaged on a Zeiss Axiovert microscope with a cooled CCD camera (Photometrics, Tucson, AZ) controlled by Metafluor 2.75 software (Universal Imaging, West Chester, PA). Dual excitation ratio imaging used excitation filters 400DF15 and 495DF10 altered by a filter changer

(Lambda 10-2, Sutter Instruments, San Rafael, CA), a 505DRLP dichroic mirror and a single emission filter, 535DF25. Fluorescence images were background-corrected by manual selection of background regions. Exposure time was 200–1000 ms, and images were taken every minute.

Dopamine induced hydrogen peroxide in PC12 cells ---Rat pheochromocytoma cells were maintained in DMEM supplemented with 10% horse serum, penicillin and streptomycin. roGFP-FA was expressed in PC12 cells using modified pEFGP-N1 as expression vector and Lipofectin Plus as transfection reagent. After 24–72 h of incubation at 37°C in culture medium, the cells were washed twice with Hanks' balanced salt solution; imaging dishes were maintained at 37^{o}C throughout the experiment.

Exposure of roGFP-FA expressing cells to environmental toxicants---Human HeLa and HepG2 cells were maintained in DMEM supplemented with 10% fetal bovine serum, 1% penicillin/streptomycin. roGFP-FA was expressed using modified pEFGP-N1 as expression vector and Fugene as transfection reagent. After 24–72 h of incubation at 37 °C in culture medium, the cells were washed twice with Hanks' balanced salt solution and imaged as above. Cell media were treated with solutions of either Sodium arsenite (0.2-25 μM), β-naphthoflavone (1 or 25 μM), benzo(α)-pyrene (1 or 25 μM), benzo(α)-anthrecene (1 or 25 μM), 3-methylcholanthrene (1 or 25 μM) or 2,3,7,8-Tetrachlorodibenzo-p-dioxin (TCDD, 4 and 100 nM), for 24 hours at 37^{o}C.

Effects of formaldehyde pre-treatment on roGFP-FA oxidation and reduction---

RoGFP-FA was subcloned into pRSETB (Invitrogen) using BamHI and EcoRI restriction sites. The plasmid encodes a fusion protein of the insert and an N-terminal

extension containing a $(His)_6$ tag, enabling purification by nickel affinity chromatography. The construct was expressed in the JM109 strain of Escherichia coli. Concentrated protein (50–200 μM) was reduced with 10mM DTT and diluted to the required concentration following removal of DTT (using Centri-spin 20 columns (Princeton Separations Inc.)). A 2% Formaldehyde solution was prepared fresh for each experiment.

C. Results

RoGFP2-FA in rat neurons---When roGFP2-FA was expressed in cerebellar primary neurons the excitation ratio in the cytoplasm of the cell body was found to be elevated (Figure 2.1). An excitation ratio of 0.5 is significantly higher than that observed in other cell cultures tested including NR6, HeLa, HeK293, PC12 and HL60. Addition of aldrithiol (200μM) to the media resulted in a slow oxidation of the redox probe. Full oxidation required 10 minutes as compared to 1-2 minutes observed in NR6 cells (Figure 2.2). Reduction of the probe by the neuron was rapid and occurred immediately upon washout of oxidant. Addition of DTT reduced the protein to an excitation ratio of 0.2 similar to the maximal reduced values obtained in other cell lines.

Reaction of cytoplasmic roGFP2A in PC12 cells to dopamine--- roGFP2-FA was expressed in the cytoplasm of PC12 cells. Cells were maintained at 37^{o}C for the duration of the experiment. Exogenous addition of dopamine (1mM) to PC12 cells had no acute effects upon the excitation ratio of roGFP2-FA (Figure 2.3A). We also tested roGFP-sec147 a more sensitive mutant with selenocysteine at position 147 (see chapter 3), in the same cell line using an equal concentration of dopamine but

prolonged the experiment up to 45 minutes. Likewise no change in excitation ratio was observed.

Exploring the effects of environmental pollutants on cytoplasmic redox state---Polycyclic hydrocarbon compounds are of concern due to their increasing prevalence in the environment. They are metabolized in the liver by a family of enzymes called cytochrome P450 particularly by CYP1A. Reactive oxygen species have been detected in association with the metabolism of these compounds. We examined the reaction of two cell lines expressing roGFP2-FA to a 24 hour exposure to five common environmental toxicants; Arsenic, β-naphthoflavone, benzo(α)pyrene, 3-methylcholanthrene, and dioxin (TCDD). Human hepatoma (HepG2) and HeLa cells expressing cytoplasmic roGFP2-FA were exposed to up to four concentrations of toxicant for 24 hours before imaging. Four concentrations of sodium arsenite were examined, 0.2, 1,4 and 25 μM. β-naphthoflavone, benzo(α)pyrene and 3-methylcholanthrene were tested at two concentrations: 1 and 25 μM. The two concentrations used for dioxin were lower; 4 and 100nM. Cells treated with benzo(α)pyrene fluoresced brightly at 530nm when excited at 400nm, and since this interfered with data acquisition for roGFP2-FA, the compound was not investigated further. The images for all five toxicants in HeLa and HepG2 cells are given in Figures 2.4 and 2.6 respectively. Average excitation ratios for each of the concentrations tested are given in Figures 2.5 and 2.7 respectively. Addition of toxicants to the cells for 24 hours did not affect their morphology. Sodium arsenite had a small but significant effect on the excitation ratio at higher concentrations in both cell types. β-naphthoflavone caused no significant change in excitation ratio in either cell type. 3-methylcholanthrene induced a small but highly significant increase

in excitation ratio in HeLa cells and a larger (also highly significant) ratio change in HepG2 cells, but in either case only at the highest concentration tested (25 μM). Dioxin was found to have a significant increase the excitation ratio only at the highest concentration tested (100nM) and only in HeLa cells. Addition of Aldrithiol to cells treated with β-naphthoflavone and TCDD (toxicants generally found to have no effect) resulted in robust excitation ratio changes indicating the toxicants had not impaired the probes ability to oxidize (Figure 2.8).

Capping roGFP thiols with formaldehyde---Redox GFPs are reversible indicators they allow for continuous nondestructive monitoring of redox potential, however there are situations where it would be beneficial to allow the probe to equilibrate with the environment and then be able to "freeze" the probe at the particular oxidation state e.g. equilibration of tumors *in vivo*. Disulfide bonds of oxidized roGFP are stable, and withstand most laboratory tissue and cell processing. RoGFP thiols are sensitive to air oxidation unless maintained under reducing conditions. Once the probes are equilibrated, capping free thiols would prevent disulfide formation in air allowing us to determine redox potential in tissues/cells despite subsequent disruption. Formaldehyde is a common tissue fixative, which we tried because it is known to react with thiols. Two redox proteins, RoGFP2 and roGFP2-FA, in their reduced form were exposed *in vitro* to 2% formaldehyde for 5 minutes and subsequently tested for ability to oxidize in the presence of aldrithiol (200μM). Pretreatment with formaldehyde only partially inhibited roGFP2 from oxidation by aldrithiol, whereas formaldehyde treated roGFP2-FA was fully inhibited from oxidation (Figure 2.9). Prolonged exposure (60 minutes) to formaldehyde resulted in quenching of fluorescence over the entire range of the excitation spectrum for both proteins, and

was found to quench both oxidized and reduced states (Figure 2.10). In a lipoate buffer, quenching with formaldehyde was minimized. Exposure of partially oxidized roGFP2-FA to 1% formaldehyde still prevented further oxidation by aldrithiol but only resulted in a slight reduction by DTT (Figure 2.11).

D. Discussion

The work in this chapter focused on using the double lysine mutant RoGFP2-F223KA206K (roGFP2-FA), a slightly more sensitive roGFP, in three distinct applications for redox GFPs; redox state of neuronal cultures and testing for dopamine production of hydrogen peroxide; disturbance of redox equilibria by environmental toxicants; and the potential for clamping the redox proteins so that cellular/tissue redox values can be determined despite cell disruption.

roGFP2-FA was expressed in primary neurons to investigate the resting redox of the neural cell body and for reaction to exogenous oxidants. Resting excitation ratios were found to be elevated as compared to other cells studied. While neuronal cells exhibited a robust oxidation upon addition of aldrithiol, the rate of reaction was slower than observed for other cells tested with this probe. The same was not true for the addition of reductant, which induced a rapid decrease in excitation ratio to basal levels observed in most cells. Reduction of the probe by the cellular machinery was efficient, and reduction was observed immediately upon washout of oxidant. Dopamine (DA) is converted to dihydroxyphenylacetaldehyde (DOPAL) by monoamine oxidase with hydrogen peroxide as a side product and has been reported to increase GSSG:GSH ratio in neuronal and rat pheochromocytoma (PC12) cells. Due to elevated concentrations of H_2O_2 neurons producing dopamine are considered to suffer from oxidative stress [5]. However, we did not observe any acute changes in

$$DA + O_2 + H_2O \xrightarrow{MAO} DOPAL + H_2O_2 + NH_3$$

excitation ratios of roGFP2-FA expressed in PC12 cells. Nor were any changes observed for a redox mutant with increased sensitivity to hydrogen peroxide (see chapter 3), even when cells were imaged up to an hour following administration of dopamine, a similar time frame used by Kim *et al*. [5]. It is possible that chronic administration of dopamine is required to disturb the redox equilibrium e.g. in Parkinson's disease where DA turnover is elevated, and hydrogen peroxide production by MAO has been linked to suppression of electron transport in mitochondria [6]. Hydrogen peroxide was detected in PC12 cells following stimulation with NGF using an alternative hydrogen peroxide indicator (HyPer). HyPer [7] uses a circularly permuted yellow fluorescent protein inserted into the regulatory domain of OxyR (a prokaryotic H_2O_2 sensing protein). The success of this probe is likely due to the position of the H_2O_2 sensitive cysteine which is hidden deep in a hydrophobic pocket in OxyR in contrast to the cysteine on the roGFPs which are exposed to the cytoplasmic environment.

To evaluate sensitivity of cellular redox equilibria to environmental toxicants, a series of six toxicants known to produce reactive oxygen species were studied; sodium arsenite, and four polycyclic hydrocarbons, Benzo(α)pyrene, 3-methylcholanthrene and beta-naphthoflavone and 2,3,7,8-Tetrachlorodibenzo-p-dioxin (TCDD). Chronic exposure of humans to inorganic arsenical compounds is associated with liver injury, peripheral neuropathy, and an increased incidence of cancer of the lung, skin, bladder, and liver. Arsenic contamination of drinking water is

a serious environmental problem worldwide [8]. Arsenic induced ROS in cells has been described by several authors using 2',7'-dichlorodihydrofluorescein diacetate (DCF-DA) [9,10] and ESR spin trapping [8] methods.

Polycyclic aromatic hydrocarbons (PAH) are widely distributed environmental pollutants generated from incomplete combustion of industrial waste, automobile exhaust, cigarette smoke, and various cooked foods [11], and are known to cause oxidative stress. Oxidative DNA damage caused by PAHs appears to be through induction of CYP1A1. CYP1A1 belongs to a family of enzymes (Cytochrome p450) responsible for metabolism of diverse array compounds including xenobiotics and environmental pollutants. All of the CYP1 family are transcriptionally controlled by the aryl hydrocarbon receptor (AhR). The AhR occurs in the cytoplasm of most vertebrate cells, it has a rather promiscuous binding pocket and binds a structurally diverse range of chemicals. Upon binding of a ligand to the receptor, the complex (ligand/AhR) migrates into the nucleus where it binds to the AhR nuclear translocator protein (ARNT). AhR and ARNT function together as a heterodimer and bind to the xenobiotic response elements (XRE) on the 5-prime promotor regions of *CYP1* genes. Induction of CYP1A1 leads to a leak in reactive oxygen species [12,13].

Exposure of Human hepatoma (HepG2) and HeLa cells expressing cytoplasmic roGFP2-FA to the five environmental toxicants yielded mixed results. Results for arsenic confirmed the findings of ROS detected by DCF-DA and ESR trapping [9,10]. Arsenic was found to elevate excitation ratios of roGFP2-FA. Both cell types tested responded similarly. Benzo[α]pyrene treated cells were found to fluoresce brightly following excitation at 400nm, which interfered with the excitation wavelengths of roGFP2-FA. 3-methylcholanthrene was effective at the highest

concentrations in both cell types, whereas β-naphthoflavone, an Ah receptor antagonist, did not cause any significant increase at any dose for either cell type. These latter results differs from those of Elbekai et al. [14] where BαP and β-NF but not 3-methylcholanthrene, significantly increased H_2O_2 production in Hepa 1C1C7 cells. Dioxin induced a moderate increases but only in HeLa cells and only at 100nM. Knerr et al. [13] also found HepG2 cells to be unresponsive to dioxin but detected dioxin induced ROS was detected in rat primary hepatocytes. Excitation ratio increases observed for arsenic and 3-MC confirm that exposure to these toxicants put cells are under oxidative stress and suggest that at higher concentrations of TCDD may act likewise.

Lastly the potential for clamping roGFP2-FA in a particular redox state using formaldehyde was investigated. Formaldehyde is best known for fixation of cell tissues but is also used in inactivate toxicants, and viruses for vaccines, isotope labeling of proteins, and studying protein-protein interactions [15]. Formaldehyde reacts primarily with amino and thiol groups of proteins forming methylol derivatives, Schiff bases and methylene bridges. Exposure of roGFP2 and roGFP2-FA to formaldehyde prevented any subsequent oxidation of roGFP2-FA but was only partially efficacious in preventing roGFP2 from further oxidation. For roGFGP2-FA this may be due to a more rapid reaction of the thiolate promoted by the positive charges of nearby lysines (positions 223 and 206). Alternatively formaldehyde may react with the primary amines of lysine and cysteine thiol to form a Schiff base analogous to thiazolidine formation found in free cysteine [16,17]. Cysteine containing peptides treated with formaldehyde have been shown to crosslink to the side chain of arginine [15]. Mass spectral comparison of the redox proteins before and after formaldehyde treatment

should indicate whether the lysine and/or cysteines are bridged. Prolonged exposure of the roGFP proteins to formaldehyde caused severe quenching of fluorescence. Since we did not wish to use formaldehyde in concentrations normally used to fix tissue, we investigated the effects of formaldehyde in the presence of lipoate buffer. Longer exposures to formaldehyde were possible although some minor quenching remained. RoGFP2-FA equilibrated with in lipoate buffer was partially oxidized, maximal oxidation was prevented by incubation with formaldehyde. Maximal reduction by DTT was also inhibited but in this case, DTT should at least have been able to reduce the disulfides formed before exposure to formaldehyde.

Three new applications for redox sensitive GFPs have been explored, all three exhibited promising results and warrant further exploration.

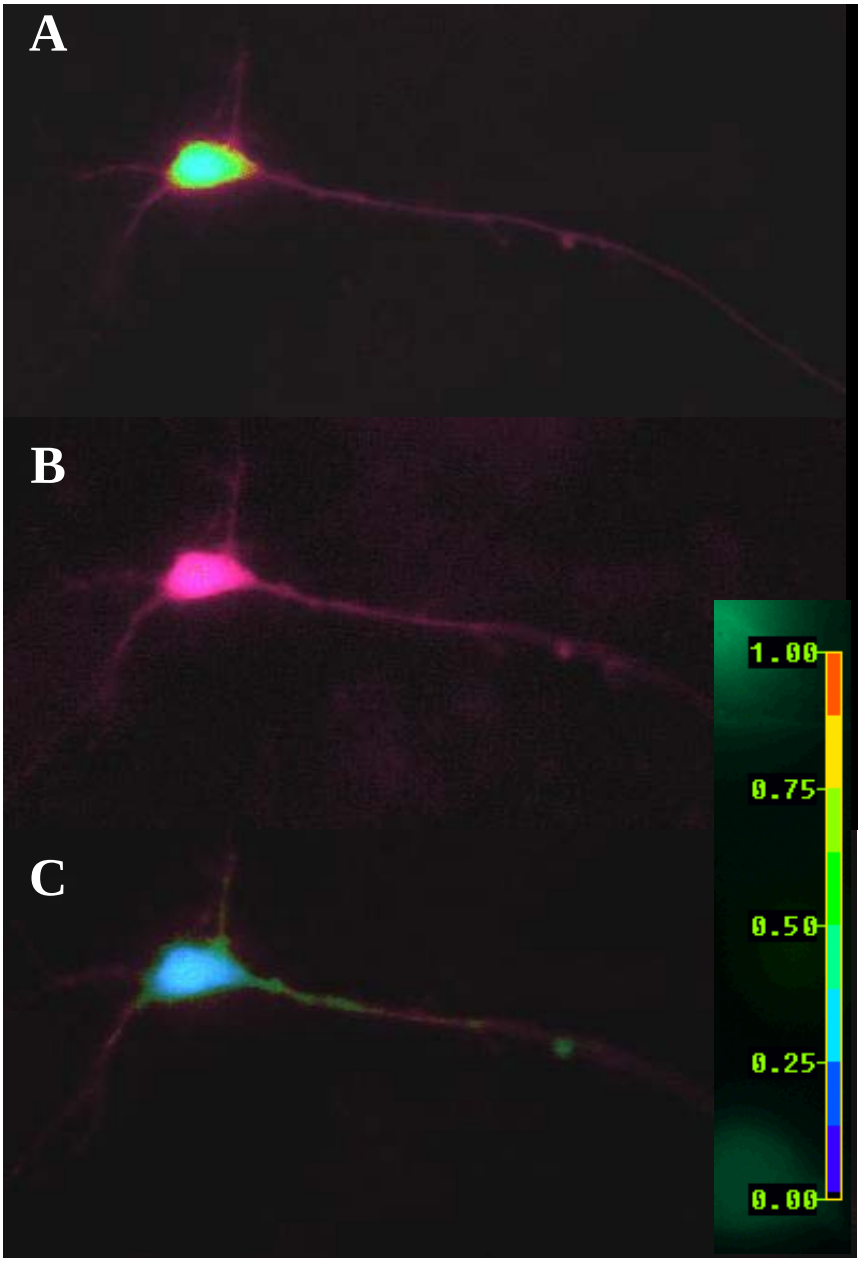

Figure 2.1. Expression of roGFP2-FA in rat cerebellar neurons. A. Pseudo-colored image for basal excitation ratio. B. Cell treated with 200 μM Aldrithiol. C. Cell treated with 10mM DTT.

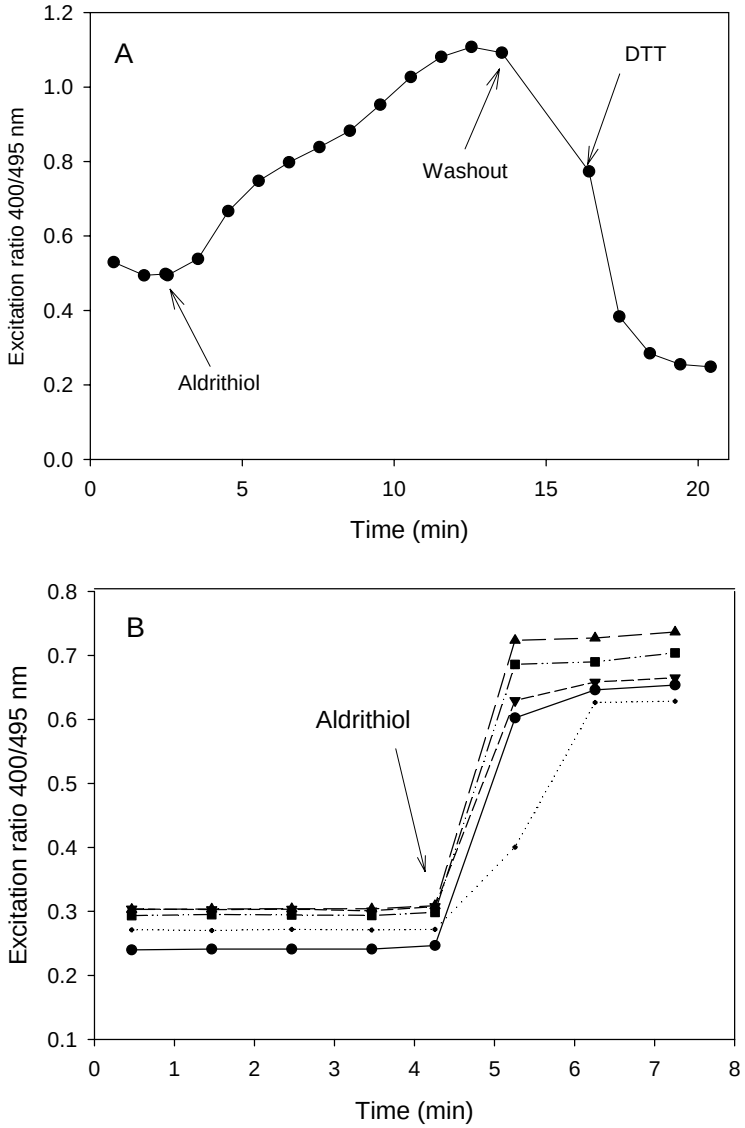

Figure 2.2. A. Oxidation and reduction of roGFP2-FA in rat cerebellar neuron, oxidation was induced by 200 μM Aldrithiol, when oxidation had reached a plateau removal of oxidant was sufficient to observe reduction, maximal reduction was achieved by the addition of 1mM DTT. B. Oxidation of roGFP-2A in NR6 cells using 200 μM Aldrithiol.

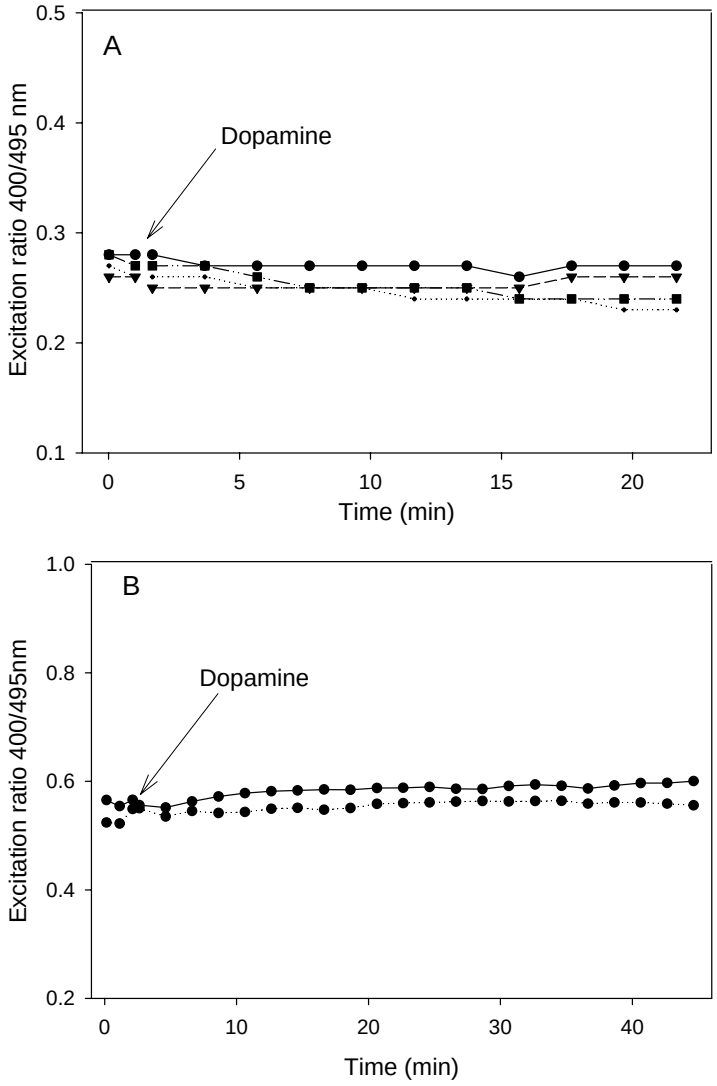

Figure 2.3. A. PC12 cells expressing roGFP2-FA exhibit no reaction to dopamine (1mM). B. PC12 cells expressing roGFP2-Sec147 do not respond to exogenous dopamine (1mM). Cells were transfected 48 hours prior to the experiment, those roGFP2-Sec147 were supplemented with 1μM Sodium selenite for 24 hours. Cells were maintained at 37^{o}C throughout imaging.

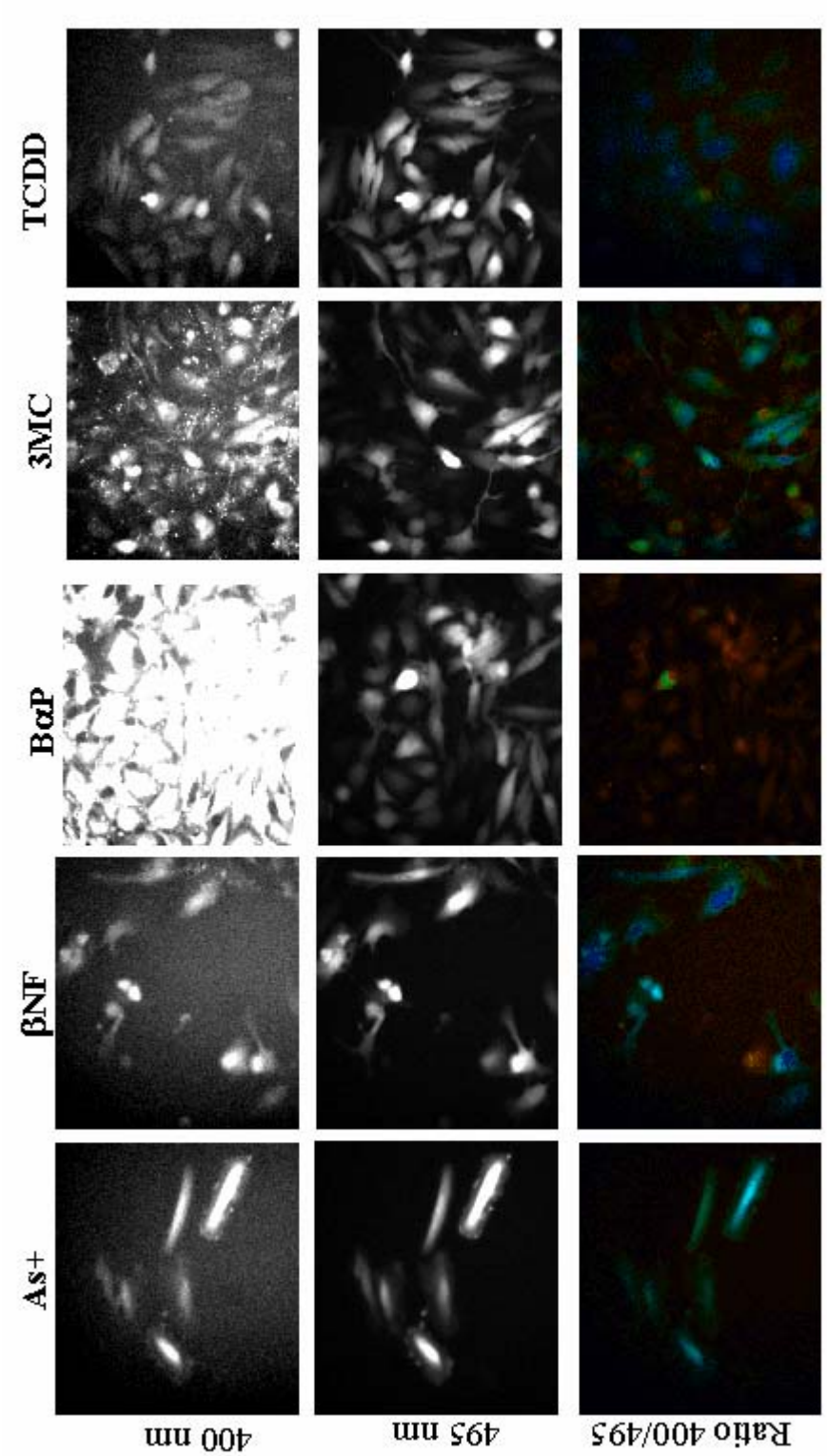

Figure 2. 4. Images of HeLa cells expressing roGFP2-FA treated with toxicant for 24hours. Upper panel fluorescence image obtained following excitation at 400nm. Middle panel fluorescence image obtained following excitation at 495 nm. Lower panel ratio of excitation images (400/495), the images are pseudo colored. Abbreviations for toxicants: Arsenic (As), β-naphthoflavone (β-NF), Benzo(α)pyrene (BαP) , 3-methylcholanthrene (3MC), and dioxin (TCDD).

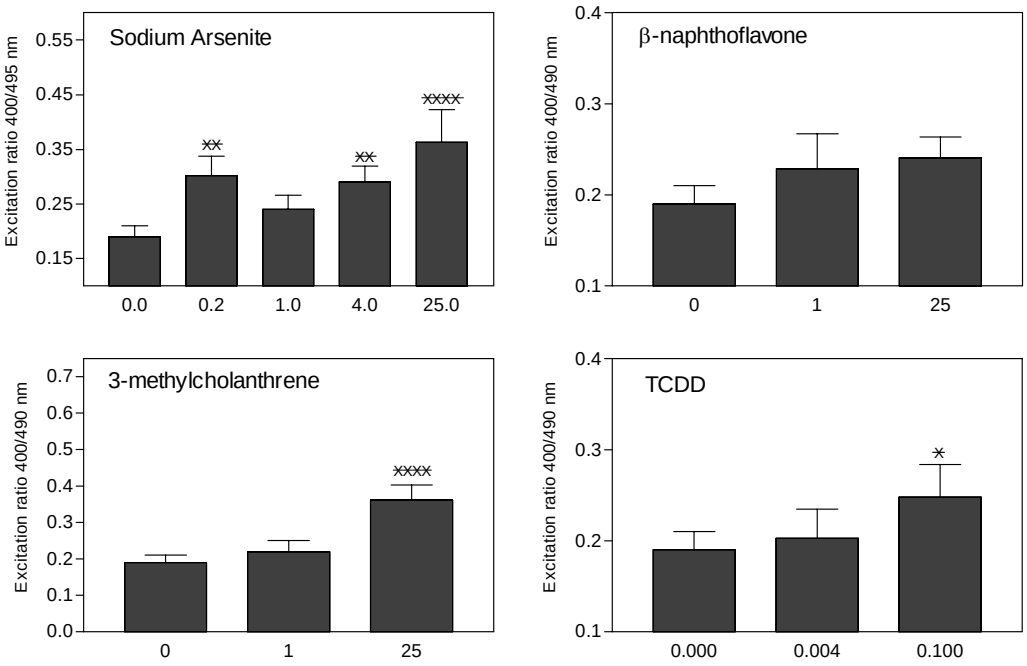

Figure 2.5. HeLa cells expressing roGFP2-FA exposed to environmental toxins. Cells were transfected 48 hours prior to the experiment; media was supplemented with toxin 24 hours prior to imaging. Concentrations (μM) of toxin are given beneath individual bars. Bars found to be significantly increased over that of the starting ratio are as indicated ****, p<0.001, ***, p < 0.005; **, p < 0.01; * p < 0.05.

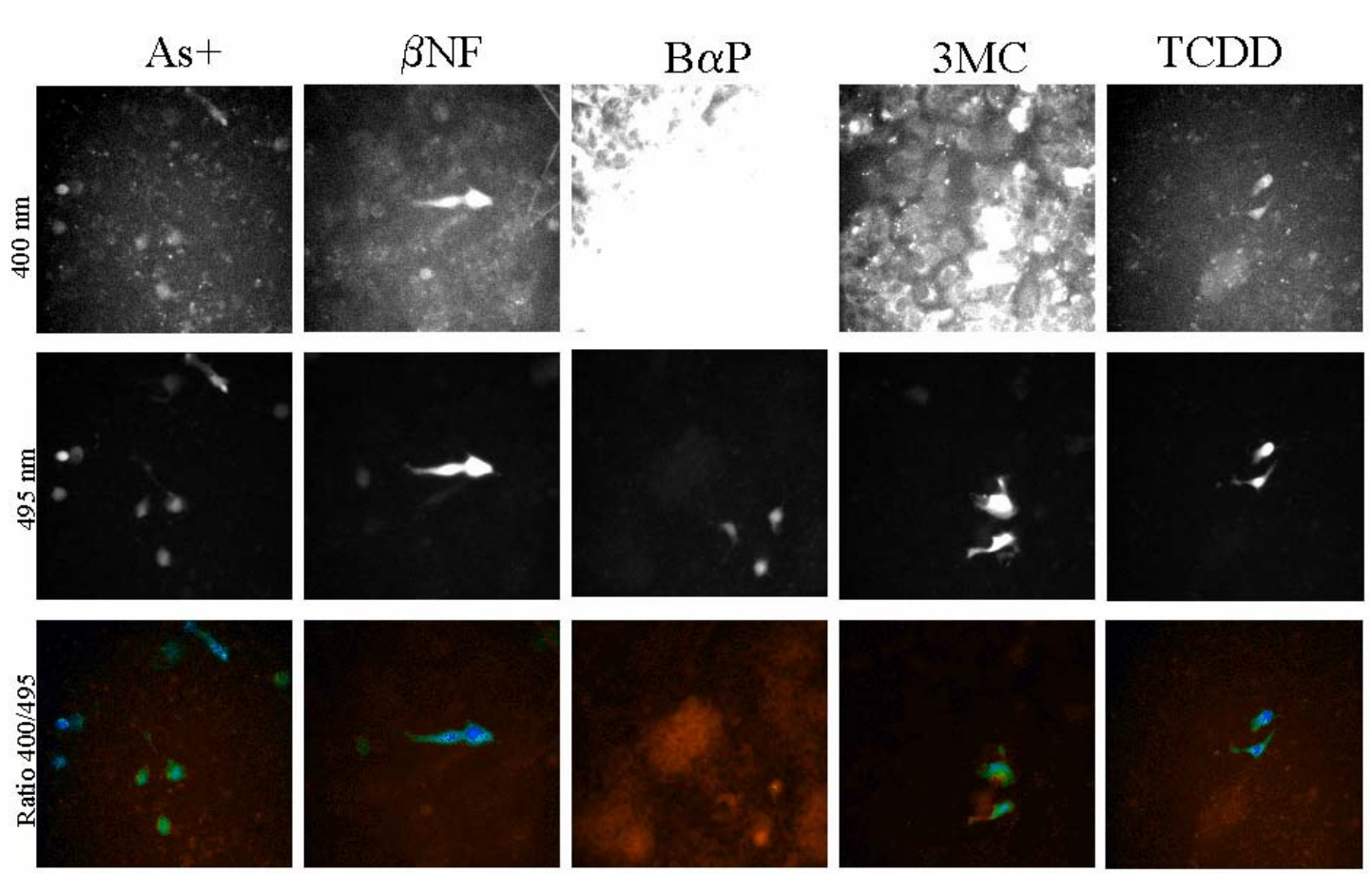

Figure 2. 6. Images of HepG2 cells expressing roGFP2-FA treated with toxin for 24hours. Upper panel fluorescence image obtained following excitation at 400nm. Middle panel fluorescence image obtained following excitation at 495 nm. Lower panel ratio of excitation images (400/495), the images are pseudo colored. Abbreviations for toxins: Arsenic (As), β-naphthoflavone (β-NF), Benzo(α)pyrene (BαP) , 3-methylcholanthrene (3MC), and dioxin (TCDD).

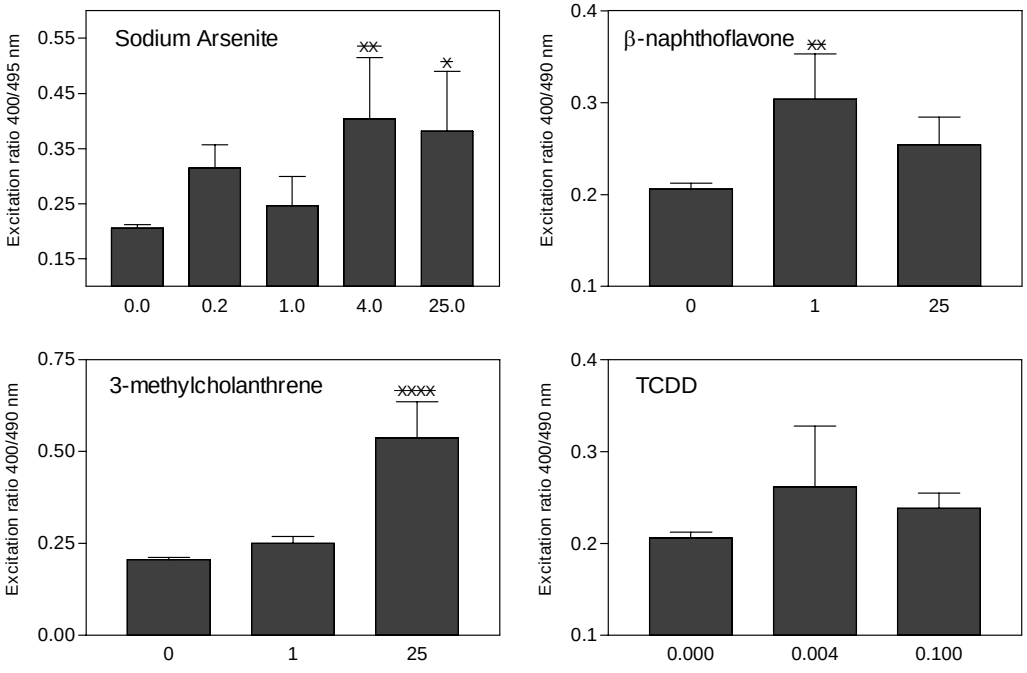

Figure 2.7. HepG2 cells expressing roGFP2-FA exposed to environmental toxins. Cells were transfected 48 hours prior to the experiment, media was supplemented with toxin 24 hours prior to imaging. Concentrations (μM) of toxin are given beneath individual bars. Bars found to be significantly increased over that of the starting ratio are as indicated ****, $p<0.001$, ***, $p < 0.005$; **, $p < 0.01$; * $p < 0.05$.

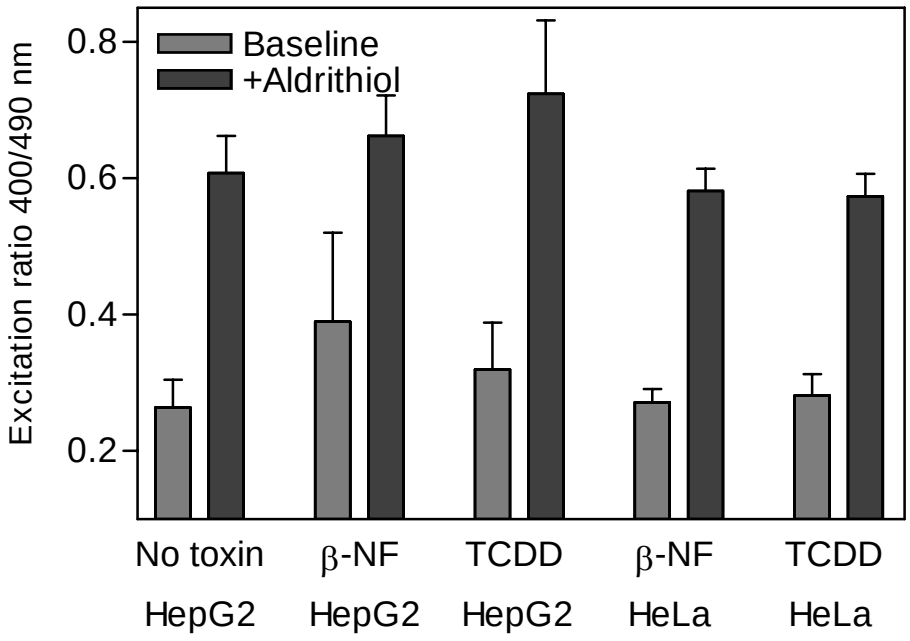

Figure 2.8. Oxidation of HepG2 and HeLa cells expressing roGFP2-FA exposed to environmental toxins. Cells were transfected 48 hours prior to the experiment, media was supplemented with toxin 24 hours prior to imaging, no significant change in excitation ratio was observed. Upon addition of aldrithiol (200μM) excitation ratios were found to increase to levels obtained for untreated cells

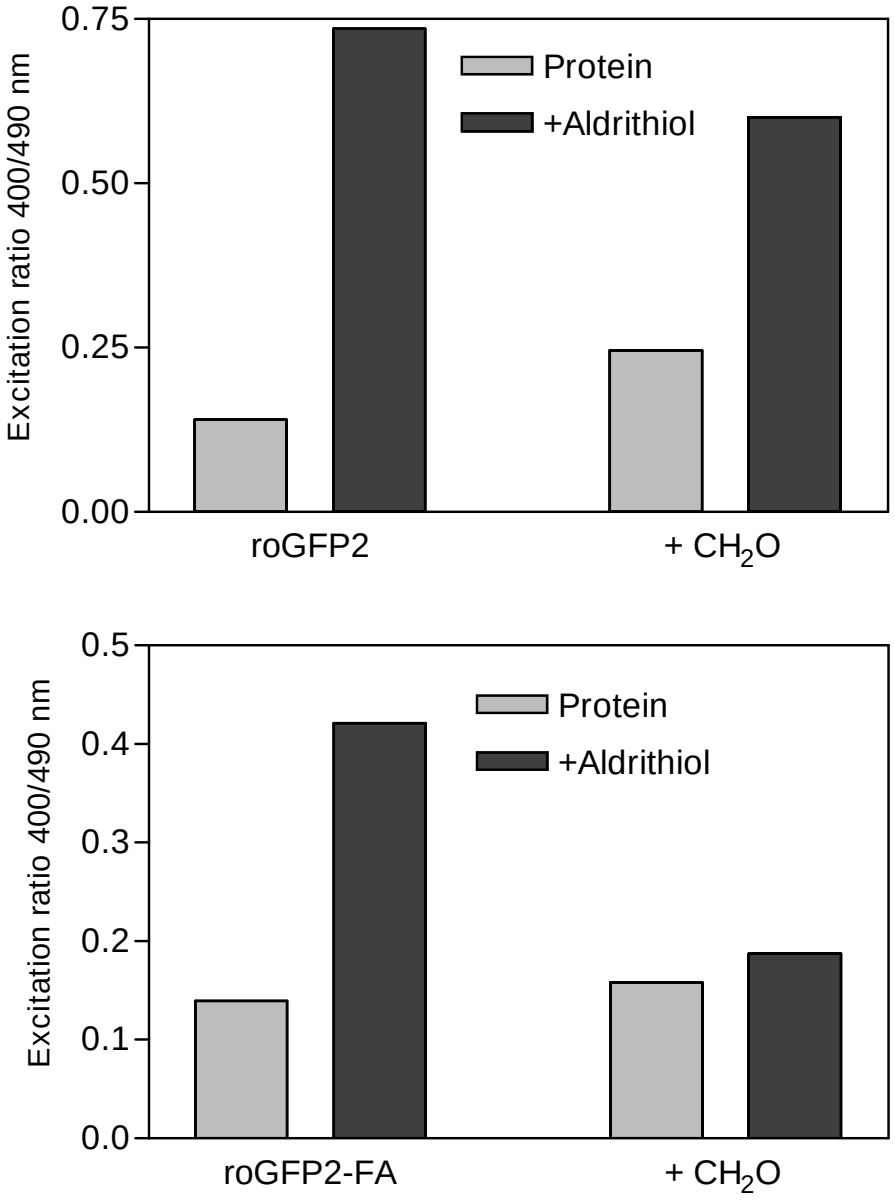

Figure 2.9. Inhibition of oxidation of roGFP2 and roGFP2-FA by formaldehyde. The proteins in their reduced form were co-incubated with 1% formaldehyde for 5 minutes in PBS buffer. Oxidation was induced by the addition of 200μM Aldrithiol.

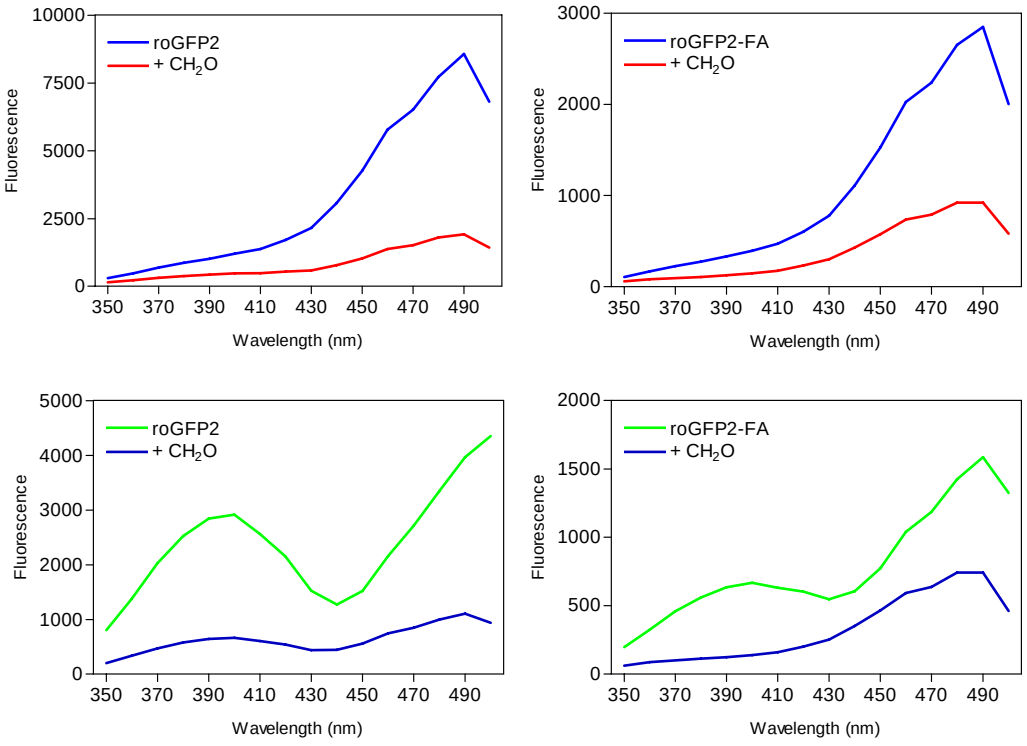

Figure 2.10 Quenching of roGFP2 and roGFP2-FA by formaldehyde. The proteins (1μM) reduced and oxidized were incubated in the presence of 1% formaldehyde for 1 hour. Excitation spectra for reduced protein, reduced protein incubated with formaldehyde, oxidized protein and oxidized protein incubated with formaldehyde.

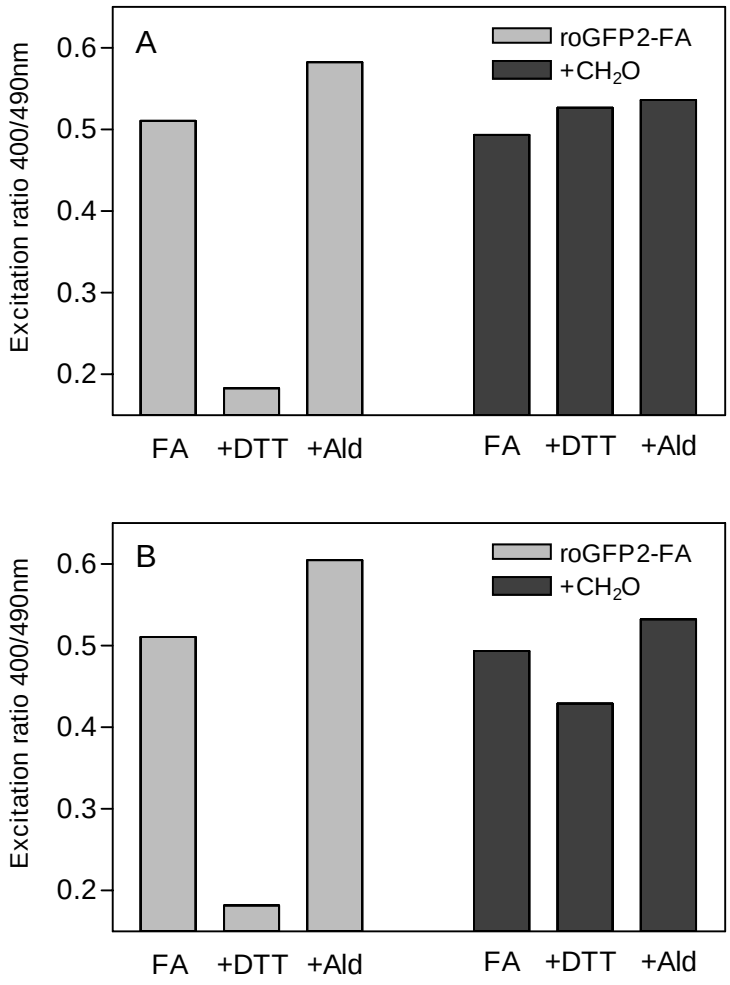

Figure 2.11. Inhibition of oxidation/reduction of roGFP2-FA by formaldehyde in lipoate buffer. RoGFP2-FA was equilibrated in a 10mM lipoate buffer (50/50 oxidized:reduced lipoate) for 1 hour at 37^{o}C. A second 1 hour incubation followed in the presence of 1% formaldehyde or PBS buffer. Proteins were oxidized by aldrithiol (200μM) or reduced using DTT (10mM). A) Excitation ratios for proteins in the presence of oxidant or reductant for 5 minutes B. Excitation ratios for proteins in the presence of oxidant or reductant for 60 minutes.

F. References

1. Kim JR, Yoon HW, Kwon KS, Lee SR, Rhee SG. Identification of proteins containing cysteine residues that are sensitive to oxidation by hydrogen peroxide at neutral pH. Anal Biochem 2000;283:214-221.

2. Dooley CT, Dore TM, Hanson GT, Jackson WC, Remington SJ, Tsien RY. Imaging dynamic redox changes in mammalian cells with green fluorescent protein indicators. J Biol Chem 2004;279:22284-22293.

3. Cannon MB, Remington SJ. Re-engineering redox-sensitive green fluorescent protein for improved response rate. Protein Sci 2006;15:45-57.

4. Hansen RE, Ostergaard H, Winther JR. Increasing the reactivity of an artificial dithiol-disulfide pair through modification of the electrostatic milieu. Biochemistry 2005;44:5899-5906.

5. Kim JR, Kwon KS, Yoon HW, Lee SR, Rhee SG. Oxidation of proteinaceous cysteine residues by dopamine-derived H2O2 in PC12 cells. Arch Biochem Biophys 2002;397:414-423.

6. Cohen G, Farooqui R, Kesler N. Parkinson disease: a new link between monoamine oxidase and mitochondrial electron flow. Proc Natl Acad Sci U S A 1997;94:4890-4894.

7. Belousov VV, Fradkov AF, Lukyanov KA, Staroverov DB, Shakhbazov KS, Terskikh AV, Lukyanov S. Genetically encoded fluorescent indicator for intracellular hydrogen peroxide. Nat Methods 2006;3:281-286.

8. Liu SX, Athar M, Lippai I, Waldren C, Hei TK. Induction of oxyradicals by arsenic: implication for mechanism of genotoxicity. Proc Natl Acad Sci U S A 2001;98:1643-1648.

9. Kitchin KT, Ahmad S. Oxidative stress as a possible mode of action for arsenic carcinogenesis. Toxicol Lett 2003;137:3-13.

10. Sun X, Li B, Li X, Wang Y, Xu Y, Jin Y, Piao F, Sun G. Effects of sodium arsenite on catalase activity, gene and protein expression in HaCaT cells. Toxicol In Vitro 2006.

11. Cherng SH, Hsu SL, Yang JL, Yu CT, Lee H. Suppressive effect of 1-nitropyrene on benzo[a]pyrene-induced CYP1A1 protein expression in HepG2 cells. Toxicol Lett 2006;161:236-243.

12. Park JY, Shigenaga MK, Ames BN. Induction of cytochrome P4501A1 by 2,3,7,8-tetrachlorodibenzo-p-dioxin or indolo(3,2-b)carbazole is associated with oxidative DNA damage. Proc Natl Acad Sci U S A 1996;93:2322-2327.

13. Knerr S, Schaefer J, Both S, Mally A, Dekant W, Schrenk D. 2,3,7,8-Tetrachlorodibenzo-p-dioxin induced cytochrome P450s alter the formation of reactive oxygen species in liver cells. Mol Nutr Food Res 2006;50:378-384.

14. Elbekai RH, Korashy HM, Wills K, Gharavi N, El Kadi AO. Benzo[a]pyrene, 3-methylcholanthrene and beta-naphthoflavone induce oxidative stress in hepatoma hepa 1c1c7 Cells by an AHR-dependent pathway. Free Radic Res 2004;38:1191-1200.

15. Metz B, Kersten GF, Hoogerhout P, Brugghe HF, Timmermans HA, de Jong A, Meiring H, ten Hove J, Hennink WE, Crommelin DJ, Jiskoot W. Identification of formaldehyde-induced modifications in proteins: reactions with model peptides. J Biol Chem 2004;279:6235-6243.

16. Huang TC, Huang LZ, Ho CT. Mechanistic Studies on Thiazolidine Formation in Aldehyde/Cysteamine Model Systems. J Agric Food Chem 1998;46:224-227.

17. Kallen RG. The Mechanism of Reactions Involving Schiff Base Intermediates,Thiazolidine Formation from L-Cysteine and Formaldehyde. J Am Chem Soc 1971;93:6236-6248.

Chapter Three

Green Fluorescent Protein Redox Indicator Employing Selenocysteine-cysteine Pair as Redox Sensor

A. Introduction

The twenty-first naturally occurring amino acid, selenocysteine (Sec) is the first addition to the genetic code to be discovered [1]. Only a small number of proteins are known to incorporate Sec. These include oxidoreductases such as glutathione peroxidase, thioredoxin reductase, bacterial formate dehydrogenase, phospholipid hydroperoxide and type I iodothyronine 5'-deiodinase. SelR and SelM until recently were two orphan selenoproteins, SelR has been identified as a methionine sulfoxide reductase [2] and SelM belongs to a new thioredoxin-like family [3,4]. All the aforementioned proteins contain a single Sec but selenoprotein P contains multiple copies (7-10). While its precise role has not been determined it is considered to be an antioxidant [1]. Selenocysteine is structurally identical to cysteine except selenium replaces sulphur. At physiological pH Sec is more fully ionized than the thiol group of Cys due to a lower pKa value (5.2) as compared to that of Cys (pKa = 8.3). Like for other amino acids the body produces a specific tRNA for Sec incorporation into proteins [5]. It is an unusual amino acid in that further translation components are required for its expression in proteins. Selenocysteine tRNA serves both as a mode of transfer to the protein by recognition of its codon and as a scaffold for the biosynthesis of Sec. It is first charged with a serine by seryl-tRNA synthase and then converted to Sec-tRNA by selenocysteine synthase [1,6]. Expression of Sec in proteins

requires not only its specific tRNA but also the presence of a Selenocysteine Insertion Sequence (SECIS, also known as the selenium translation element) downstream of the open reading frame, in the 3'untranslated region (3'UTR) [7-9]. All selenoproteins incorporate the Sec at a specific codon, (UGA, opal), which normally functions as a stop codon. Use of UGA/TGA as a Sec codon does not prevent use of UGA as a stop codon elsewhere in the same organism [6].

Bacterial expression of Sec proteins requires four genes SelA which encodes selenocysteine synthase, SelB a selenocysteine specific elongation factor [10], SelC the specific tRNA and SelD the selenophosphate synthethase which forms selenophosphate from ATP and reduced selenium [11]. A quaternary complex is formed when SelB recognizes the Sec-tRNA, GTP and the SECIS element, which can then interact with the ribosome. The SECIS element in bacteria immediately follows the stop codon [12,13] (see figure 3.1.A.) The efficiency of incorporation of selenocysteine in bacteria is low about 7-10%. This inefficiency is caused by the slow rate of insertion and by stalling of the ribosome at the UGA codon [11].

A distinction between eukaryote and prokaryote SECIS elements is that in eukaryotes it is not immediately downstream of the UGA codon but in the 3'UTR of the mRNA, up to 4000 base pairs away [1] (see figure 3.1.B). In mammalian cells the presence of a SECIS element allows almost complete flexibility on the position of the UGA codon [7]. There is a minimal spacing requirement of 51-111 nucleotides between the UGA codon and the SECIS element [14], but the upper limit is not known. Although sequences of SECIS elements vary, they all have a conserved stem-loop structure, two helices separated by an internal loop, the conserved sequences include A/GUGA at the 5'base stem; AA in the hairpin loop; and GA at the 3'base of the stem [15].

Additional factors involved are accessory binding proteins which include a specific elongation factor (EFsec), SECIS Binding Protein 2 (SBP2), an RNA binding protein (SECp43) an autoimmune antigen SLA/LP and a ribosomal protein (L30) [16]. The mammalian efficiency of Sec insertion for some selenoproteins are very high, particularly PHGPx expression in the testis, [17]

Many groups are interested in replacing cysteines with selenocysteine. Proteins synthesized with heterologous selenium include Azurin where Sec replaced Cys bound to copper. This protein was synthesized using a ligation method called Expressed Protein Ligation [18]. Several groups have reported use of the bacterial selenoprotein machinery to produce artificial selenoproteins [12,19,20]. Selenopeptides have been expressed on the coat protein of phage [21] employing the SECIS element from formate dehydrogenase of *E.coli*. The first demonstration of incorporation of selenium into a heterologous mammalian protein was by Shen et al. [8]. The SECIS element was shown to be sufficient for incorporation of a Sec at a UGA codon in Rab5b, a GTP-binding protein. The native 3'UTR of Rab5 and the stop codon were replaced with coding sequence for Glutathione peroxidase (GPx. Codon 63 (UGU) which is normally transcribed as cysteine was mutated to UGA. Transfection of the construct in COS1 cells demonstrated that the opal codon and 3'UTR were sufficient to express Sec in a heterologous protein.

In collaboration with Dr. Remington's laboratory (U. Oregon, OR) we have developed redox sensitive GFPs based on cysteine residues close to the chromophore, that allow real time visualization of the oxidation state of the indicator (Chapter One). Ratios of fluorescence from excitation at 400 and 490 nm indicate the extent of oxidation and thus the redox potential while canceling out the amount of

indicator and the absolute optical sensitivity. Because the indicator is genetically encoded, it can be targeted to specific proteins or organelles of interest and expressed in a wide variety of cells and organisms. Cytoplasmic redox GFPs respond to a variety of oxidants, but not to hydrogen peroxide stimulated by growth factors or to exposure to anoxia/hypoxia even under glucose-free media or serum starvation conditions known to sensitize cells to oxidative damage. However roGFPs do detect superoxide generated during the oxidative burst of stimulated macrophages. From our studies with roGFPs it appears that the cells possess a strong mechanism for prohibiting oxidation of the cytoplasm. Unless this method is disabled, small oxidative insults are not detected by our sensors. To detect a chemically significant change in thiol-disulfide redox status the reaction would have to be highly compartmentalized.

We hoped to increase the sensitivity of RoGFPs to oxidation and thereby detect small or localized alterations in redox state of the cell. Harnessing the sensitivity of selenocysteine to oxidation would be one means of optimizing roGFPs. By employing the 3'UTR of glutathione peroxidase and an opal codon at each of the cysteine residues of our redox probes we were able to create selenoGFPs, which did indeed have a greater sensitivity to oxidation.

B. Methods

Construction and Expression of a mammalian vector for roGFP with selenocysteine---Two separate constructs were made the first with Sec replacing Cys147, the second with Sec replacing Cys204. The UGA codon was inserted at either position using Quik-Change reactions (Stratagene,CA) and the following primers:

Sec147 forward: CTGGAGTACAACTACAACTGACACAACGTCTATATCATG

Sec147 reverse: CATGATATAGACGTTGTGTCAGTTGTAGTTGTACTCCAG

Sec204 forward: AACCACTACCTGAGCACCTGATCCGCCCTGAGCAAAGACC

Sec204 reverse: GGTCTTTGCTCAGGGCGGATCAGGTGCTCAGGTAGTGGTT

Both roGFP1 and roGFP2 where used as templates. cDNA obtained from the Quik-change reaction was transformed in *E.coli* (DH5α). SCS110 bacteria were transformed using purified plasmids in order to digest with Xba1, which requires non-methylated DNA. The purified plasmids were digested with BsrG1 and Xba1. The 3'UTR was obtained by PCR from a construct of Glutathione peroxidase in pCMV4 kindly supplied by Dr. Peter Newburger (University of Massachusetts, MA). Primers for the PCR were as follows:

Forward: GAGCTGTACAAGAGCTGGGCCTAGGGCGCCCCTCCTACCCCGGCT

Reverse: GGCACTGGGGAGGGGTCACA

A band of approximately 400 nucleotides was observed on a 1% agarose gel as expected. The PCR product was restricted with BsrG1 and Xba1 and ligated into the pN1 vector containing the UGA-modified GFPs. Correct alignment for the sec147 and Sec204 constructs were confirmed by sequencing in both forward and reverse directions. The plasmids were expanded in *E.coli* (DH5α), purified and expressed in HeLa and Cos7 cells. SBP2 in pCDNA4 was a gift from Peter Copeland (UMDNJ-Robert Wood Johnson Medical School, NJ) and was used as received.

Construction and Expression of a bacterial vector for roGFP with selenocysteine---A quick change reaction on roGFP2-UGA-147 to mutate position 179 Ala-Ser was performed in order to insert a Blp1 restriction site primers; Forward primer:AGGACGGCAGCGTGCAGCTCAGCGACCACTACCAGCA Reverse primer: TGCTGG

TAGTGGTCGCTGAGCTGCACGCTGCCGTCCT. A PCR reaction was used to create the SECIS sequence placing TVAGL at position 151-156. Forward primer: GGGCCCGGGATCCACCGGCCGGCCACCATGGTGAGCAAGGGCGAGGAGCT Reverse primer :ACCTTGATGCCGTTGCTCAGCTTGTCGGCCATGATATAG. The PCR product and vectors (roGFP in pRSET or pBAD) were cut with Nco1 and BsRG1 and ligated.

For bacterial Sec204, roGFP2-UGA-204 was mutated to have Afe1 site at position 216. forward primer: GACCCCAACGAGAAGCGCTATCACATGGTCCTGCTGGAG Reverse primer: CTCCAGCAGGACCATGTGATAGCGCTTCTCGTTGGGGTC A PCR reaction was performed to create the SECIS sequence. Forward primer: GGGCCCGGGATCCACCGGCCGCCACCATGGTGAGCAAGGGCGAGGAGCT. Reverse primer ;ATCTATAGCGCTTGTGCAGACCTGCAACCGTCAGGGCGGATCAGGTGCTCA GGTAGTGGTTGTCGG. The PCR product and vectors (roGFP in pRSET or pBAD) were cut with Nco1 and BsRG1 and ligated

Construction of Epidermal growth factor receptor with C-terminal fusion of Sec147--- The vector for pN1-EGFR-eGFP was provided by Alexander Sorkin (University of Colorado, CO). eGFP at the C terminal was replaced by Sec147 by restriction with SacII and Xba1. Although Sec147 and the EGFR construct were both in the same vector EGFR-eGFP had been inserted using Nhe1 and Xba1 which removed the SacII site form the 5' Multiple Cloning Site.

Fluorescent Imaging---Cells were imaged on a Zeiss Axiovert microscope with a cooled CCD camera (Photometrics, Tucson, AZ) controlled by Metafluor 2.75 software (Universal Imaging, West Chester, PA). Dual excitation ratio imaging used excitation filters 400DF15 and 495DF10 or 480DF20 altered by a filter changer (Lambda 10-2, Sutter Instruments, San Rafael, CA), a 505DRLP dichroic mirror and a single emission filter, 535DF25. Fluorescence images were background-corrected by

manual selection of background regions. Exposure time was 200–1000 ms, and images were taken every minute.

C. Results

Although the redox potential and sensitivity of roGFP is well poised, lack of an oxidation response to physiological stimulus led us to explore new options for monitoring oxidation. The slow response rate in cytoplasm and insensitivity to hydrogen peroxide at low micro-molar concentrations suggested the need for a faster responding sensor. Many of the cells reductive enzymes contain selenocysteine at their active site and as the translational machinery for incorporation of this amino acid has been elucidated, we thought it a good candidate for improving the redox indicators utility. Unlike disulphides, diselenides have not been identified in proteins although the redox potential of selenocysteine-selenocysteine (-488mV) suggest it is possible [22] even so we concentrated on creating cysteine-selenocysteine pairs.

A paper by the Newburger laboratory [8] described the minimal requirements for insertion of selenocysteine into heterologous eukaryotic proteins, we adapted the method for insertion of selenocysteine into our roGFPs. Codons corresponding to positions 147 and 204 of the protein were individually mutated at the opal codon (TGA) for both roGFP1 and roGFP2. The native stop codon of GFP was removed and replaced with nucleotides corresponding to the last three amino acids of Glutathione peroxidase (GPx) and the full length of its 3'UTR including the polyadenylate tail (the vector for GPx was a generous gift from Dr. Newburger).

The four constructs (roGFP1 and 2 with Sec at positions 147 or 204) were expressed in HEK293 cells and media supplemented with 1-5μM sodium selenite (Figure 3.2.A). All four constructs were expressed poorly as compared to roGFP

constructs (which in turn are poorly expressed when compared to GFP). The transfection efficiency was comparable to roGFP but the fluorescence emitted following excitation at both 400 and 495 nm wavelengths was much diminished. For most subsequent experiments the acquisition protocol was altered to increase the fluorescence observed at 490nm peak by using a wider dicroic (480/30). Constructs derived from “wild-type GFP” and possessing Sec at position 147 were the dimmest of the four constructs. Because we worried that a substantial fraction of the fluorescence observed at 400 may be due to auto-fluorescence we did not proceed further with these constructs. Constructs based on “enhanced GFP” were only slightly brighter and in HeK293 cells exhibited distinct excitation ratios whether the selenocysteine was expressed at position 147 or 204 (Figure 3.2.B).

Sec2-147 was tested in five cell lines HEK 293, HeLa, NR6, PC12 and COS7. Expression varied between cell lines (Figure 3.3.A). PC12 cells exhibited the greatest expression of Sec2-147 albeit lower than that usually observed for roGFP2, but transfection efficiency in these cells was generally found to be low ≈30%. HeLa cells expressed the least well under these conditions. HEK293, NR6 and COS7 cells all exhibited intermediate expression. The excitation ratio observed also varied between cell lines with HeLa and Cos7 cells expressing considerably higher excitation ratio than the other three cell lines (Figure 3.3.B). It should be noted that the excitation ratios in all cell lines were much higher than those found for roGFP2 (usually ~0.2).

To confirm selenocysteine incorporation we investigated the dependence of expression of Sec2-147 and Sec-204 upon exogenously applied selenium. Expression of both constructs in COS7 cells was heavily dependant upon added selenium. The average fluorescence at 480nm increased ~5 fold in the presence of

selenium for both constructs (Figure 3.3A) although not shown similar results were observed in HEK293 cells. To determine whether read-through of the stop codon at positions 147 and 204 was contributing to the observed fluorescence, two roGFP mutants were prepared with the UGA codon at either position (Δ3'UTR) but lacking the SECIS element (no 3'UTR). During translation they would be unable to insert Sec. Read-through of the stop codon would result in a serine replacement at either position and resulting proteins would fluoresce. As shown in Figure 3.4 A and B, there does not appear to be any read through of the UGA codon as only auto-fluorescence was observed. Thus we are confident that the fluorescence we observe for our original constructs is due to a selenocysteine protein.

Transfection conditions usually saturate the cell's Sec insertion machinery, so truncated protein is expected even in the presence of a SECIS element [23]. Low expression of the Sec constructs was a concern and several attempts were made to optimize them. We found that addition of sodium selenite for the first 24 hours following transfection followed by an additional 24 hours growth in fresh media lacking selenium improved expression slightly, and increased expression in HeLa cells to that of HEK293 and COS7 cells. Insertion of selenocysteine requires several accessory proteins, including Selenocysteine Binding Protein 2 (SBP2) analogous to the SelB in bacteria and co-expression of this protein can increase the levels of transiently expressed selenoproteins [17]. We tried co-expressing SBP2 (kindly provided by Dr. P. Copeland) with both Sec2-147 and Sec2-204 in Hek293, HeLa and Cos7 cells, results for HeLa cells are given in Figure 3.5. None of the cells lines exhibited dramatic improvement in expression with SBP2 with a maximum of 20% increase in expression observed.

The constructs were tested for sensitivity to low micro-molar concentrations of hydrogen peroxide. We chose to test 20μM hydrogen peroxide a concentration we knew from previous studies not to induce changes in excitation ratio for cytoplasmic roGFP2. Although the basal excitation ratios for Sec GFPs are consistently higher than those found for GFPs, we observed a rapid change in excitation upon addition of hydrogen peroxide (Figure 3.6). The excitation ratio returned to baseline upon washout of the peroxide. However the extent of excitation ratio increase was small, barely 0.2 units as compared to 0.6-0.8 for a maximal reaction of roGFP2. Increasing the concentration of hydrogen peroxide to 100μM did not increase the maximal excitation ratio (Figure 3.7.A) nor did application of 200μM Aldrithiol a stronger oxidant (Figure 3.7.B).

The high basal excitation ratio exhibited by the selenoGFPs was not altered by addition of strong reducing agents such as dithiothreitol (DTT). To investigate whether selenocysteines on the SecGFPs were partially or fully oxidized in the cytoplasmic milieu, we used a more powerful reductant tributyl phosphine (Bu_3P). Millimolar concentrations were found to lower the excitation ratio (Figure 3.7). Changes in ratio were due to increases in emission following excitation at 480 nm and small decreases for 400nm excitation, consistent with reduction of selenide-sulfide bonds of roGFP. Washing out of Bu_3P followed by addition of oxidants yielded small excitation ratio increases, but as Bu_3P is organic and hydrophobic, it might not be easily removed.

Once we had demonstrated improved sensitivity to hydrogen peroxide over the redox GFPs, we next focused on detecting physiological generation of hydrogen peroxide by epidermal growth factor (EGF) [24]. Sec2-147 was expressed in NR6 cells

and supplemented with selenium for 24 hours; the cells were then incubated in media lacking FBS for an additional 24 hours. NR6 cells, which endogenously express high levels of the EGF receptor, were exposed to EGF (8nM) for up to twenty minutes without any change of excitation ratio being observed (Figure 3.9.A). To investigate whether redox perturbations generated by EGF are localized a fusion construct of EGFR and sec2-147 was synthesized. Expression of the fusion construct in NR6 cells was on the membrane as expected, and although expression was poor it was not much poorer than that of the roGFP-EGFR fusion. Stimulation with EGF once again failed to generate changes in excitation ratio of the SecGFP (Figure 3.9.B).

While positions 147 and 204 were considered optimal for the roGFPs they were only one of six originally described by Hanson et al. [25], placing cysteines at positions 149 and 202 also generated a ratiometric probes (roGFP3 and 4 [25]) and similar redox probes based on YFP cysteines at the same positions has also been described [26]. We prepared a roGFP4 mutant with Sec at position 149 and tested it for sensitivity to hydrogen peroxide. The expression levels in COS7 cells were similar to those of the previous constructs, however there was no reaction to the addition of 20μM hydrogen peroxide as seen for Sec2-147 (Figure 3.10).

We noted a difference in behavior for the Sec GFPs derived from roGFP1. When pre-exposed to 400nm light, they were found to exhibit increased fluorescence emission following excitation at 480nm and a slight decrease in emission fluorescence following excitation at 400 nm i.e. exposure to 400nm light produced a increase in excitation ratio (480/400). Although the ratio increases following 10-30 second bouts of illumination were small they were additive (Figure 3.11.A). In the course of preparing Sec4-149 we also prepared a mutant with cysteine at position

149 and selenocysteine at position 204. Expression levels of this mutant in Cos7 cells was similar for other mutants however upon addition of 100μM hydrogen peroxide the excitation ratio was observed to increase, caused by increased emission following 480nm excitation (Figure 3.11.B).

Many attempts were made to purify the SecGFPs from cells, but this was made difficult by the low expression and a tendency of the stable cell lines to stop producing fluorescent protein. Other difficulties included alteration in behavior of the Sec2-204 construct when an N-terminal histidine tag was included for nickel purification. We were never able to produce enough protein for *in vitro* studies or to demonstrate the presence of selenocysteine by mass spectral analysis. An alternative approach was attempted in which we attempted to harness the bacterial Sec insertion machinery for expression of the protein in *E.coli*. This proved to be difficult since the SECIS element in bacteria immediately follow that of the stop codon [12,13] (see Figure 3.1). Following the method described by Bar-Noy and Moskovitz [27] who were successful in expressing a mammalian methionine sulfoxide reductase in *E.coli*, we incorporated into roGFP the minimal requirements described; the SECIS element (the loop region and conserved distance from UGA to loop) of Formate dehydrogenase H [28]. For bacterial Sec147 the SECIS loop (GGUUGCAGGUCUGCACC) was incorporated 11 nucleotides away from the UGA codon at position 147, positions 151-156 (YIMADK) were mutated to (TVAGLH). For Sec204 mutation of positions 208-212 (SKDPNE) were mutated to (TVAGLH), Asp at 216 was mutated to Tyr for ease of insertion of the PCR product. Since a 3'UTR is not required for prokaryotic translation the natural stop codon for GFP was reintroduced. Mutants were generated in which the amino acids required for the

SECIS element were introduced to the GFP constructs, we had predicted that fluorescent forms of the protein would occur since most of the amino acids were loops of the GFP β-barrel (Figure 12). However fluorescent proteins were not observed following expression in E.coli (JM109) with induction with IPTG or LMG194 with induction by arabinose. The constructs were fused to the 3'UTR of GPx and expressed in COS7 cells, again no fluorescence was observed.

D. Discussion

Using reversible ratiometric redox GFP we had found that cells possess a strong mechanism for maintaining a reducing environment in the cytoplasm, which was not overcome by physiological means of generating reactive oxygen species. We anticipated that having a greater propensity to oxidize incorporation of selenocysteine would increase the sensitivity of Redox GFPs. We hoped the new sensors would be able to overcome the cells reductive machinery enough to detect small or localized alterations in redox state of the cell. The minimal requirements for insertion of selenocysteine into mammalian proteins were first described for rab5b by Shen et al. [8] we adapted the method for insertion of selenocysteine into roGFP. Codons corresponding to positions 147 and 204 of the protein were individually mutated to the opal codon (TGA) for both roGFP1 and roGFP2. Nucleotides corresponding to the stop codon of the GFP were replaced with those of Glutathione peroxidase (GPx) and the full length of the enzyme's 3'UTR including the polyadenylate tail. Glutathione peroxidase is a tetrameric enzyme that metabolizes hydrogen peroxide and many organic peroxides [29,30].

Expression of the constructs was poor is all cell types tested and although some improvements were made by optimizing the length of exposure to sodium

selenite and co-expression with an accessory protein SBP2 the fluorescence of these proteins remained too dim to be truly useful. Replacing cysteine with selenocysteine in another redox GFPs (roGFP4) did not yield a redox sensitive protein but was equally dim. We are confident the fluorescence observed is due to the selenocysteinyl-GFP and were able to demonstrate a sharp dependence of fluorescence on supplemented selenium. Furthermore since green fluorescent proteins have been used as markers for UGA read through [3], the roGFP constructs have an innate monitoring system. Positions 147 and 204 were mutated to UGA in constructs lacking SECIS elements, these constructs were found not to exhibit any fluorescence, indicating that for our proteins read through of the UGA stop codon is minimal. Read through has been observed however for other proteins [31].

SecGFPs were indeed found to be more sensitive to hydrogen peroxide, and detected concentrations of exogenous peroxide that redox GFPs could not, however the dynamic range of the sensors appeared to be much diminished oxidation only resulted in an excitation ratio change of 0.2 units as compared to 0.6 –0.8 for roGFP. In most cells Sec147 exhibited a higher basal excitation ratio (~0.5) than roGFP (~0.2) examination of the effect of reductants on the sensor determined that a strong reductant like DTT was insufficient to fully reduce the protein. Peptides containing selenocysteine and diselenide can have redox potentials below that of DTT (-326mV) [32]. Tributylphosphine a stronger reductant was capable of reducing the protein to levels observed for roGFP. We believe the dynamic range of SecGFP is similar to roGFP but the sensitivity to oxidation and perhaps an inability of the cell to fully reduce the proteins results in elevated basal ratios and small responses to oxidants.

It is unfortunate that we were unable to produce enough protein to confirm these findings *in vitro*.

Although we were successful in improving the sensitivity to hydrogen peroxide, we found that SecGFPs could not detect hydrogen peroxide produced by EGF. An attempt was made to determine whether hydrogen peroxide induced by EGF stimulated is localized, by targeting the sensor to the epidermal growth factor receptor, it failed to generate a response (data not shown). We are now more confident peroxide production by growth factor stimulation does not in fact disturb the overall thiol-disulfide redox equilibrium of the cell. This is highlighted by a recent report of a redox sensor [33] capable of detecting cellular H_2O_2 production, in this sensor the sensing cysteine is buried within the protein and not accessible to the cells reduction machinery (see chapter 2). Excitation ratios for Sec147 in cells starved of FBS were low, which while contrary to or theory that serum starvation causes oxidative stress, supports our theory that the elevated basal ratios observed in other experiments, are due to cellular oxidation and not limitations of the probes dynamic range.

A phenomenon observed for some SecGFP constructs but not roGFPs was an increased excitation ratio in response to prolonged illumination at 400nm in the case of roGFP1Sec 147 or in response to hydrogen peroxide for roGFP4-Ser 202Sec204. The former is likely explained by fluorescent and non-fluorescent states of GFP, transitions between these states can reveal themselves as blinking or photobleaching of the emission [34]. Dickson et al. [35] first described such photo-conversion in yellow fluorescent protein. In GFP UV illumination causes a proton transfer from the neutral chromophore to the glutamate residue at position 222,

photoisomerization results in an increase in absorbance at 475 and concomitant decrease at 395nm. The reaction of roGFP4-Ser 202Sec204 may be more akin to excitation ratio changes observed for singlet oxygen sensors (see chapter four).

The selenocysteine redox sensors would need to be further optimized for fluorescence emission before they could have general utility. New GFPs have been described as having super folding capabilities[37] perhaps these mutations in conjunction with the selenocysteine insertion machinery would improve brightness. Improved expression would allow purification for mass spectral analysis and *in vitro* spectral studies on the protein. Only when the proteins are bright enough to be useful would the basal excitation ratio be taken under consideration.

.

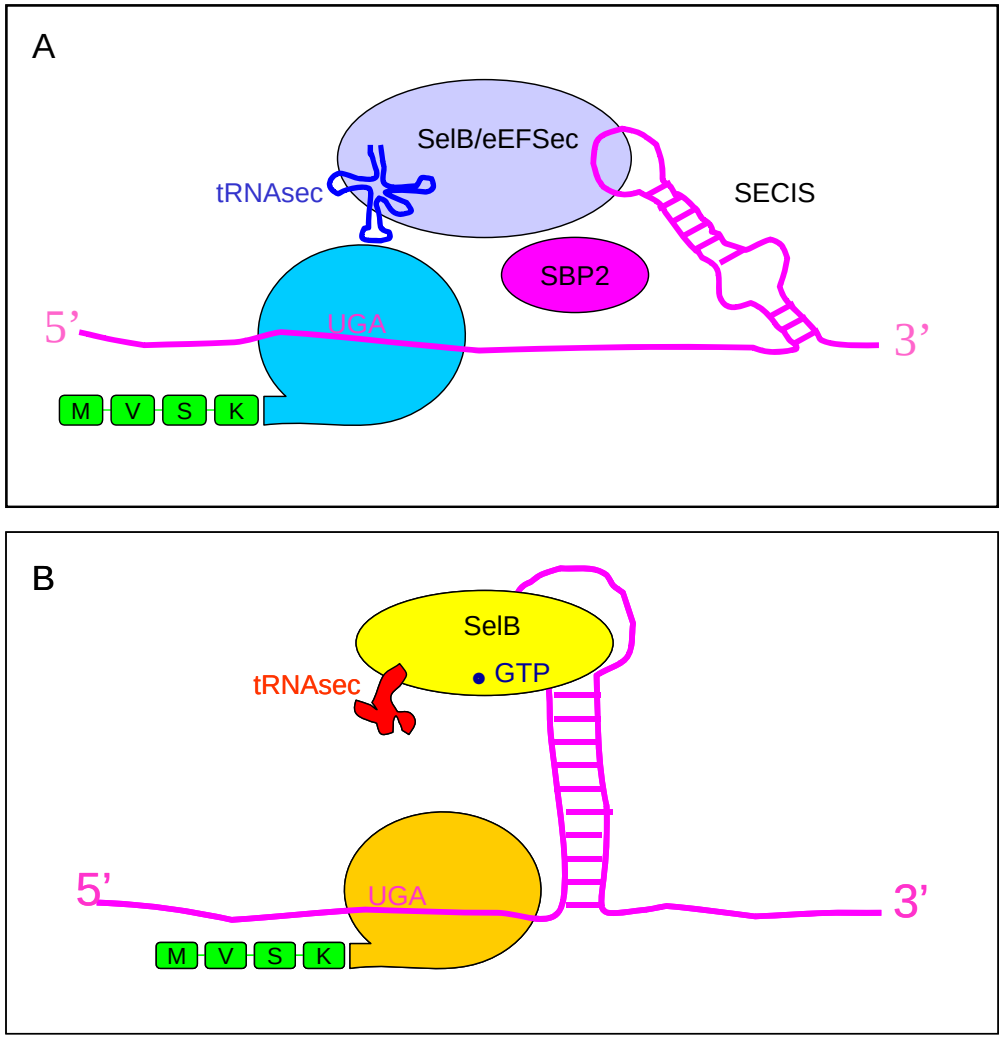

Figure 3.1. Selenocysteine incorporation models for mammalian and bacterial expression A) Model for selenocysteine incorporation in eukaryotes B) model for selenocysteine incorporation in prokaryotes

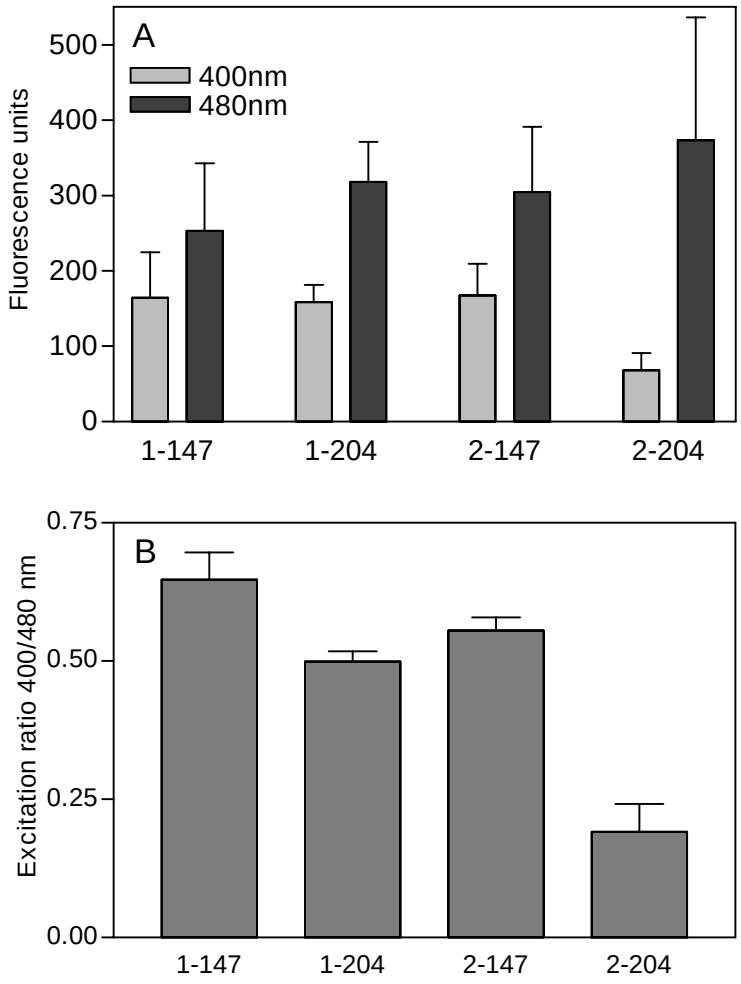

Figure 3.2. Selenocysteine GFPs expressed in cytoplasm of HEK293 cells. Cells were transiently transfected with vector and supplemented with 5μM sodium selenite. A. Average values for emission fluorescence following excitation at 400 or 480 nm for mutants of roGFP1 and roGFP2 with Sec at either position 147 or 204. B. Average excitation ratios for the same four mutants.

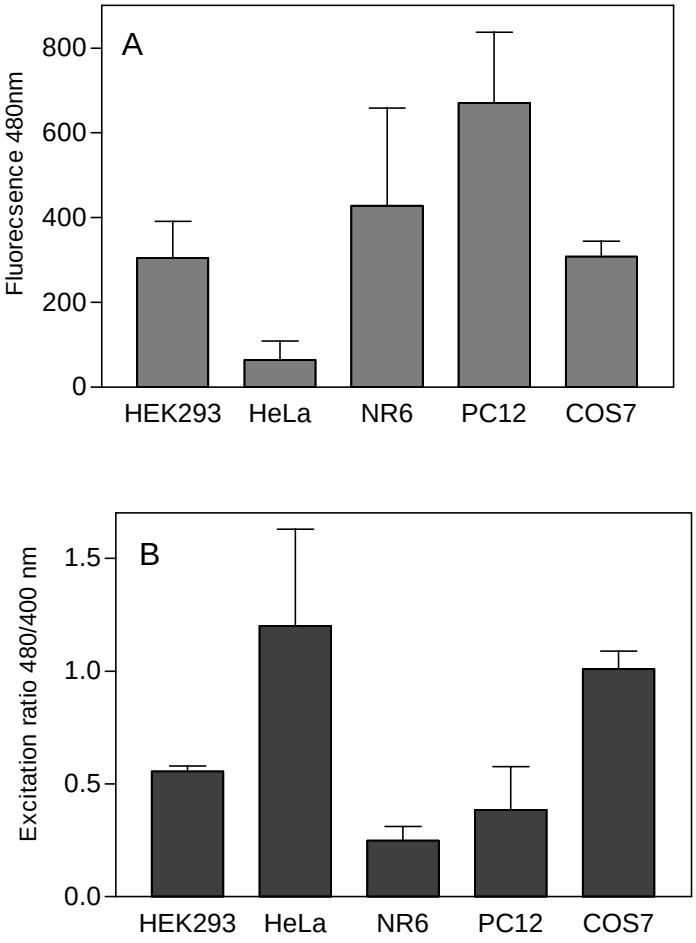

Figure 3.3. Sec2-147 expressed in five different cell lines. Cells were transiently transfected with vector and supplemented with 5μM sodium selenite. A. Average values for emission fluorescence following excitation 480 nm. B. Average excitation ratios for Sec2-147 in each cell line.

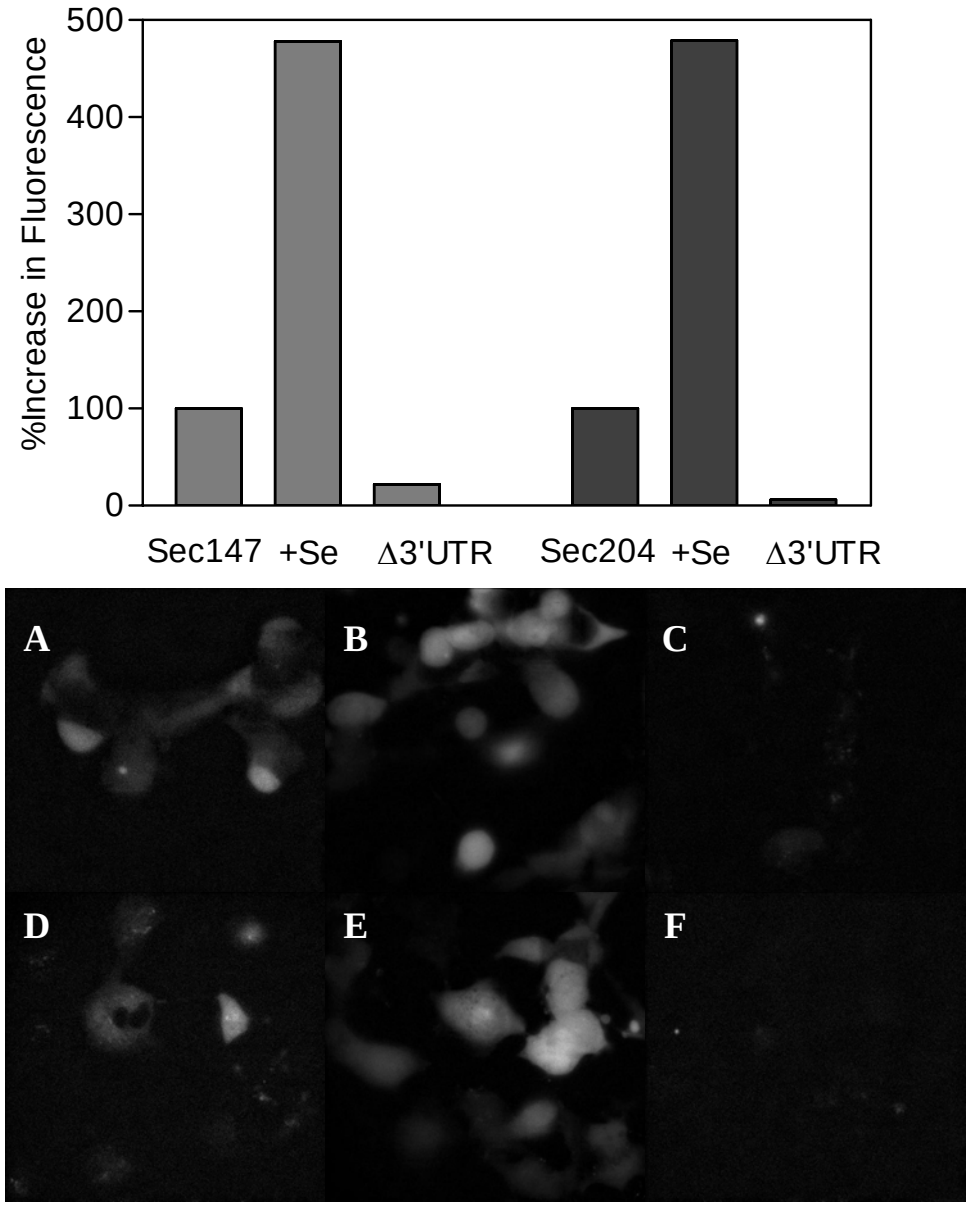

Figure 3.4. Dependence of Sec2-147 and Sec2-204 expression on Selenium. Upper graph: Sec2-147 and Sec2-204 were expressed in COS7 cells. In control conditions (Sec2-147 and Sec2-204) cells were grown in the absence of sodium selenite, media was refreshed after 24 hours cells were imaged after 48 hours. Selenium fed cells (+Se) were supplemented with 1μM sodium selenite for 24 hours then replaced with fresh media. Cells expressing the proteins with solely the stop codon (Δ3'UTR) were grown in the same conditions as the control cells. The graph depicts the average fluorescence following excitation at 480nm as a percentage of that obtained for the control condition. Lower panel. Images of cells obtained at 480nm excitation: A and B images for Sec2-147 with/without Selenium, C. Sec147-Δ3'UTR. D and E, images for Sec2-204 with/without Selenium F. Sec204-Δ3'UTR.

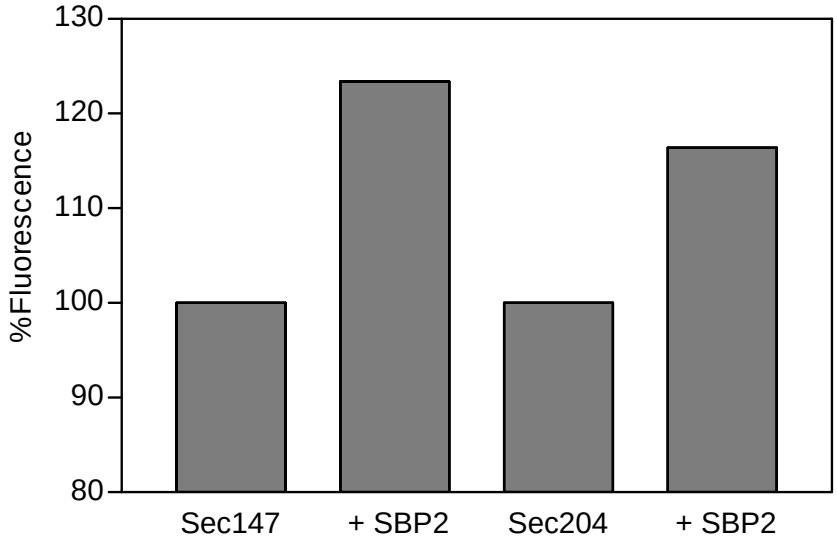

Figure 3.5. Dependence of Sec2-147 and Sec2-204 expression on SBP2. Sec2-147 and Sec2-204 expressed in HeLa cells. Cells were transiently transfected with vector for SecGFP with or without cotransfection with vector for SBP2. Cells were supplemented with 5μM sodium selenite. Bars represent the percent fluorescence observed for excitation at 480nm.

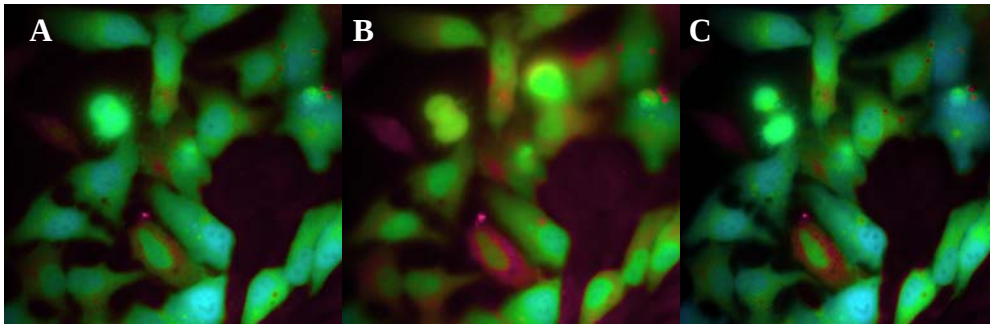

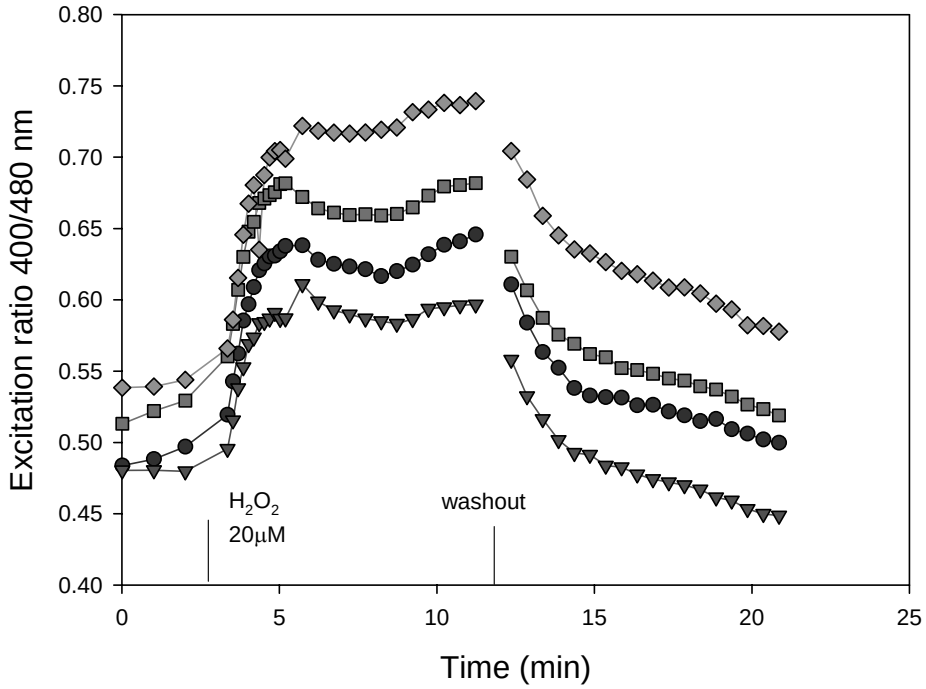

Figure 3.6. Oxidation of Sec2-147 expressed in HeLa upon stimulation with exogenous hydrogen peroxide. Images were taken at 10 second intervals following application of 20μM hydrogen peroxide. Washout consisted of removal of peroxide solution, a single wash with HBSS and replacing the original volume (2mls) HBSS. Upper panel: Excitation ratios for cells A) Before addition of peroxide B) Cells exhibiting maximal response and C) Final images following washout or peroxide. All images are pseudo-colored

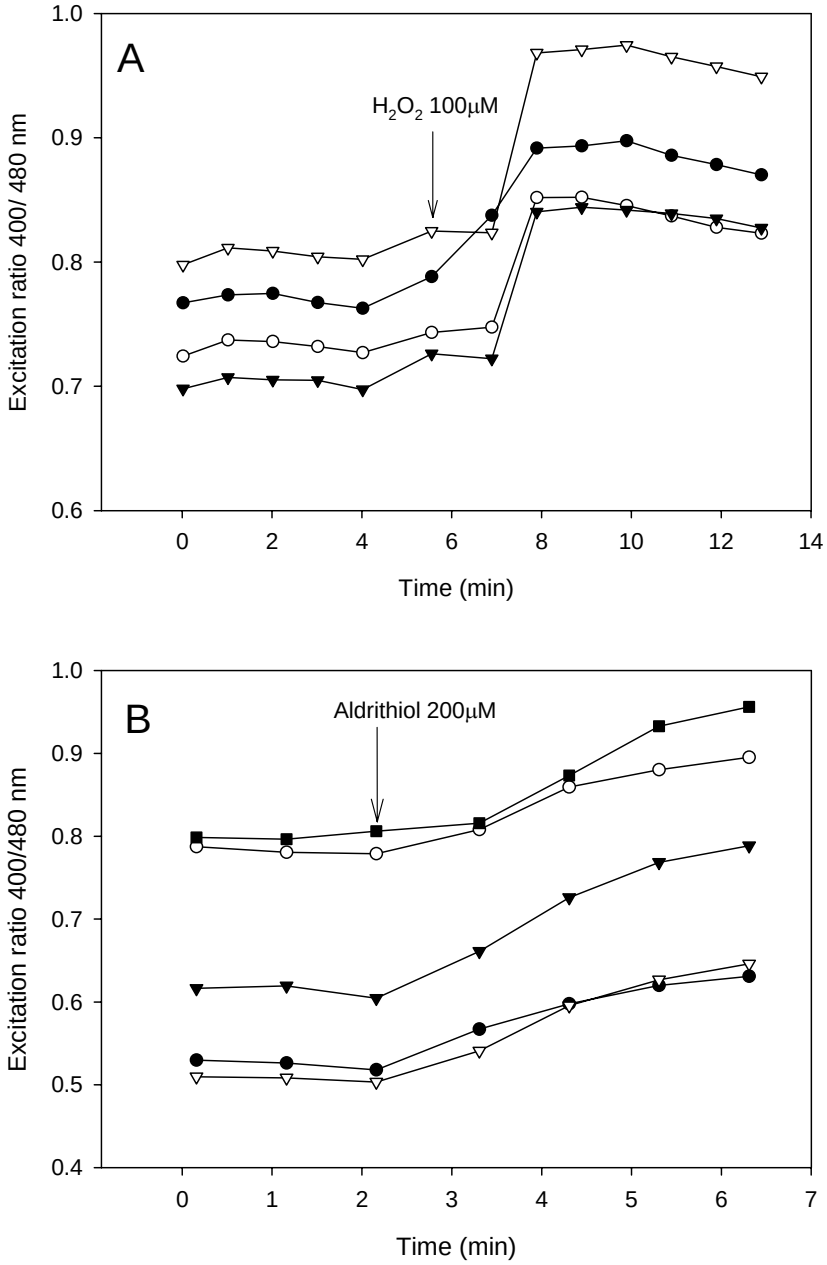

Figure 3.7. A. Oxidation of Sec2-147 expressed in HeLa cells upon stimulation with 100μM Hydrogen peroxide. B. Oxidation of Sec2-204 expressed in NR6 cells upon stimulation with 200 μM Aldrithiol.

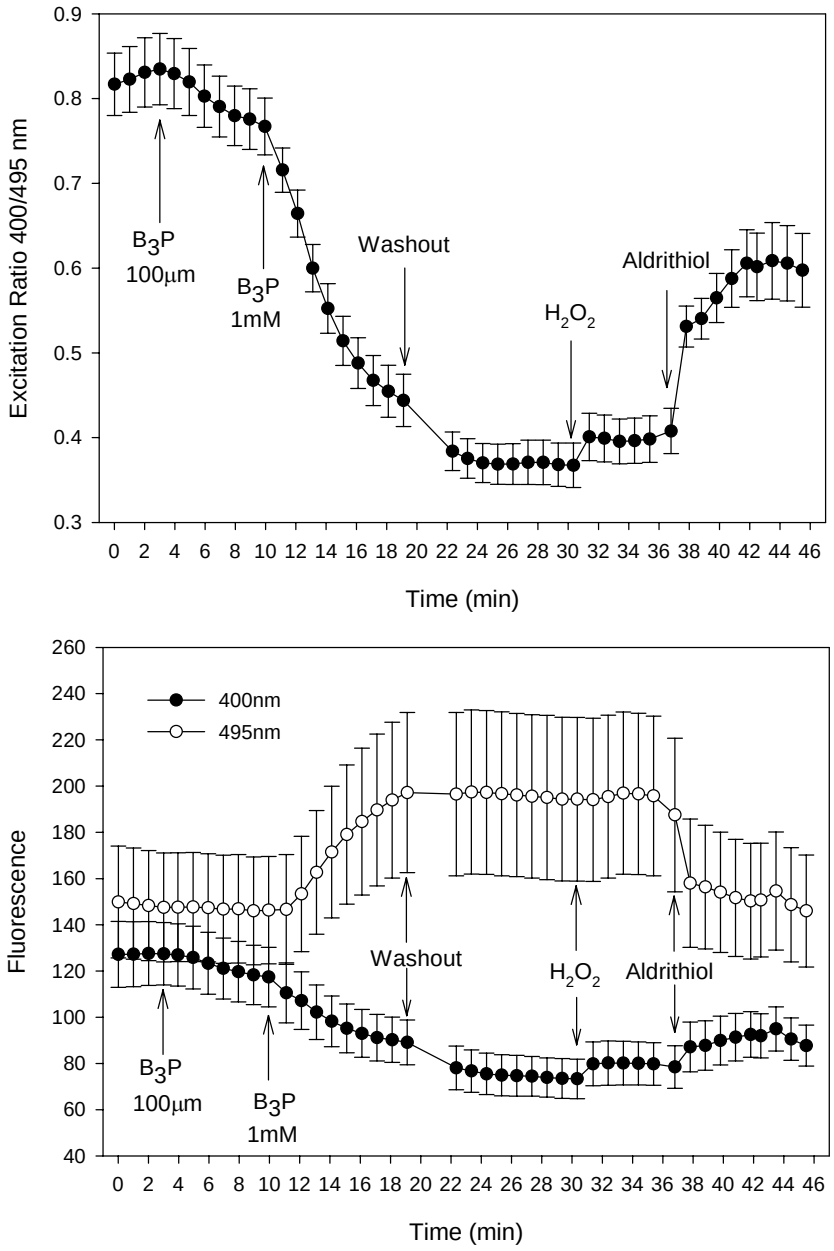

Figure 3.8 Reduction of Sec2-204 expressed in COS7 cells upon stimulation with tributylphosphine. A. Excitation ratios B. Emission at 530/25 following excitation at 400 and 495nm. Cells were treated by 100μM followed by 1mM Bu_3P. Cells were washed with HBSS then treated with 20μM hydrogen peroxide followed by washout and addition of 1mM Aldrithiol.

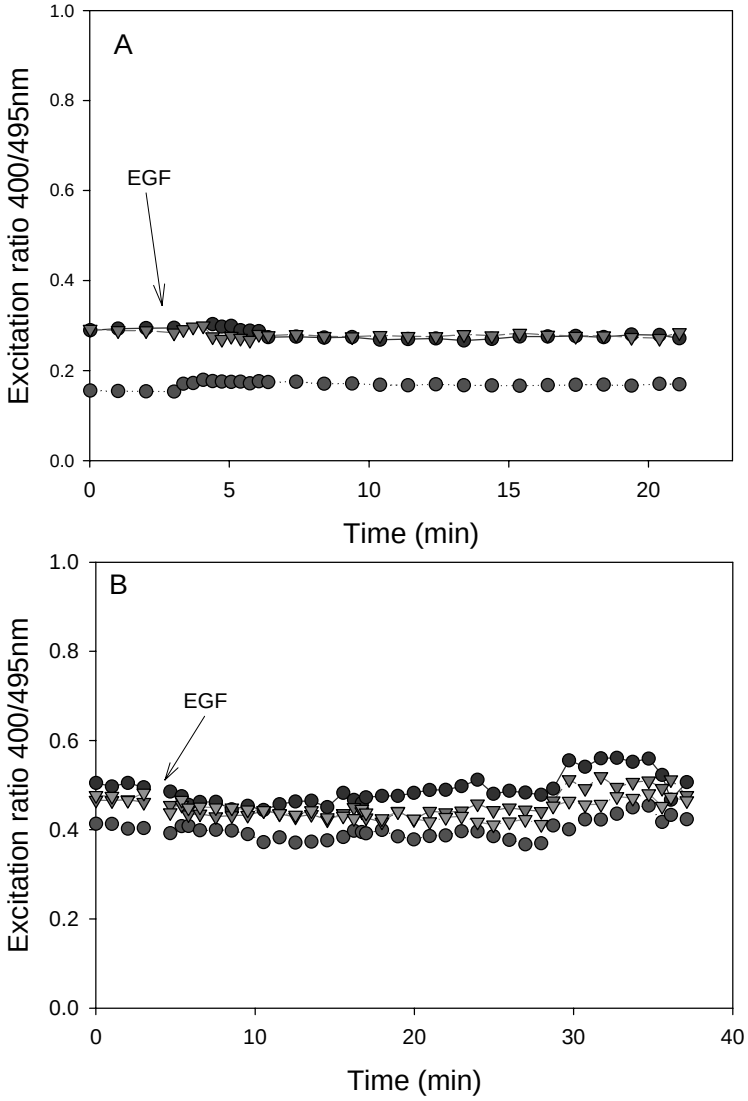

Figure 3.9. Epidermal growth factor stimulation of cytoplasmic and EGFR targeted Sec147. A. Sec2-147 expressed in cytoplasm of NR6 cells. B. Epidermal growth factor receptor fusion with Sec147 at C-terminal expressed in PC12 cells. Cells were starved of FBS for 24 hours prior to the experiment. EGF (8nM) was added at times indicated by the arrow.

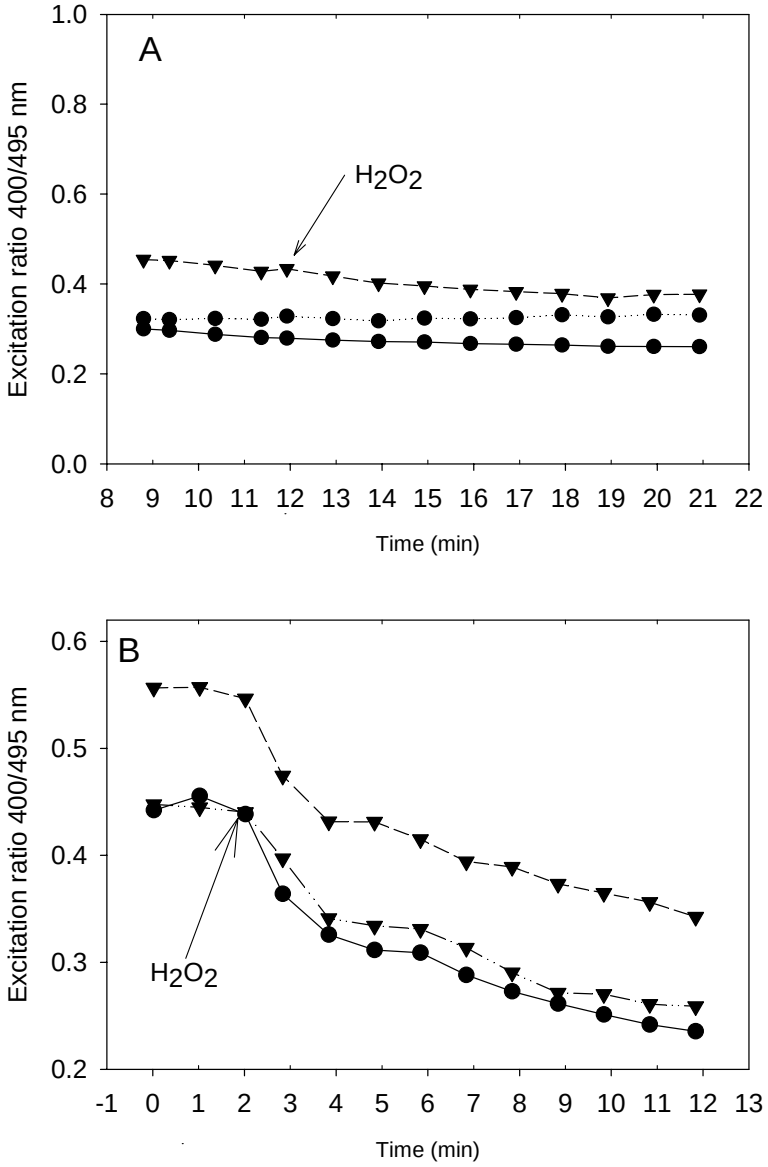

Figure 3.10. Responses to Hydrogen peroxide by two additional selenocysteine mutants. A) roGFP4 mutant in which the 149-202 cysteines are replaced by 149Sec-202Cys and B) roGFP 149C-204Sec, in which positions 147 and 202 were both serine.

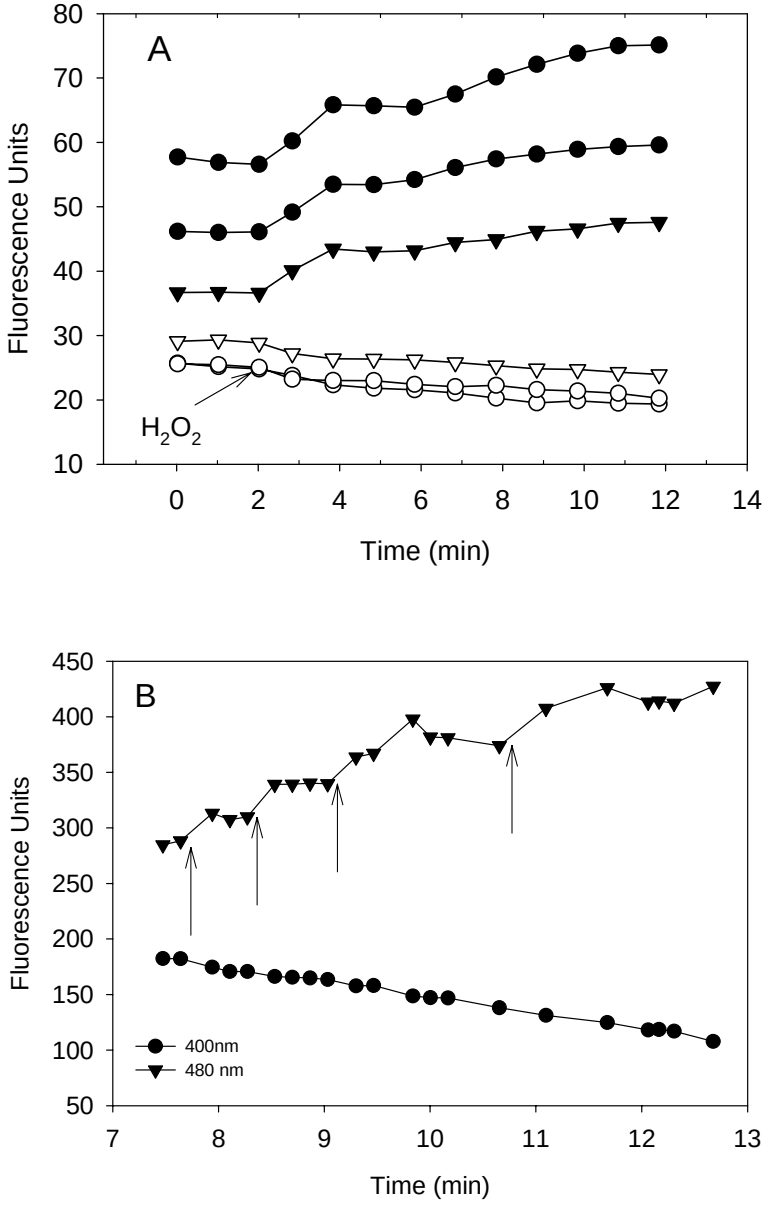

Figure 3.11. Individual excitation wavelengths for both roGFP 149C-204Sec and sec147 exhibit altered reactions. A) roGFP 149C-204Sec shows fluorescence increases for excitation at 495 nm (solid symbols) and concomitant decreases for excitation at 400nm (open symbols) following addition of H_2O_2 and B) roGFP1-Sec147 shows similar increases/decrease if illuminated for 10sec intervals (arrows).

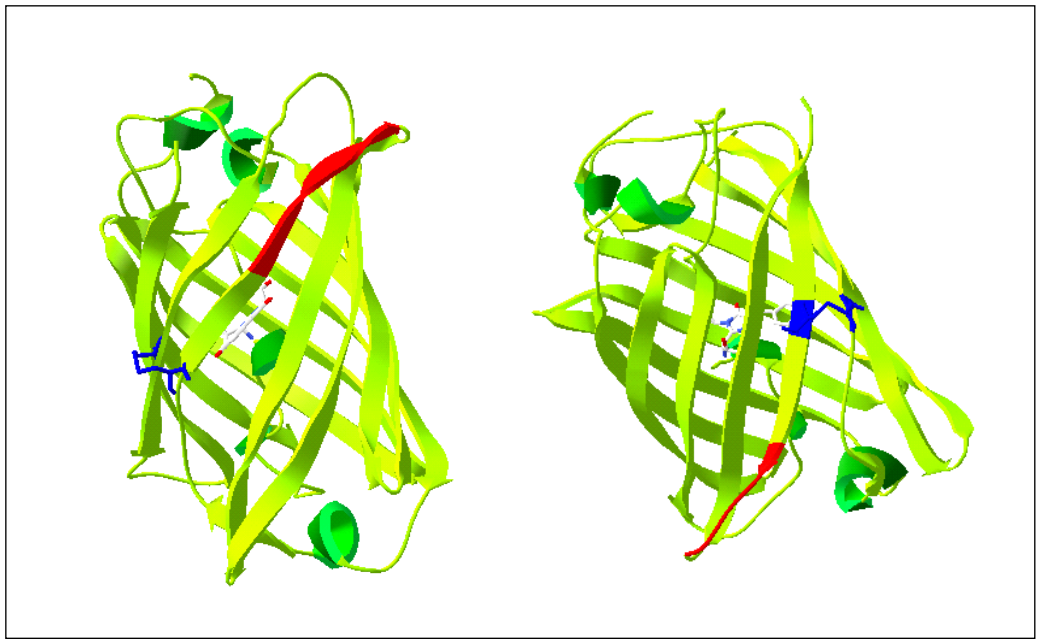

Figure 3.12. Location of mutations used for bacterial expression of Sec147 (left) and Sec204 (right). Amino acids mutated for SECIS loop are shown in red positions 147 and 204 are shown in blue.

F. References

1. Driscoll DM, Copeland PR. Mechanism and Regulation of Selenoprotein Synthesis. Annu Rev Nutr 2003.

2. Kryukov GV, Kumar RA, Koc A, Sun Z, Gladyshev VN. Selenoprotein R is a zinc-containing stereo-specific methionine sulfoxide reductase. Proc Natl Acad Sci U S A 2002;99:4245-4250.

3. Korotkov KV, Novoselov SV, Hatfield DL, Gladyshev VN. Mammalian selenoprotein in which selenocysteine (Sec) incorporation is supported by a new form of Sec insertion sequence element. Mol Cell Biol 2002;22:1402-1411.

4. Ferguson AD, Labunskyy VM, Fomenko DE, Arac D, Chelliah Y, Amezcua CA, Rizo J, Gladyshev VN, Deisenhofer J. NMR structures of the selenoproteins Sep15 and SelM reveal redox activity of a new thioredoxin-like family. J Biol Chem 2006;281:3536-3543.

5. Leinfelder W, Zehelein E, Mandrand-Berthelot MA, Bock A. Gene for a novel tRNA species that accepts L-serine and cotranslationally inserts selenocysteine. Nature 1988;331:723-725.

6. Commans S, Bock A. Selenocysteine inserting tRNAs: an overview. FEMS Microbiol Rev 1999;23:335-351.

7. Berry MJ, Banu L, Harney JW, Larsen PR. Functional characterization of the eukaryotic SECIS elements which direct selenocysteine insertion at UGA codons. EMBO J 1993;12:3315-3322.

8. Shen Q, Chu FF, Newburger PE. Sequences in the 3'-untranslated region of the human cellular glutathione peroxidase gene are necessary and sufficient for selenocysteine incorporation at the UGA codon. J Biol Chem 1993;268:11463-11469.

9. Low SC, Berry MJ. Knowing when not to stop: selenocysteine incorporation in eukaryotes. Trends Biochem Sci 1996;21:203-208.

10. Forchhammer K, Leinfelder W, Bock A. Identification of a novel translation factor necessary for the incorporation of selenocysteine into protein. Nature 1989;342:453-456.

11. Suppmann S, Persson BC, Bock A. Dynamics and efficiency in vivo of UGA-directed selenocysteine insertion at the ribosome. EMBO J 1999;18:2284-2293.

12. Arner ES. Recombinant expression of mammalian selenocysteine-containing thioredoxin reductase and other selenoproteins in Escherichia coli. Methods Enzymol 2002;347:226-235.

13. Chen GF, Fang L, Inouye M. Effect of the relative position of the UGA codon to the unique secondary structure in the fdhF mRNA on its decoding by

selenocysteinyl tRNA in Escherichia coli. J Biol Chem 1993;268:23128-23131.

14. Martin GW, III, Harney JW, Berry MJ. Selenocysteine incorporation in eukaryotes: insights into mechanism and efficiency from sequence, structure, and spacing proximity studies of the type 1 deiodinase SECIS element. RNA 1996;2:171-182.

15. Berry MJ, Martin GW, III, Tujebajeva R, Grundner-Culemann E, Mansell JB, Morozova N, Harney JW. Selenocysteine insertion sequence element characterization and selenoprotein expression. Methods Enzymol 2002;347:17-24.

16. Small-Howard AL, Berry MJ. Unique features of selenocysteine incorporation function within the context of general eukaryotic translational processes. Biochem Soc Trans 2005;33:1493-1497.

17. Mehta A, Rebsch CM, Kinzy SA, Fletcher JE, Copeland PR. Efficiency of mammalian selenocysteine incorporation. J Biol Chem 2004;279:37852-37859.

18. Berry SM, Gieselman MD, Nilges MJ, Der Donk WA, Lu Y. An engineered azurin variant containing a selenocysteine copper ligand. J Am Chem Soc 2002;124:2084-2085.

19. Johansson L, Chen C, Thorell JO, Fredriksson A, Stone-Elander S, Gafvelin G, Arner ES. Exploiting the 21st amino acid-purifying and labeling proteins by selenolate targeting. Nat Methods 2004;1:61-66.

20. Arner ES, Sarioglu H, Lottspeich F, Holmgren A, Bock A. High-level expression in Escherichia coli of selenocysteine-containing rat thioredoxin reductase utilizing gene fusions with engineered bacterial-type SECIS elements and co-expression with the selA, selB and selC genes. J Mol Biol 1999;292:1003-1016.

21. Sandman KE, Benner JS, Noren CJ. Phage display of selenopeptides. J Am Chem Soc 2000;122:960-961.

22. Jacob C, Giles GI, Giles NM, Sies H. Sulfur and selenium: the role of oxidation state in protein structure and function. Angew Chem Int Ed Engl 2003;42:4742-4758.

23. Lescure A, Gautheret D, Krol A. Novel selenoproteins identified from genomic sequence data. Methods Enzymol 2002;347:57-70.

24. Bae YS, Kang SW, Seo MS, Baines IC, Tekle E, Chock PB, Rhee SG. Epidermal growth factor (EGF)-induced generation of hydrogen peroxide. Role in EGF receptor-mediated tyrosine phosphorylation. J Biol Chem 1997;272:217-221.

25. Hanson GT, Aggeler R, Oglesbee D, Capaldi RA, Tsien RY, Remington SJ. Investigating mitochondrial redox potential with redox-sensitive green fluorescent protein indicators. J Biol Chem 2004;279:13044-13053.

26. Ostergaard H, Henriksen A, Hansen FG, Winther JR. Shedding light on disulfide bond formation: engineering a redox switch in green fluorescent protein. EMBO J 2001;20:5853-5862.

27. Bar-Noy S, Moskovitz J. Mouse methionine sulfoxide reductase B: effect of selenocysteine incorporation on its activity and expression of the seleno-containing enzyme in bacterial and mammalian cells. Biochem Biophys Res Commun 2002;297:956-961.

28. Zinoni F, Birkmann A, Stadtman TC, Bock A. Nucleotide sequence and expression of the selenocysteine-containing polypeptide of formate dehydrogenase (formate-hydrogen-lyase-linked) from Escherichia coli. Proc Natl Acad Sci U S A 1986;83:4650-4654.

29. Arthur JR. The glutathione peroxidases. Cell Mol Life Sci 2000;57:1825-1835.

30. Stadtman TC. Selenium biochemistry. Mammalian selenoenzymes. Ann N Y Acad Sci 2000;899:399-402.

31. Guimaraes MJ, Peterson D, Vicari A, Cocks BG, Copeland NG, Gilbert DJ, Jenkins NA, Ferrick DA, Kastelein RA, Bazan JF, Zlotnik A. Identification of a novel selD homolog from eukaryotes, bacteria, and archaea: is there an autoregulatory mechanism in selenocysteine metabolism? Proc Natl Acad Sci U S A 1996;93:15086-15091.

32. Besse D, Siedler F, Diercks T, Kessler H, Moroder L. The redox potential of selenocystine in unconstrained cyclic peptides. Angew Chem Int Ed Engl 1997;36:883-885.

33. Belousov VV, Fradkov AF, Lukyanov KA, Staroverov DB, Shakhbazov KS, Terskikh AV, Lukyanov S. Genetically encoded fluorescent indicator for intracellular hydrogen peroxide. Nat Methods 2006;3:281-286.

34. Nifosi R, Ferrari A, Arcangeli C, Tozzini V, Pellegrini V, Beltram F. Photoreversiible dark status in a tristable green fluorescent protein varient. J Phys Chem 2003;107:1679-1684.

35. Dickson RM, Cubitt AB, Tsien RY, Moerner WE. On/off blinking and switching behaviour of single molecules of green fluorescent protein. Nature 1997;388:355-358.

37. Pedelacq J.D., Cabantous S., Tran T., Terwilliger T.C., Waldo G.S. Engineering and characterization of a superfolder green fluorescent protein. Nature Biotechnol. 2006;24:79-88.

Chapter Four

Singlet Oxygen Sensitive Green Fluorescent Proteins (SOS:GFPs)

Ratiometric Irreversible Indicators

A. Introduction

Singlet oxygen, an excited state of molecular oxygen results from the promotion of an electron to a high energy orbital. Molecular oxygen exists in a triplet state ($^3\Sigma_g^-$) it has two electrons with parallel spins in two degenerate π^* orbitals. Upon excitation to the singlet state ($^1\Delta_g$) the two electrons occupy a single π^*orbital with opposite spins. Although other excited states of oxygen exist they are not formed in biological systems [1] and of these only singlet oxygen has a sufficient half-life to react chemically. Since the energy of formation is only 94 kJ mol-1 (23 kcal mol^{-1}) above the ground state singlet oxygen is easily formed, it has a relatively long half-life (~10^{-6} secs) and is thereby capable of causing considerable damage *in vivo*, oxidizing lipids, DNA, and proteins (reviewed in [1,2]) and is involved in sunburn, development of cataracts and skin cancer. Biological sources of singlet oxygen occur in a number of systems notably the immune systems defense against bacteria. Singlet oxygen for killing pathogens can be generated by peroxidases (myeloperoxidase) [3], oxygenases (lipoxygenase or cyclooxygenase) or by the reaction of hydrogen peroxide with hypochlorite or peroxynitrite [1,4].

Chemical reactions that generate singlet oxygen include but are not limited to; oxidation of hydroperoxide, the disproportionation of hydrogen peroxide by molybdate ions [5,6], thermolysis of polycyclic aromatic endoperoxides (such as 1,4-

dimethylnaphthalene), or the reduction of ozone by triphenylphosphite [4]. Photosensitized production of singlet oxygen is a common means of producing singlet oxygen in biological systems. Photosensitizers are often fluorescent molecules in which singlet oxygen is produced by a Type II mechanism [7]:

$$P + h\nu \rightarrow P^*$$

$$^1P^* \rightarrow ^3P^*$$

$$^3P^* + O_2\ (\Sigma_g^-) \rightarrow P + O_2\ (^1\Delta_g)$$

where P denotes a photosensitizer in the ground state, $^1P^*$ an excited singlet state, and $^3P^*$ an excited triplet state. Photosensitizers can also initiate photochemistry by a Type I mechanism in which singlet and triplet states of the photosensitizer react directly with a molecule to produce radicals or radical ions [7]. Rose bengal and methylene blue are two widely used water soluble photosensitizers [8,9]. Rose bengal is a xanthene based dye that absorbs in the 450-500nm range, has a high quantum yield of singlet oxygen (0.75-0.8) [10,11] and binds to the plasma membrane of mammalian cells [12]. Methylene blue is a phenothiazine, absorbs in the 550-700nm range and has a lower singlet oxygen quantum yield of 0.52 [8]. Photosensitizers capable of crossing the cell membrane are tend to localize in subcellular entities, lysosomes, the inner mitochondrial membrane or nucleus, thus limiting reactions of singlet oxygen to these subcellular compartments. Genetically targetable photosensitizers have been recently introduced, such as the biarsenical fluorescent dyes FlAsH and ReAsH which been used to generate singlet oxygen in biological systems [13,14]. However, the quantum yield for ReAsH is low (0.04).

There are four current methods for the detection of singlet oxygen, 1) chemical traps such as 2-(9,10-dimethoxyanthracenyl)-*tert*-butylnitroxide for use in conjunction

with ESR spectroscopy (a potential problem with many chemical traps is formation of endoperoxide from non singlet oxygen source [1]) 2) Perturbation methods either by quenching by e.g. azide, 1,4-diazabicyclo[2.2.2]octane (DABCO), or anthracene dipropionic acid (ADPA) or by using deuterated solvent to decrease inactivation rate or 3) Chemiluminescence; relaxation of singlet oxygen to the ground state can be observed by monitoring emission at 1268nm, or when two molecules of singlet oxygen collide and they can be monitored at 634 and 703nm (Dimol emission) [1] and 4) Fluorescent indicators based on diphenylanthracene-fluorescein conjugates [15,16], when singlet oxygen forms the endoperoxide on the diphenylanthracene dye the conjugation is altered and the molecule becomes fluorescent.

In the cell the major biological target for singlet oxygen are proteins, they are composed of sensitive amino acids and occur in high concentrations. The five amino acids most susceptible to oxidative degradation are histidine, tryptophan, cysteine, methionine and tyrosine [2,17,18] the peptide backbone is relatively insensitive to cleavage [19]. Histidine is the most sensitive to singlet oxygen (with a quench constant of 3-4 x 10^7 M^{-1} s^{-1} [19,20]) from the initial endoperoxides formed by $^1O_2$ additions across the imidazole [19] many products are formed. Tryptophan residues are the only side-chain to have both significant physical and chemical quenching of singlet oxygen [21] and it is also unusual in that its derivatives are photosensitizers. Arginine and Lysine can be photooxidized by singlet oxygen but only at high pH when they are in the un-protonated form.

Previous efforts to detect reactive oxygen species (ROS) by roGFP following a physiological stimulus lead us to two conclusions; firstly the generation of ROS must be very localized, and/or limited in quantity or localization, and secondly the cell's

ability to reduce any oxidized product is difficult to overcome using reversible sensors. We reasoned that an irreversible sensor might be advantageous in this situation since it would negate any effects of the reduction machinery and would accumulate as long as the stimulus produced ROS. However since we wished to develop a sensor that was an endogenously expressed protein we were limited to the natural amino acids. There have been numerous studies on the oxidation of proteins. Oxidation can cause non-sulphydryl based cross-linking in peptides and proteins [22-25] and even in some cases intramolecular cross-linking [26,27]. By employing the reactions that amino acid side chains naturally undergo during oxidation, we anticipated that we could harness the natural oxidative processes, to develop irreversible ROS sensing GFPs.

Oxidative intra-or inter-protein cross linking can occur by several methods following oxidation: 1) Oxidation of two cysteine residues 2) Reaction of 2 carbon centered or 2 tyrosine radicals, the dienone alcohol formed upon oxidation of tyrosine by singlet oxygen can undergo Michael reactions with nucleophiles such as thiols and amines, which may contribute to protein cross-linking [2]. Tyrosine may also generate phenoxyl radicals which may dimerize to di-tyrosine, however this may require an radical mediated electron mediated transfer involving transfer agents such as Fe ions [28]. 3) Lysine residues interacting with carbonyl groups of oxidized proteins, malondialdehyde or glycation/glyoxidation derived carbonyls or lipid peroxidation products [29]. 4) Histidine residues are thought to be of particular importance in protein aggregation, as proteins lacking histidines do not cross link [2,23,30]. Many reactions that give rise to aggregates are considered “dark reactions” as they independent of continuing $^1O_2$ production [2]. Histidine derivatives can cross link with lysine, cysteine, tryptophan and tyrosine or other histidine residues [22,23,26] in reactions analogous to

Schiff base /Amadori reactions [31]. Another amino acid thought to be involved in cross linking is tryptophan, oxidative degradation results in kynurenines and N-formylkynurenin [32]. These compounds are better photosensitizers than tryptophan itself and thus can generated further singlet oxygen production under prolonged exposure to light [2]. Kynurenine reacts preferentially with cysteine though reactions with histidine and lysine also occur [33].

A rational approach was taken for the discovery of the green fluorescent based singlet oxygen sensors (SOS-GFP). The redox sensitive indicator (roGFP2) [34,35] described in Chapter one was used as a starting point. It was reasoned that since the cysteines at positions 147 and 204 yielded optimal signals for changes in excitation spectra upon oxidation/reduction, these two positions were likely affect the excitation spectra upon oxidation or cross linking. Our initial mutations involved histidine, tryptophan and lysine and were expanded to include additional amino acids with sensitivities to oxidation, methionine, tyrosine, proline and arginine. When expressed in cells the mutants exhibited a wide range of excitation ratios. The mutations did not show any response to the exposure to hydrogen peroxide, only a couple showed a slight response following exposure to menadione. There was a strong response to singlet oxygen in particularly for mutations expressing histidine at position 147. The histidine mutations were evaluated for specificity and sensitivity to singlet oxygen. The most reactive/sensitive mutations were then used in three different biological settings to sense singlet oxygen generated form a nearby source.

B. Methods

GFP Mutations--- Positions 147 and 204 of roGFP2 in either pRSETb or pN1 were mutated using QuikChange reaction method (Stratagene, CA), The codon sequence

VGB was used to in the forward and reverse primer to simultaneously generate eight amino acids (V, G, A, L, R, P, M, and T). A tetracysteine motif FLNCCPGCCMEG [36] was added to the C-terminal of SOS-HH, and SOS-HV by swapping GFP coding regions of SOS-HH with GFP-4C in pCDNA3 through restriction with HindIII and BsrGI.

HH-PLGLAG-4C---: The construct was composed of SOS-HH a GGGGGGS linker, the MMP cleavage site (PLGLAG) a second linker GFKSGSGSGS and the tetracysteine sequence FLNCCPGCCMEG. The c-terminal tag was generated by consecutive PCR reactions using forward and reverse primers as follows: reaction 1) overlapping primers CAGCCAAGCTTCGGAATTCCATTTAGGTACCGGGC TCCATGCAGCAGCCGGGGCAGCAATTCAAAAAGCTGCCGCTGCCGCTGCCGCT and TGGCGGCTTTAAGAGCGGCAGCGGCAGCGGCAGCTTTTTGAATTGCTGC reaction 2) the product of the first reaction was used as template for a second reaction using the following primers forward: AGCTGTACAAGGGCGGCGGCGGCGGCGGCAGCCCCC TCGGCCTCGCTGGCGGCTTTAAG and reverse: TGGCGGCTTTAAGAGCGGCA GCGGCAGCGGCAGCTTTTTGAATTGCTGC. The full-length tag was restricted with BsrG1 and EcoR1 and inserted into SOS-HH in pBAD restricted with the same enzymes.

FKBP-SOS-GFP—This construct was generated by PCR. cDNA of SOS-HH and HV with restriction sites EcoRI and KpnI at the C terminal were obtained from SOS-HH in pN1 by PCR reactions using the following primers: forward: GCAGAGCTGGTTTAGTGA ACCGTCAG and reverse ATGGAATTCATCATCGGTACCCTTTACTTGTACAGCTCGTCCA TGCCGA. The PCR reactions were cut with SalI and EcorI and ligated to the C-terminal FKBP in pRSETb cut with the aforementioned restriction enzymes. A

correction to put the GFP in frame was necessary, so a quick Change reaction was performed to insert an adenosine (forward primer CCGGGATCCAACATGGTGAGC, reverse GCTCACCATGTTGGATCCCGG). For mammalian expression FKBP-HH and FKBP-HV was cut with XhoI and BsrGI and ligated to SOS-HH in pN1 cut with the same enzymes (preFKBP-HH). A PCR reaction was then performed to generated a start codon and include a Kozak sequence and a BglII restriction site at the N-terminal of FKBP, the primers used were: forward TGCAGATCTGCCACCATGCTCGAGGGA

GTG and reverse GTTTCAGGTTCAGGGGGAGGTGTGGGAGG, pre-FKBP-HH in pN1 was used as template. The PCR reactions were restricted and ligated into pre-FKBP-HH restricted with BglII and BsrGI.

FRB-4C--- The tetracysteine motif was expanded from SOS-HV-4C using PCR and forward primer, CATAAGCTTCATGTCGACGGCGGCGGCGGCGGCGGCAGCTTTTTGAAT TGCTGCCCCGGC and reverse primer ATGGAATTCTTAGGTACCCTCCATGCAGCA. The PCR reaction was cut with SalI and EcoRI and ligated to FRB in pRSETb. For mammalian expression a PCR was performed using forward primer: TGCGGATCCCTCGCCACCATGTGGCATGAA and pRSETb reverse primer: CTAGTTATTGCTCAGCGGTGG on FRB in pRSETb. The PCR reaction was restricted using BamHI and EcoRI and ligated into pCDNA3 vector cut with the same enzymes.

FRB-mO-HIY---. To replace the tetracysteine motif with mOrange, the FRB and GGGGSSSS linker cDNA with HindIII restriction site at both the N and C terminals was generated using GTAAAGCTTCTCGCCACCATGTGG for the forward primer and TGCAAGCTTAAGCTGCCGCC as the reverse primer. The PCR reaction was cut

and ligated in pCDNA3 containing mOrange-HIY [37]. For bacterial expression the FRB-mO construct was restricted with HindIII and EcoRI and ligated to pRSETb restricted with the same enzymes.

ReAsH staining in cells of constructs with 4C motifs--- A stock solution of ReAsH was diluted 10x in 2mM ethane dithiol (EDT) and then added to 2mLs cell media (DMEM no FBS) or HBSS at a final concentration of 0.5-1μM. Cells were incubated in 1-2 mL ReAsH solution for 0.5-1hour at 37°C. Then washed twice with HBSS or 10μM EDT, followed by two ten-minute incubations in 0.25-1mM BAL/HBSS at 37°C. Finally the cells were washed twice with HBSS before imaging.

ReAsH staining of proteins with 4C motifs *in vitro*---Proteins containing the tetracysteine tag were expressed in *E.coli* (LMG194 or JM109). Bacteria were pelleted and treated with 8-10mls of B-Per I (Pierson, IL) to lyse cell walls. The lysate was centrifuged and supernatants were shaken in the presence of nickel coated beads for 3 hours at 4°C of 1mM TCEP and 10mM mercaptoethane sulfone to minimize oxidation of cysteine residues. Aliquots of protein were incubated with dye (3x concentration protein) for 1-2 hours at room temperature. Samples were concentrated (Microcon 30MW Millipore,MA) and resuspended in 100μM EDT followed by three similar washes (concentration and resuspension) in PBS buffer. Extent of ReAsH coupling was determined by an absorbance scan of wavelengths that included both protein and ReAsH, and using the extinction coefficients of 60,000 for ReAsH and 44,000 for SOS-GFP (protein treated with 1N NaOH).

Generation of Singlet oxygen in Cells---Singlet oxygen was generated using one of three sources, Rose bengal, ReAsH or GFPs. Rose bengal was dissolved in methanol before dilution to concentrations of interest (0.1-6μM) and was added to

directly to HBSS in the imaging dish. Cells were illuminated using 568nm light for 1-2 minutes. ReAsH was directed by means of a tetracysteine tag to a protein of interest, after staining with ReAsH using the protocol described above, cells were illuminated on the microscope using 568nm light for 1-3 minutes or as described in each Figure). A one-minute illumination was estimated to be 534 Joules/cm^2.

Singlet oxygen generation *in vitro*---Photosensitization: Rose bengal was dissolved in methanol before dilution to concentrations of interest (0.1-6μM). Illumination of assay wells (96well plate) was achieved using a solar simulator (Spectra Physics, CA) and employing a 568/55 filter for 1 minute or as described in each experiment. Proteins stained with ReAsH were illuminated for 10 minutes or more on the solar simulator using the same filter. All plates were sealed actively cooled while under the solar simulator.

Disproportionation of Hydrogen peroxide--- A second source of singlet oxygen was achieved by exposing the proteins to a hydrogen peroxide (10-50mM) in the presence of sodium molybdate (10-50mM) in PBS buffer pH 7.4, final volume 150μl, and incubating for 5-20 minutes at room temperature.

Reactivity of SOS-GFPs with various ROS/RNS---SOS-GFPs (1μM) were incubated in conditions which generated a) hydroxyl radicals; ferrous perchlorate (100μM) and hydrogen peroxide (1mM), b) hypochlorite ions; sodium hypochlorite (NaOCl, 3μM) 30 mins 37^{o}C, c) Superoxide; Potassium superoxide (KO2, 100μM) 30 mins 37^{o}C, d) hydrogen peroxide (H_2O_2, 1mM), e) RNO 2-2'-Azobis(2-amidinoppropane)-dihydrochloride (100μM) 30 mins 37^{o}C, f) nitrous oxide radicals (NaNONO , 1,1-diethyl-2-hydroxy-2-nitrosohydrazine 10 μM) 30 mins 37^{o}C.

Fluorescent Imaging---Cells were imaged on a Zeiss Axiovert microscope with a cooled CCD camera (Photometrics, Tucson, AZ) controlled by Metafluor 2.75 software (Universal Imaging, West Chester, PA). Dual excitation ratio imaging used excitation filters 400DF15 and 495DF10 altered by a filter changer (Lambda 10-2, Sutter Instruments, San Rafael, CA), a 505DRLP dichroic mirror and a single emission filter, 535DF25. Fluorescence images were background-corrected by manual selection of background regions. Exposure time was 200–1000 ms, and images were taken every minute

C. Results

GFP Mutations

Amino acid side chains undergo a variety of oxidative reactions some of which include cross linking, we planned to use such natural oxidative processes, to develop irreversible ROS sensing GFPs. Positions 147 and 204 yielded optimal signals for changes in excitation spectra upon oxidation/reduction, thus were likely affect the excitation spectra upon oxidation or cross linking. Initially the cysteine residues at positions 147 and 204 were mutated individually to histidine, tryptophan and lysine and later mutations for combinations of the three amino acids were made. Mutants were expressed in COS7 Hek293 or HeLa cells, basal excitation ratios did not differ between cell lines. Excitation ratios of mutants with 147C-204X were not significantly altered from 147C-204C (roGFP). Most mutants with lysine at 147 exhibited elevated excitation ratios, but all mutants with histidine or tryptophan at position 147 were significantly higher as was the 147Y-204Y (YY) mutant.

One form of protein cross-linking involves the side chains of lysine with carbonyl groups. Oxidation of the side chains of lysine, arginine, proline, leucine and threonine

has been shown to yield carbonyl derivatives [29,38,39]. To explore the possibility of developing intra-molecular cross-linkage stimulated by ROS, three additional series of mutations were generated by replacing the 147-C in roGFP2 with histidine, tryptophan or lysine and eight amino acids at position 204. By using a minimum of nucleotides we were able to express the four amino (arginine, proline, leucine and threonine) acids of interest and four additional amino acids (valine, alanine methionine and glycine) with a single nucleotide codon sequence (VGB which encodes for G,C,A at the first position of the codon, T,G,C at the second and G at the third). Although methionine was were not expected to generate cross-links they are affected by oxidation so there was some interest in including this amino acid. The library also included two series where position 204 was fixed as cysteine or lysine and the position 147 was varied by using VGB codon sequence. Proline at position 204 was observed to have elevated excitation ratios and four mutants were test with proline at position 147. All mutations expressed in cells are shown in Figure 4.1. Although we observed unusual basal ratios for many of the mutants, they were not found to increase the excitation ratio upon exogenous addition of 100μM H_2O_2 or menadione (data not shown) however a number of mutant exhibited changes in excitation ratio when exposed to singlet oxygen generated by Rose bengal. The responses were irreversible excitation ratios did not decrease when illumination ceased. Increases in excitation ratio were dependant on dose of light. Since the excitation ratio response to singlet oxygen generally involved a more distinct change at the 495nm wavelength the excitation ratios for the mutants were subsequently expressed as 495/400nm, excitation ratios will increase in response to singlet oxygen. Because the basal ratio of the mutants varied widely we compared their

response by increase over basal ratio (Figure 4.2). The double histidine mutant (HH) gave the greatest response to singlet oxygen followed by HT, HV and HL. Mutants with tryptophan at position 147 did not generate large responses and resulted from loss of fluorescence emission at both wavelengths. Most ratio changes for mutants besides tyrosine were due fluorescence decreases at both wavelengths (Table 4.1). Five mutants were found to have significantly reduced excitation ratios (Figure 4.2.B) KW, CH, LK, YT and YY. Of these only CH exhibited an increase in fluorescence from excitation at 400nm and a concomitant decrease for 490nm. The role played by the amino acid at position 204 is intriguing as neither the basal ratio nor the reaction to singlet oxygen can be judged by similarity of amino acids at position 204, although a full combinatorial examination of amino acid mutants might be more revealing. The time course of reaction to illumination of cells expressing SOS-HH preincubated with Rose bengal is given in Figure 4.3.

Singlet Oxygen Sensing Proteins *In Vitro*

The proteins were next compared to a more established singlet oxygen sensor 9,10-anthracenedipropionate $ADPA^{(2-)}$ are a common means for detection of singlet oxygen, these molecules lose their fluorescent properties when the endo-peroxide form of the molecule is formed following exposure to singlet oxygen. The three most responsive singlet-oxygen-sensing proteins (SOS-HH, SOS-HV and SOS-HT) were expressed as His_6-tagged proteins in bacteria and purified using Nickel beaded columns. Equal concentrations of SOS-HH and ADPA were exposed to equivalent doses of singlet oxygen as produced by photosensitized Rose bengal (1μM). The solutions were simultaneously illuminated (568nm) on a solar simulator for a series six intervals of ten-second duration followed by a second interval of one-minute

duration (total dose= 17 Joules/cm^2). The methods for monitoring the effects of singlet oxygen are different for each compound, SOS-GFPs require collection of an excitation ratio and the polycyclic aromatic compound requires monitoring fluorescent emission. The two data sets cannot be gathered simultaneously, in order to compare the two, data presented in Figure 4.4 has been converted to a Molar concentration of ADPA or SOS-HH remaining. Deactivation of singlet oxygen by solvent is much greater than with ADPA 3 x10^5 s^{-1} versus 5 x 10^3 s^{-1} ([ADPA]x k), therefore the rate equation for singlet oxygen can be considered independent of ADPA concentration, the decay of ADPA follows first-order kinetics [40]. Using first order rate constant for ADPA ~1 x 10^8 M-1 s-1 [40-42], we were able to determine the concentration of singlet oxygen produced by Rose bengal and use this SO concentration to determine the rate constant for SOS-HH (1.26 x $10^8 \pm 2.6e^7$).

Quenching Of Singlet Oxygen Generated From Rose bengal By Sodium Azide--- A shortcoming of Rose bengal as photosensitizer is that it undergoes auto-degradation during irradiation (photobleaching) leading to type I reactions and as a result may form adducts to other reactants. These adverse reactions were demonstrated by the inability of Sodium azide (10mM), an efficient singlet oxygen quencher, to inhibit the excitation ratio increases of SOS-HV observed with illumination in the presence of Rose bengal. Complete failure to quench the reaction is occurs at higher concentrations of Rose bengal (4 μM or higher, Figure 4.5). Only at concentrations of Rose bengal below 1μM was there greater than 50% inhibition by azide. The concentration of azide was not limiting as increasing the concentration to 50 mM did not improve inhibition. Since much of the excitation ratio increases

observed with higher concentrations of Rose bengal are not singlet oxygen mediated only concentrations below 1μM Rose bengal were subsequently used.

Singlet oxygen by hydrogen peroxide and molybdate---The disadvantages of Rose bengal as a source of singlet oxygen led us to explore a second source for singlet oxygen: the disproportionation of hydrogen peroxide by Molybdate ions

$$2H_2O_2 + MoO_4^{2-} \rightleftharpoons 2H_2O + MoO_6^{2-}$$
$$MoO_6^{2-} \rightarrow MoO_4^{2-} + {}^1O_2$$
$$HMoO_6^{2-} \rightleftharpoons H^+ + MoO_6^{2-}$$
$$H_2O_2 \rightleftharpoons H^+ + HO^{2-}$$
$$2H_2O_2 + MoO_6^{2-} \rightleftharpoons 2H_2O + MoO_8^{2-}$$
$$MoO_8^{2-} \rightarrow MoO_6^{2-} + {}^1O_2$$
$$HMoO_8^{-} \rightleftharpoons H^+ + MoO_8^{2-}$$

(MoO_4^{2-}) to singlet oxygen and water [5,6,43]. At low concentrations of peroxide a yellow precipitate is formed (MoO_6^{2-}) whereas is excess peroxide a red-brown precipitate is formed (MoO_8^{2-}). While the reaction is efficient in alkaline conditions it is dramatically decreased at pH 7 [15,43] and we are forced to use high concentrations of peroxide. Incubation of the SOS-GFPS with the individual components of the reaction; hydrogen peroxide had no effect on excitation ratio while molybdate ions slightly decreased the excitation ratio, the drop in ratio was intensified when low concentrations of hydrogen peroxide were added, however upon mixing the components the excitation ratio increase as expected (Figure 4.6.A.). Molybdate was not the only metal found to affect the excitation ratio, Nickel, and Zinc and to a lesser extent iron and copper increased ratios Figure 4.6.B.

Reactions of SOS-GFPs and a selection of non-histidine mutants were exposed to singlet oxygen generated *in vitro* by the disproportionation of hydrogen

peroxide. The GFP mutants with histidine at position 147 exhibited similar responses to $^1O_2$ generated from Hydrogen peroxide disproportionation as they did to that generated from Rose bengal, HH yielded the greatest increase in ratio and HC exhibited a decrease in ratio. Mutants with amino acids other than histidine at position 147 with the exception of MM exhibited a decrease in ratio, or no significant change in ratio (most ratio changes due to decreases in fluorescent emission at both 490nm, Figure 4.7.).

The excitation spectral changes for HH before and after exposure to singlet oxygen generated by the disproportionation of hydrogen peroxide are given in Figure 4.8.A. Increases at 490 nm and decreases at 400 nm are similar to those observed for reaction to singlet oxygen from Rose bengal. Increases in excitation ratios however were fully inhibited in the presence of sodium azide, therefore ratio changes are caused solely by singlet oxygen (Figure 4.9.B). Quenching by azide yielded excitation ratios below that of the starting ratio, to those observed when only molybdate ions are present. We also observed sudden drop in fluorescence at 410nm for ADPA when the H_2O_2/MoO_4^{2-} complexes. Molybdate complexes are yellow and absorb strongly at 350-400nm (Figure 4.9.C), the tail of the absorption peak is sufficient to cause interference at 340nm where ADPA absorbs. Such interference does not account for the excitation ratio changes of SOS-GFP since the complexes do not emit at 530nm. To compare the reactivity of SOS-HH and ADPA, we used the comparable concentrations of hydrogen peroxide and molybdate but the two optimal concentrations for HH and ADPA (1μM and 50μM respectively). Using ADPA as standard we estimated the singlet oxygen concentrations generated at each concentration of H_2O_2 (Figure 4.10). From these concentrations we estimated the rate

constant for SOS-HH as we had using Rose bengal as photosensitizer, which in this experiment was estimated to be $2.49e^{8}$ M^{-1} s^{-1} similar to that estimated for Rose bengal.

Buffer pH influences SOS-GFP excitation ratios--- pH was found to affect the resting excitation of proteins *in vitro*. In acidic conditions the excitation ratios are similar to oxidized form of roGFPs i.e. 490/400 excitation ratios are high. As the solution becomes more basic the 490/400 excitation ratio decreases to resemble that seen for the oxidized form of roGFP Figure 4.11. As pH increased there was a corresponding increase in fluorescence emission for both wavelengths (Figure 4.11A) this increase was observed before and after singlet oxygen exposure. To factor out this effect excitation spectra were normalized to an isosbestic point at 440nm, it is then apparent that excitation ratio changes in response to pH due to solely to increased emission following excitation at the 400nm wavelength 4.12 D and F. For SOS-HH the excitation ratio is maximal at pH 6.2 decreases steadily as pH rises and levels off after pH 8, whereas the excitation ratio of HT-SOS is not at maximal values at pH 6.2 indicating a lower pKa for this mutant. (Figure 4.11 C and E). The double histidine mutant (HH) resulted in greater sensitivity to pH reflected in the larger dynamic range and sharper decrease observed when SOS-HH is titrated in pH buffer compared with SOS-HT. Exposure to singlet oxygen abolished the 400nm sensitivity to pH, the SOS-GFPs resemble the reduced form of roGFP (Figure 4.11 B).

Selectivity of SOSGFP for singlet oxygen--- Several other species of ROS and reactive nitrogen species (RNS) that can be generated intracellularly were tested. SOS-HH and SOS-HT were exposed to: hydroxyl radicals ($OH^{\cdot}$), perchlorate ions,

peroxyl (RNO), Superoxide ions (O_2^-), hydrogen peroxide and nitrous oxide radicals ($NO^{\cdot}$). SOS-GFPs were found to respond solely to singlet oxygen (Figure 4.12).

Effect of singlet oxygen on SOS protein structure---Singlet oxygen destroys the sidechains of several amino acids including histidine, exposure to singlet oxygen has a detrimental effect on most proteins. SDS-PAGE of the SOS proteins following singlet oxygen exposure generated by the disproportionation of hydrogen peroxide reveals a smearing of the GFP band at ~33KDa (Figure 4.13B) singlet oxygen induces many reactions and/or structural changes. No bands were observed corresponding to protein dimmers, suggesting that intermolecular cross-linking does not occur. These results are mirrored by mass spectral analysis the profile for protein digests following singlet oxygen treatment indicate a loss of many protein fragments without the corresponding increases at other peaks of higher or lower masses which would be expected for a simple oxidation reaction (Figure 4.13C).

Singlet oxygen does not cross cell membranes---SOS-GFPs showed similar excitation ratios when expressed in different cell types (HeLa, COS7, HEK293). We have previously demonstrated that production of singlet oxygen by illumination of Rose bengal in stained cells can influence the excitation of cytoplasmic SOS-GFPs. (Figure 4.3). To investigate whether singlet oxygen generated by Rose bengal traverses cell membranes into adjacent cells, COS7 cells expressing cytoplasmic SOS-HH were stained with 1 μM Rose bengal and a portion of the cell was exposed to illumination at 568nm for one minute. The excitation ratio for the whole cell was observed to increase as expected for a freely mobile GFP. However the adjacent cells did not exhibit any significant increase in excitation ratio (Figure 4.14).

Protein proximity assays--- The sensitivity and selectivity of SOS-GFPs has been demonstrated. One of the many possible applications for such proteins would be to combine the ability to produce and sense singlet oxygen in order to demonstrate the proximity of two proteins. Attachment of a singlet oxygen source protein A and a SOS-GFP to protein B, would ideally not induce excitation ratio increases when far apart but would when in close proximity (100nm or less, Figure 15A). Two approaches are possible for testing this system; a) the proteins are triggered to associate or b) proteins are induced to dissociate. Prior to undertaking testing discreet proteins, we first attached a singlet oxygen generator to the C-terminal of SOS-HH and SOS-HV. Membrane permeant dyes that specifically bind to cysteine-rich hexapeptide motifs (CCXXCC) on proteins have been developed in our laboratory. The dyes are biarsenical fluorescent molecules, both a green fluorescent (FlAsH) and a red fluorescent dye (ReAsH) have been developed [13,14] they have a distinct advantage of not being fluorescent until bound. The original binding motif was recently optimized to enhance binding affinity and contrast [36] the new tetra-cysteine tag used in this study was FLNCCPGCCMEP. For proteins expressed *in vitro* the tetracysteine tag was attached to the C-terminal of the SOS-GFPs separated by a heptapeptide linker (SGSGSGS). The protein expressed well *in vitro*, fluorescence was not affected by addition of the linker and tetracysteine tag. The tetra-cysteine motifs were stained with ReAsH, (details for staining procedure are given in the Materials and Methods section), The spectra for ReAsH stained SOS-HH before and after illumination are given in Figure 4.16A the presence of ReAsH could be confirmed by determining fluorescence resonance energy transfer (FRET) between the GFP and the biarsenical dye Figure 4.16 B. Maximal excitation ratios ratio

changes were observed after 10-15 minutes illumination Figure 4.16 C. Singlet oxygen generation and detection were confirmed for a homologous construct.

A mammalian vector for the SOS-GFP-4C construct was expressed in COS7 cells to determine whether detect singlet oxygen would be detected in the cytoplasm. The cells were stained with ReAsH (1μM) for 2.5 hours then washed with EDT and BAL to minimize background staining (see Methods) the resting excitation ratio for stained SOS-HV-4c was higher than for SOS-HV. Upon illumination of cells with 568nm light for 1 min the excitation ratio increased by 14%, illumination for a further 3 minutes decreased the excitation ratio by another 16% (Figure 4.17). As observed for *in vitro* experiments the ratio changes are solely due to increases at 495nm, with negligible decreases at 400nm. SOS-HH-4C with and without ReAsH staining exhibited higher basal ratios than SOS-HH. Illumination of unstained SOS-HH-4C did not alter the excitation ratio. A small ratio increase was observed for cells stained with ReAsH but expressing SOS-HH lacking a tetracysteine tag, this signal is due to singlet oxygen generated by ReAsH that is stained non-specifically.

SOS-HH response to Actin targeted ReAsH---Increasing the level of difficulty would be to detect singlet oxygen generated from a more remote source. An Actin–4C construct was co-expressed with cytoplasmic SOS-HV. ReAsH staining was modified to obtain highly specific staining on Actin filaments; the concentration of ReAsH was halved, washes were for longer duration, and all staining/washing procedures were carried out in HBSS rather than DMEM. Under these conditions ReAsH stained cells expressing SOS-GFPs without 4C did not exhibit increases in ratio due to background staining. There was a dramatic increase in excitation ratio for SOS-HV following a one-minute illumination at 568nm (Figure 4.19). The ratios continued to

increase beyond the time scale of illumination and reached a plateau in about one and half minutes.

Monitoring the enzymatic release of the tetracysteine tag---Having demonstrated that singlet oxygen can be detected from ReAsH at a proximal site and that with many copies of ReAsH we can detect singlet oxygen from a remote site. We next investigated the ability of this system to monitor the release of the tetracysteine tag by enzymatic cleavage. Two tetracysteine fusion constructs with different enzyme cleavage sites were used. The first was SOS-HH-4C, which has a natural cleavage site for Trypsin at the GFP C-terminal just before the linker (DEL**K**YGSGS). The second was an SOS-HH fusion of a metalloproteinase (MMP) cleavage site (PLGLAG) flanked by two linkers between the GFP and the tetracysteine tag.

Trypsin cleavage *in vitro* could be monitored by loss of FRET, the tetracysteine tag was cleaved following at least 2 hours incubation at 37^{o}C. Although Trypsin cleavage of ReAsH stained SOS-HH-4C reduced the response to singlet oxygen (Figure 4.20 d) the reduction was not complete unless the tryptic fragments were physically separated from each other prior to illumination (Figure 4.20 e). Singlet oxygen can travel up to 100nm in solution and we were concerned that the concentration of ReAsH was sufficient to affect SOS-HH post-cleavage. Using diluted samples of the protein-ReAsH complex demonstrated that this was indeed the case, concentrations of protein below 0.5μM exhibited minimal increases in excitation ratio following Trypsin cleavage (Figure 4.21). Cleavage of SOS-HH-PLGLAG-4C with MMP9 required longer incubations, sub-micromolar concentrations of protein were used and this enzyme was also found to abolish singlet oxygen detection (data not shown).

Monitoring protein association by singlet oxygen sensing---As a final demonstration of the power of SOS-GFPs to sense protein-protein interactions we attempted to detect association of two distinct proteins. SOS-HH was fused to the N- or C- terminus of the FK506 binding protein (FKBP) [44] and a tetracysteine tag was fused to the C-terminus of the binding domain (FRB) of FKBP-rapamycin associated protein (FRAP) [45,46]. FKBP and FRB bind in the presence of rapamycin, singlet oxygen production should be detected in this system only after the proteins have been co-incubated with rapamycin. We were unable to detect singlet oxygen by FKBP-SOS-HH following illumination of FRB-4C before or after rapamycin addition in either the *in vitro* proteins or those expressed in cells. Failure of this experiment was ultimately attributed to the failure of the protein constructs to associate upon exposure to rapamycin, FRET between SOS-HH and ReAsH was not detected, nor were complexes of the correct size retained in 30MW microcon columns (Millipore, MA).

D. Discussion

By mutating positions 147 and 204 of roGFP2 we have developed singlet oxygen sensors. As they based on GFP they are genetically encoded and thus can readily be expressed in any cell/tissue of interest. Furthermore since the reaction to singlet oxygen is monitored through changes in excitation ratio the proteins are not influenced by the concentration. The reaction to singlet oxygen is irreversible, allowing small signals to be detected. Singlet oxygen sensing GFPs (SOS-GFPs) are very specific for singlet oxygen, other reactive oxygen species were found to be ineffective. The proteins were identified from a series of mutations in which we replaced the cysteines of the redox GFPs with amino acids thought to be sensitive to oxidation, histidine, tryptophan and lysine. Originally we had surmised that we might

induce cross-linking from oxidized side-chains of histidine, tryptophan and lysine as has been described in nature [23-25,27,47]. Photodynamic cross-linking can occur in which the interaction of singlet oxygen with either normal or reactive species of a photoactivatable amino acid or free amine group [22].

Expression of the first set of mutations in cells revealed elevated excitation ratios (400/490) as compared to roGFP2, such elevated ratios were unexpected as we had theorized that only after oxidatively induced cross-linking would we observe any alteration in excitation ratio. An expanded series of mutations were synthesized including additional amino acids thought to play a role in oxidation/cross-linking (tyrosine, methionine, arginine, threonine, leucine and proline [38,39,48-50]. Elevated excitation ratios were found for many of the mutations. There is no simple explanation for the difference in excitation ratio among the mutants but it appears that amino acids at position 147 have a greater influence than those at position 204. Although the bulky amino acids (those with cyclic side chains Trp, Tyr, Pro, His) at position147 exhibited higher basal ratios, mutants with less bulky side chains were also elevated (Leu, Met and Lys), and yet arginine a similarly sized amino did not result in elevated ratios. At position 204 the amino acid most likely to yield elevated ratios was glycine. Likewise charge was not a consideration as both histidine and lysine were elevated and arginine was not. A full set of all possible combinations of these amino acids at the two positions would be needed to answer the question.

In cells the mutants did not react to hydrogen peroxide but most were found to react to singlet oxygen produced by photosensitized Rose bengal. However most of these reactions involved an ablation of fluorescence following treatment. Exceptions were examples containing histidine at position 147 or 204, for these mutants singlet

oxygen treatment induced an increase in fluorescence at 525nm when excited at 490nm and induced less fluorescence when excited at 400nm. Since following singlet oxygen exposure a greater change was found to occur at the 490nm wavelength, we reversed excitation ratios and thenceforth used 490/400nm. Tyrosine double mutants did in fact give an increase in the 400/490 ratio similar to that seen for redox GFP and as we would have originally predicted but the ratio change was not pronounced and furthermore was a result of decreases in fluorescence for both excitation wavelengths. For the tyrosine mutants and some tryptophan mutants the initial ablation of fluorescence has a modest recovery.

The three mutants with the greatest dynamic range were SOS-HH, SOS-HV and SOS-HT. To examine their properties more closely we expressed the three proteins in a bacterial system and employed a histidine tag on the N-terminus for purification. The excitation ratios found for the proteins *in vitro* were not significantly different from those found in cell cytoplasm indicating that the ratios found in the cell are due to unmodified proteins singlet oxygen (nor any other ROS) is not present at any detectable amount. Additionally the N-terminal His-tag does not seem to affect the protein excitation ratio.

The SOS-GFPs were compared to 9,10-Anthracene dipropionic acid (ADPA) one of the few water-soluble singlet oxygen quenchers available [51,52]. Singlet oxygen was initially produced as it had been in the cell using 568nm illumination of Rose bengal. At pH 7 Rose bengal exists as a dianion with a maximal absorption at 568nm (ε=72,800M-1cm-1) giving an excited state capable of generating singlet oxygen [9]. The comparison of sensitivity to singlet oxygen by SOS-GFPs and ADPA was hindered by the differences in monitoring the two molecules. SOS-GFPs were

monitored by following changes in fluorescence at 530nm following excitation at one of two excitation wavelengths, whereas ADPA was monitored by decreases in emission following excitation at 397nm. The former requires an excitation scan gathered at a single emission wavelength while the latter requires an emission scan generated by a single excitation wavelength, and the two could not be carried out simultaneously. To ensure the dose of light was identical the two were illuminated simultaneously. The rate constants of the two sensors were very similar. Detection of singlet oxygen was similar to that of ADPA suggesting that the GFP does not behave as a singlet oxygen sink, with only a few molecules of singlet oxygen generating a response. It remains to be determined whether singlet oxygen need to interact only with His 147 or His, Thr or Val at position 204, to generate a signal or whether singlet oxygen hitting amino acids other than these two sites can generate signal. SOS-HH was found to be more sensitive at lower concentrations this may be due to protein aggregation at higher concentrations, which is not unknown for GFP [53] and can easily be remedied by an Ala206Lys mutation.

Rose bengal suffers from one major disadvantage as a photosensitizer, it photo-bleaches. During illumination it undergoes Type I reactions in which radical forms are generated not only destroying the photosensitizer but which may form adducts with other molecules. The failings of Rose bengal were evident by the lack of inhibition of singlet oxygen production with sodium azide. Only at low concentrations of Rose bengal was sodium azide inhibition complete. Indications of Rose bengal adducts to the protein were seen by the diminished fluorescence at high concentrations of Rose bengal.

An alternative source for singlet oxygen is the disproportionation of hydrogen peroxide by Molybdate or tungsten ions [5,6,43]. Although the reaction produces quantitative amounts of singlet reaction it is optimal in alkaline conditions [6] and is not widely used for biological studies. At pH 7 we found that concentrations of hydrogen peroxide in the 10-30mM range were required to generate sufficient singlet oxygen for detection by either ADPA or the SOS-GFPs. The singlet oxygen produced was efficiently inhibited by sodium azide. One small disadvantage of this system was interference from the yellow diperoxo- (MoO_6^{2-}) and brown tetraperoxo- species (MoO_8^{2-}). In experiments using ADPA for singlet oxygen detection method correction for absorbance at 410nm by these species was made. In experiments using SOS-GFPs a decrease in ratio was observed which is not attributable to absorbance by these colored complexes since they do not fluoresce. Molybdate ions were found to decrease the basal ratio for SOS-GFPs slightly but decreases were enhanced when low concentrations of hydrogen peroxide were also present. The effect of singlet oxygen eventually overcomes the ratio decrease. Excitation ratios were also found to be influenced by other metals, notably zinc and nickel. Using the rate constant obtained from ADPA we estimate that the rate constant for SOS-HH to be $3 \times 10^9\ M^{-1}s^{-1}$.

Six mutants with histidine at position 147 and nine non-histidine mutants were exposed to singlet oxygen generated by decomposition of molybdate complexes. Excitation ratio changes were similar to those observed using Rose bengal. MM which exhibited a general increase in fluorescence but only a slight increase in excitation ratio? The changes in excitation spectra for SOS-HH were very similar to that seen for Rose bengal, yet even at the highest concentrations used (50mM)

sodium azide was able to fully inhibit the detection of singlet oxygen, indicating a much cleaner reaction. The sensitivities of ADPA and SOS-HH likewise were similar in this system.

The excitation ratios of SOS-GFPs were found to be sensitive to pH which is not surprising since GFP-S65T [54] and roGFP2 [34] are pH sensitive. For GFP the neutral or protonated chromophore (corresponding to the 400 peak) is maintained hydrogen bonding and electrostatic repulsion by Glu 222, Ser 205, His 148 and a water molecule,. The ionized or deprotonated chromophore (corresponding to peak 490) has an altered Thr 203 conformation and loss of hydrogen bonding between Ser205 and Glu222 [54]. In alkaline conditions the deprotonated form is favored. Normalized excitation spectra revealed ratio changes were predominantly due to increased emission following excitation at 400nm. For SOS-GFPs alkaline conditions permits the neutral form of the chromophore, the pH sensitivity is dependant on His 147 as singlet oxygen destroys pH sensitivity. Histidine at position 204 also plays a role as replacement of His by Thr reduces range of the 400nm peak. The pH titration curve most resembles that observed of a pH sensor based on E2GFP (F64L/S65T/T203Y/L231H) [55], but in this case the protonated form is stabilized by tyrosine at 203, it would be interesting the effect of mutating Thr203 in SOS-HH. Since pH predominantly effects the 400nm peak and singlet oxygen exposure predominantly effects 490nm peak, we have a means in a biological setting to distinguish between ratio changes due to pH shifts or those due singlet oxygen exposure.

Other reactive oxygen and nitrogen species were found to have no effect on the excitation ratios of the SOS-GFPs, notably hydroxyl and superoxide ions were not

found to react. We are confident that we have a very selective system for the detection of singlet oxygen in biological environments.

We have not made significant headway in determining the mode of action of singlet oxygen. The chemistry of the oxidation by singlet oxygen of phenylalanine tyrosine and tryptophan are well defined but those of histidine are poorly understood [49] the major sites of attack in all cases are usually the aromatic rings with tryptophan this results in ring cleavage [49,56] products N-formylkynurenine,3-hydroxyknynurenine and kynurenine. Singlet oxygen oxidation of histidine occurs via an initial formation of an endoperoxide generates number products (up to 17 identified for benzoylhistidine) [19] including aspartic acid and urea via several intermediates including 2-oxohistidine [56]. SDS page of the proteins did not provide evidence of intermolecular cross-linking, no bands corresponding to dimers were observed. Singlet oxygen treatment generated a smearing of the band at 30,000 this was found whether the protein was SOS-GFP or another non-sensitive mutant, we are probably only seeing evidence of protein destruction by this method. Damage to proteins by singlet oxygen includes oxidation of sidechains and backbone breakage (although occurs rarely), and may result in dimerization, aggregation, conformational changes or unfolding. Mass spectral analysis was no clearer, spectra of digested protein after singlet oxygen reflected damage to protein by loss of many peaks, there was not however a concomitant rise in new peaks as would be expected for a single reaction. The only addition identified was to methionines in which oxygen was added (+16), but since methionines were not found to have a significant effect at positions 147 and 204 it is likely they are participating in a SO sink [57]. In future the surface methionines should be mutated to non-sensitive amino acids.

In experiments using membrane localized photosensitizers a small fraction of singlet oxygen generated near the cell surface was found to diffuse into the surrounding buffer [7]. Singlet oxygen molecules exist for about 4 μsec in aqueous solution and diffuse about 100nm [8] in cells the lifetime is about 0.1μsec [7] mostly quenched by biological molecules. (this would be 2.5 nm). We were concerned that singlet oxygen generated in one cell did not traverse across membranes to adjacent cells. Using Rose bengal which primarily labels membranes we produced SO in a single cell by illuminating a portion of the cell and occluding the remainder of the field with an iris shutter. There was no evidence of nearby cell responding to singlet oxygen production in the illuminated cell, the cell in question was found to have a general reaction to SO, demonstrating the speed in which cytoplasmic protein diffuses throughout the cell.

There a many potential applications for genetically encoded SOS-GFPs. Apart from ready targeting to cellular subcompartments, and direct sensing of biological production of SO, such as of UV damage to DNA lipids and proteins [1], by phagocytic destruction of invading microorganisms [3], or by photosystem II in plants [58] singlet oxygen has an important role to play in treatment for cancer. Photodynamic therapy (reviewed in [59]) involves the selective delivery of photosensitizers to tumors, exposure to light generates ROS which induces apoptosis in loaded cells. Ratiometric SO sensors have been described [60] but these consist of ADPA and a SO insensitive dye incorporated into nanoparticles and would need to be injected to cells.

We were interested in using the SOS-GFPs to develop a system for photodynamic monitoring (PDM), attaching SOS-GFPs to one subcellular entity, (e.g. proteins) and attaching a photosensitizer to a second entity (2nd protein, membrane,

etc) one could monitor conditions which bring the entities into close proximity or conversely when the entities separate. Since singlet oxygen diffuses up to 100nm in solution the entities can be large and further apart than those used in fluorescence energy transfer (FRET). Another advantage over FRET is that the relative orientation of the two entities will not critical.

The Tsien laboratory is a leader in the field for fluorescent small molecules that bind specific genetically encoded tags. Two such biarsenical tags have already been used to generate singlet oxygen to inactivate proteins by a process termed chromophore light assisted light inactivation (CALI) [61]. Incorporating the two systems was therefore trivial. At first a tetracysteine tag (FLNCCPGCCMEP) was tethered to the C-terminus of the SOS-GFPs. These constructs allowed us to demonstrate the sensitivity of the SOS-GFPs to ReAsH (which has a quantum yield of singlet oxygen at least one order of magnitude below that of Rose bengal) both *in vitro* and in the cell cytoplasm. Singlet oxygen could also be detected on a construct in which the ReAsH tag was more removed from the GFP. It was somewhat unexpected that at concentrations of 1μM singlet oxygen was detected when the tetracysteine tag was enzymatically cleaved. The fragments needed to be physically separated to demonstrate cleavage. At concentrations below 0.5 μM cleaved fragments did not need to be separated to demonstrate cleavage.

Many photosensitizers produce both singlet oxygen and superoxide, singlet oxygen usually predominates but relative amounts are dependant on the type of sensitizer, excitation wavelength and reaction conditions [2]. Like Rose bengal, ReAsH produces more just singlet oxygen upon excitation, in order to demonstrate that excitation ratio changes induced by illumination are SO derived, we used sodium

azide as a ROS quencher and deuterated water which prolongs the half-life of singlet oxygen. Both systems indicated that the signals were SO mediated.

Targeting the SOS-GFPs to proteins in the cell allowed us to demonstrate the ability of SO to traverse greater distances than FRET. The lifetime within the cells is estimated to be 0.1μs, where singlet oxygen is more likely to be quenched due to biological molecules [7]. The concentration of a chemical trap needed to trap singlet oxygen within the cell is approximately 30 fold that required in aqueous solutions [7]. Singlet oxygen produced by Actin-tethered ReAsH could alter cytoplasmic SOS-GFP excitation ratios. Illumination times in the cell were much shorter than those required *in vitro* due to the stronger light source and small volumes involved.

The biarsenical tags are not the only specifically targetable sources of singlet oxygen. Green fluorescent protein has been reported to be capable of producing singlet oxygen [62] and more recently a red fluorescent protein [63] that produces both superoxide and singlet oxygen was described. Examination of recently developed Orange and red fluorescent proteins in our laboratory [37,64] suggest capability of producing singlet oxygen. Incorporation of a GFP based generator of singlet oxygen into the PDM would make the whole system genetically encoded, allowing one to target both producer and sensor to any target of interest with minimum manipulation and until illumination noninvasive.

Our attempts to develop an assay in which the association of proteins was monitored using SOS-GFP and ReAsH were unsuccessful to date. We chose to monitor the association of FKBP and FRB by rapamycin. FK506 and rapamycin are immunosuppressants widely used in liver and kidney transplants [65], they bind to a protein known as FKBP12 which is a peptidyl-prolyl cis/trans-isomerase (or rotamase)

[66]. FKBP 12 is a 108 amino acid protein, which forms an amphiphilic β-sheet containing 5 antiparallel strands [67]. Rapamycin bound FKBP12 and forms a ternary complex with FKBP12-rapamycin associated protein (FRAP) [45,46]. FRAP is a large protein 289kDa and a minimal binding domain (FRB) has been elucidated [68]. There is no interaction between the proteins until rapamycin is present and though rapamycin binds to FKBP with moderate affinity (μM) the complex binds FRB tightly (nM) [69]. Fusions of FKBP and FRB to proteins (have been used previously in protein proximity assays [70], but in studies in which both FKBP and FRB are fusions to proteins (e.g. split luciferase or GFP) [70,71] the systems were successful if multiple FKBP units were used, [70] or the whole construct tethered [71] or if mutants of FKBP and FRB which are selective for a rapamycin analogue (Ariad Pharmaceuticals, Cambridge MA) were employed [72]. Our constructs were not induced to dimerize by rapamycin, although we tried placing the GFP and both the N- and C-terminus of FKBP, it is possible that the linkers were not optimal, or that the fusion protein/peptide interfered with the binding interface.

E. Conclusions

Singlet oxygen sensing proteins will have a wide variety of applications. Being genetically encoded gives them great power to target specific sites, and being ratiometric means one is not dependant on their concentration. When used for detection of protein proximity they would have a couple of advantages over FRET (fluorescent resonance energy transfer) constructs; they would exhibit sensitivity over greater distances (up to ~100nm) and they would be less dependant on orientation. They would need to be used with caution as singlet oxygen is cytotoxic, and one would not wish to use them with proteins that have singlet oxygen sensitive amino

acids in critical positions. The next step would be to develop genetically encoded singlet oxygen generators, which is currently underway in this laboratory.

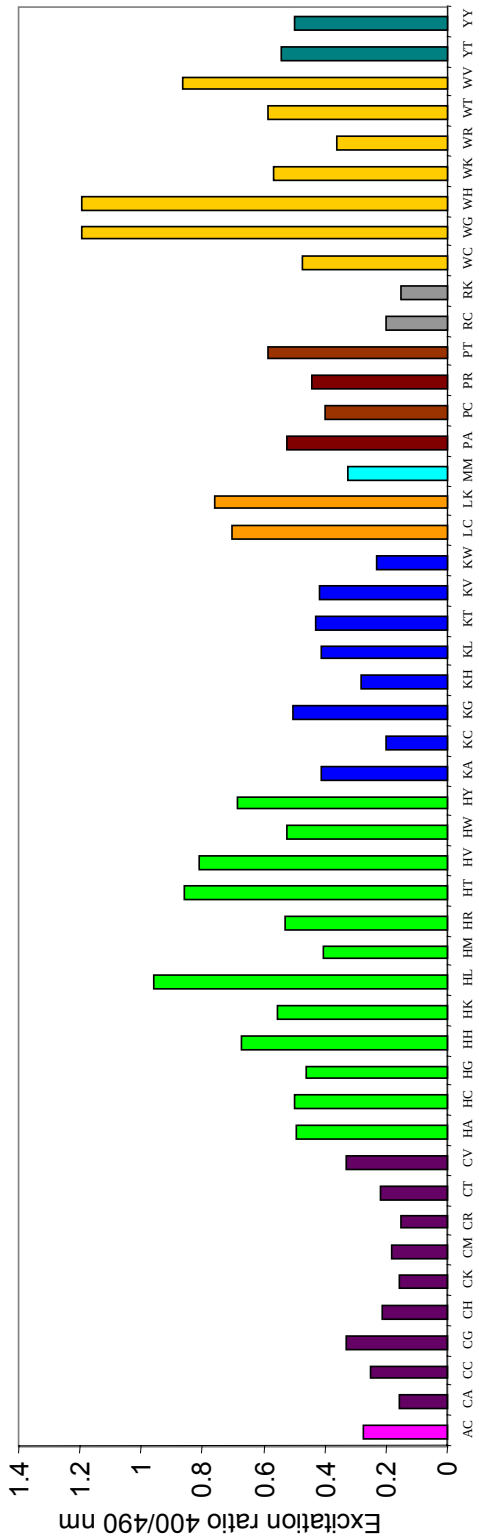

Figure 4.1: Excitation ratios of roGFP2 mutated at positions 147 and 204. Mutated proteins were expressed in the cytoplasm of Cos7 cells or Hek 293 cells. Cells transfected with 147C204W did not express fluorescent protein. RoGFP2 is represented as CC.

Table 4.1. Excitation ratios for roGFP2 mutations positions 147 and 204 before and after singlet oxygen exposure

Mutations 147/204	Pre-illumination Excitation ratio 490/400	Post Illumination Excitation ratio 490/400	Δ 400nm	Δ 495 nm
CH	4.8 ± 0.21	3.6 ± 0.15	↑	↓
HA	1.8 ± 0.27	1.9 ± 0.3	→	→
HC	1.5 ± 0.13	1.5 ± 0.19	↓	↓
HG	2.3 ± 0.23	2.5 ± 0.43	↓	↓
HH	1.5 ± 0.07	3.0 ± 0.22	↓	↑
HK	1.3 ± 0.57	1.5 ± 0.74	↓	↓
HL	1.3 ± 0.05	2.0 ± 0.17	↓	↑
HM	2.4 ± 0.06	2.5 ± 0.06	→	→
HR	2.3 ± 0.36	2.3 ± 0.37	↓	↓
HT	0.9 ± 0.03	1.64 ± 0.10	↓	↑
HV	1.1 ± 0.07	1.8 ± 0.20	↓	↑
HW	1.9 ± 0.20	2.3 ± 0.19	↓	↓
HY	1.7 ± 0.08	1.9 ± 0.08	→	→
KG	3.8 ± 0.5	3.6 ± 0.5	↓	↓
KH	4.0 ± 0.06	4.7 ± 0.12	↓	↓
KW	4.5 ± 0.61	3.2 ± 0.64	↓	↓
LC	1.8 ± 0.12	1.7 ± 0.07	↓	↓
LK	1.5 ± 0.13	1.3 ± 0.24	↓	↓
PT	1.7 ± 0.06	1.6 ± 0.06	↓	↓
WG	1.1 ± 0.09	1.6 ± 0.11	↓	↓
WH	1.5 ± 0.06	1.8 ± 0.09	↓	→
WK	2.0 ± 0.21	1.8 ± 0.20	↓	↓
WT	1.8 ± 0.05	1.7 ± 0.07	↓	↓
WV	1.3 ± 0.02	1.3 ± 0.02	→	→
YT	1.9 ± 0.07	1.6 ± 0.09	↓	↓
YY	2.0 ± 0.15	1.5 ± 0.12	↓	↓

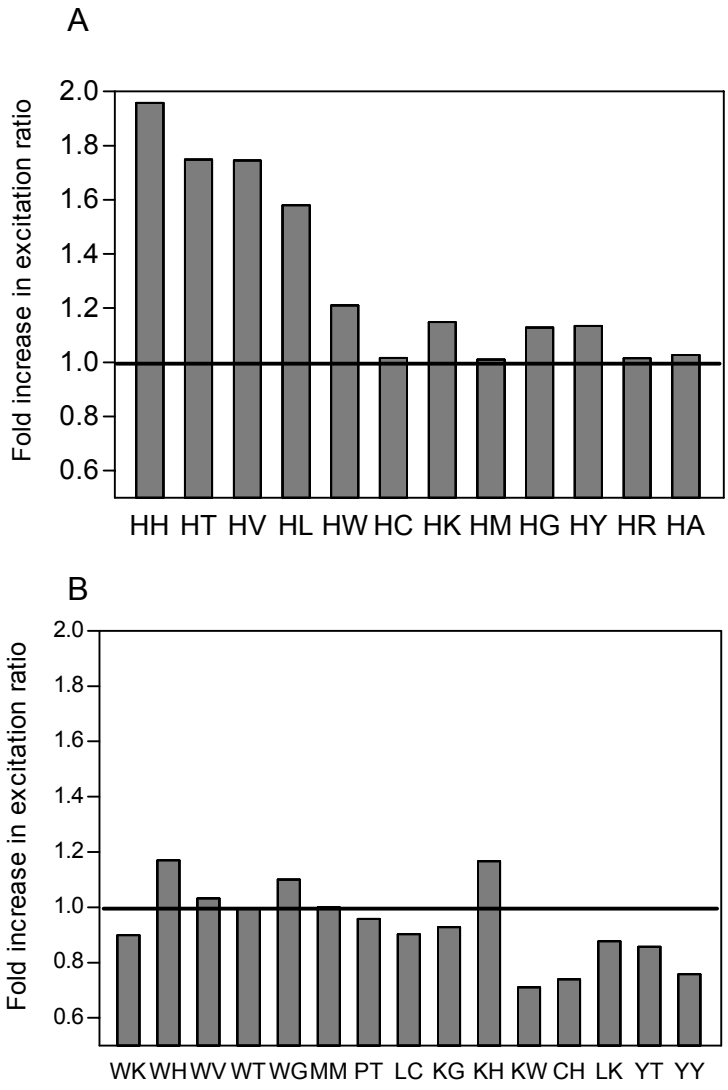

Figure 4.2*:* Specific amino acid residues are required at both positions 147 and 204 for excitation ratio increases observed following exposure to singlet oxygen. Cells expressing roGFPs147X-204Y were incubated in 5μM Rose bengal for 5 minutes then exposed to 568nm for 1 minute. A: COS 7 cells expressing roGFP2-H 147 and 12 different amino acids at position 204. B: Non histidine roGFP2 mutants exhibiting altered basal ratios were also tested for change in ratio upon singlet oxygen exposure. Y axis represents the ratio of excitation ratio before and after exposure to singlet oxygen

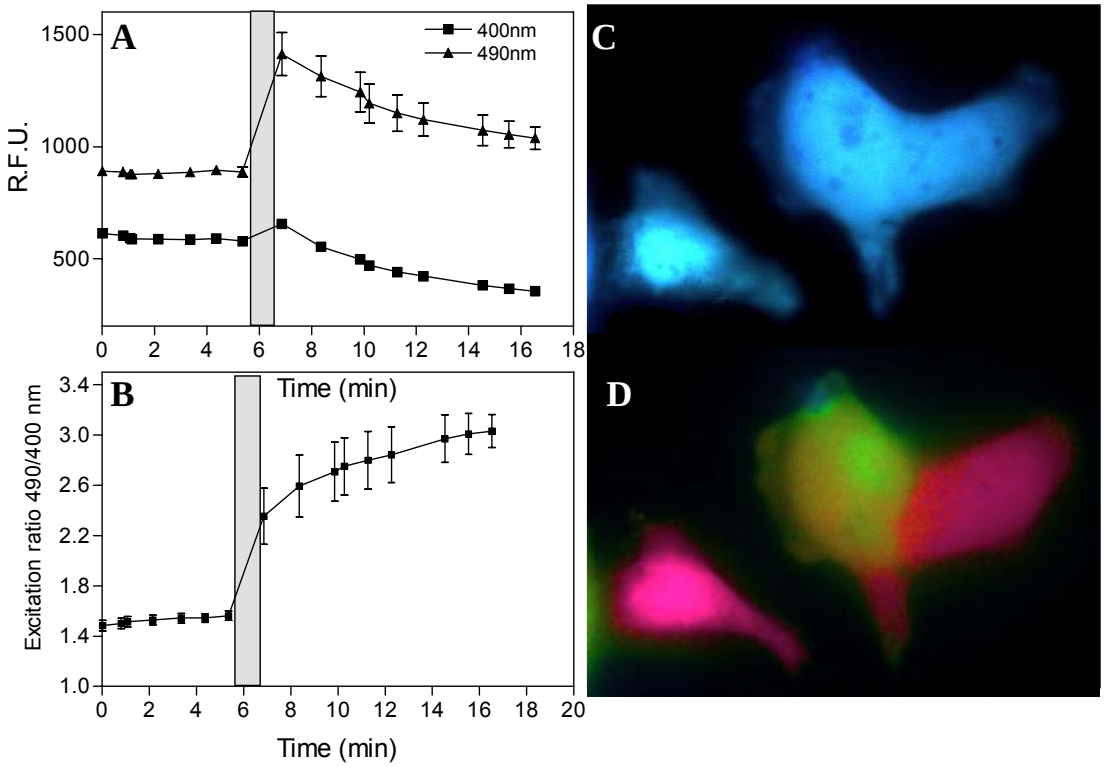

Figure 4.3: SOS-HH senses singlet oxygen in cell cytoplasm: Sos-HH was expressed in COS7 cells. Cells were stained with 5μM Rose bengal for 5 minutes and illuminated at 568nm for 1 minute (grey bar). A) Emission for individual excitation wavelengths, B) Excitation ratios 490/400 nm. Pseudo colour display of excitation ratios in cells C) prior to D) following illumination.

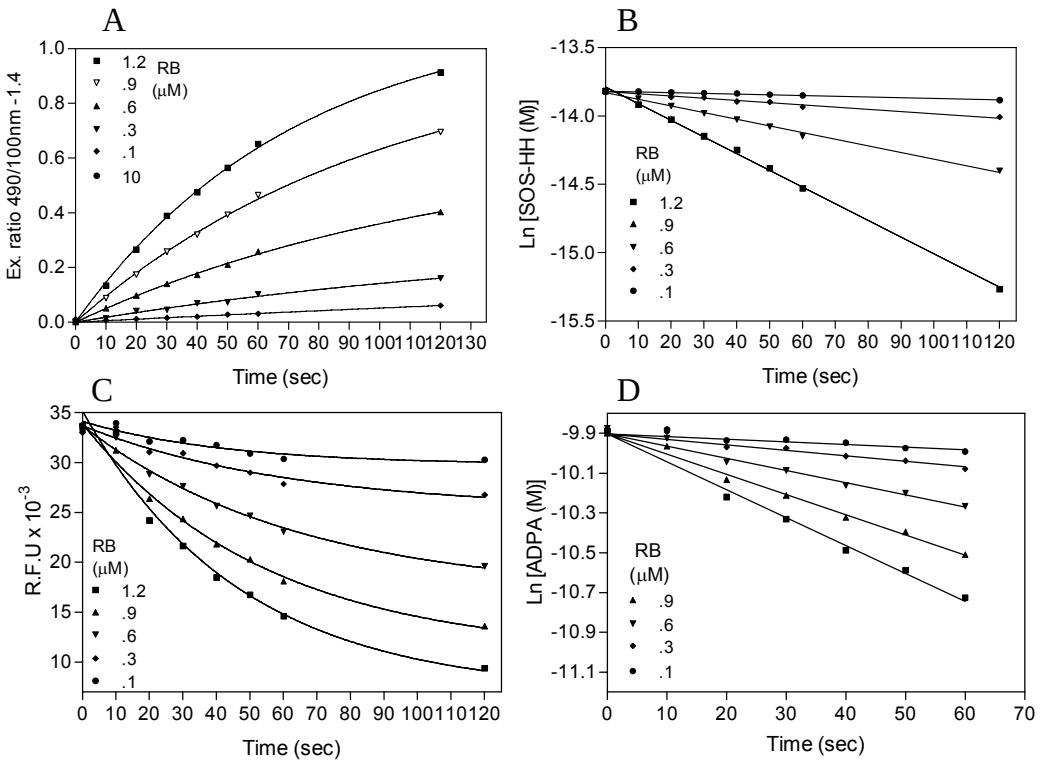

Figure 4.4 Kinetics of singlet oxygen production by the Rose bengal monitored by SOS-HH or 9,10 Anthracene dipropionate (ADPA). A: Increased excitation ratios for SOS-HH with increasing concentrations of Rose bengal. B: Plot of natural log of concentration of SOS-HH versus time. C: Inhibition of florescence emission for ADPA with increasing Rose bengal concentrations. D: Plot of natural log of concentration of ADPA versus time.

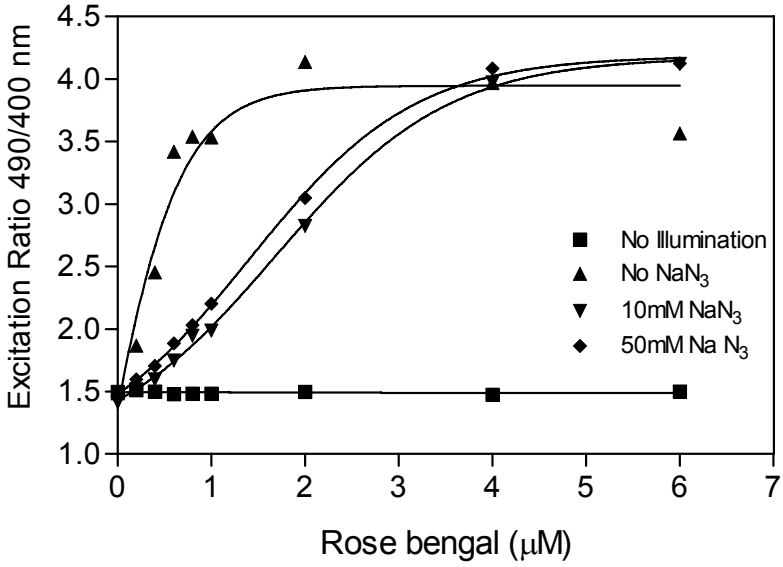

Figure 4.5: Increase in excitation ratio of SOS-HV induced by illumination of Rose bengal is only partially inhibited by sodium azide. SOS-HV (1μM) was incubated *in vitro* with varying concentrations of Rose bengal in PBS buffer (pH 7.4) with or without sodium azide. The samples were illuminated at 568 nm for 5 minutes.

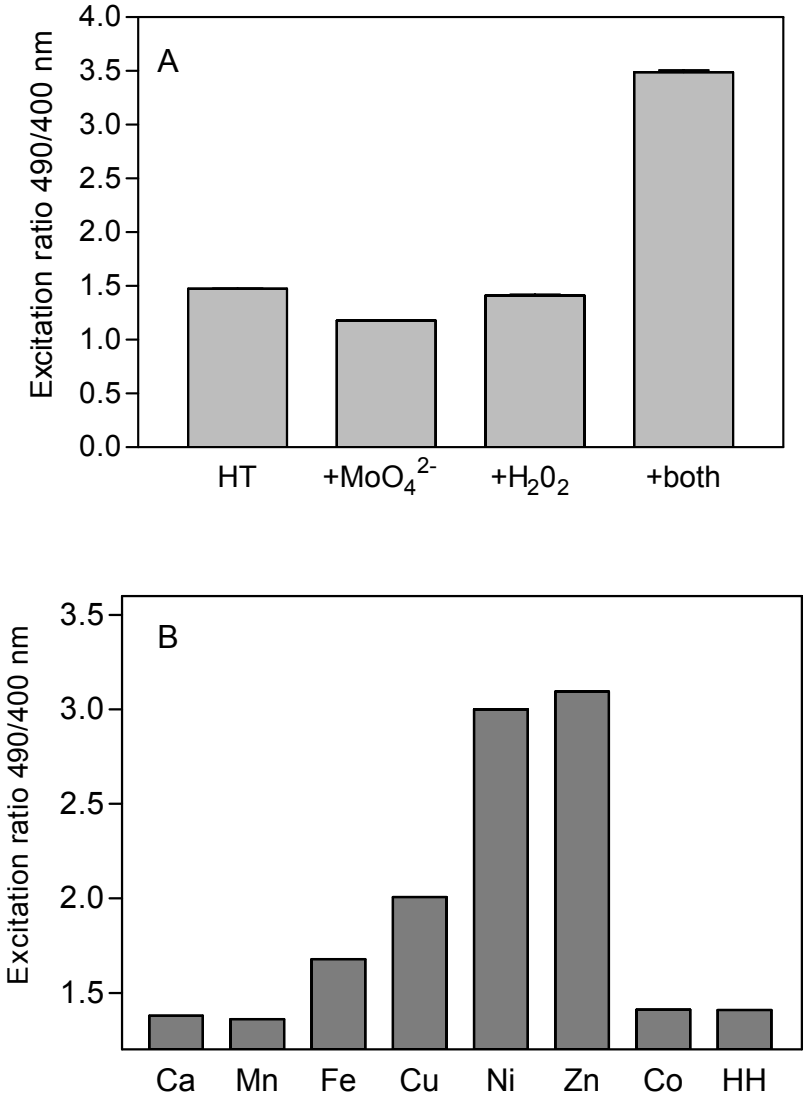

Figure 4.6: Excitation ratio adjustments for components of dispoportionation reaction and for metal ions. A. Singlet oxygen produced by molybdate and hydrogen peroxide increases the excitation ratio of SOS-HT. Molybdate ions decreased the excitation ratio. SOS-HT (1μM) was incubated with 30mM Na_2MoO_4, 30mM H_2O_2 and 30mM of each for 15 minutes in PBS buffer (pH 7.4). B. The presence of certain metals increase the excitation ratio, metals (1mM) were incubated with 1μM SOS-HH.

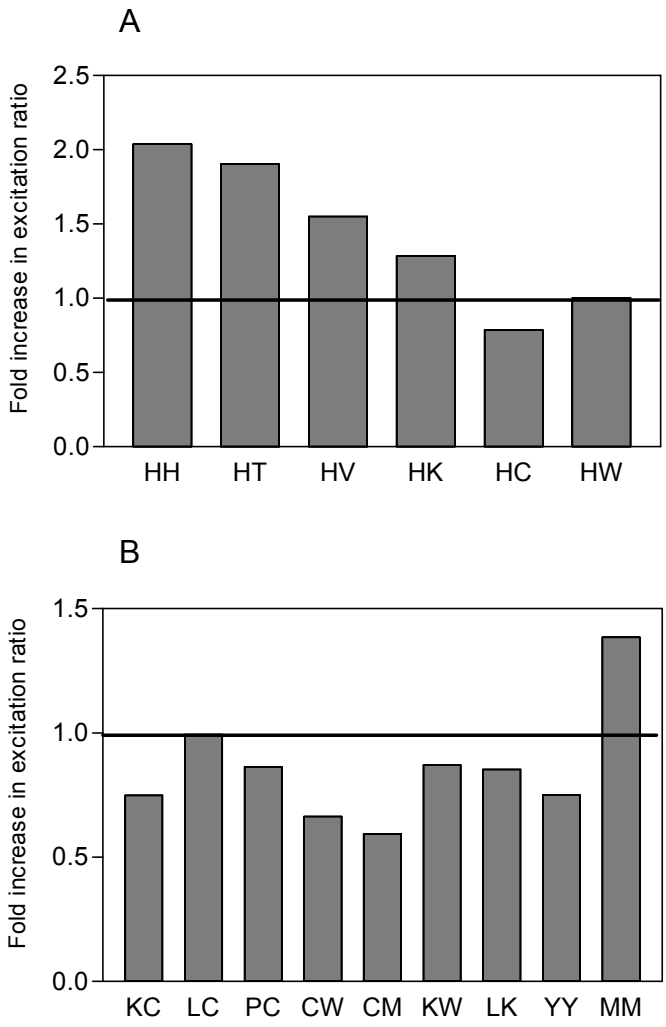

Figure 4.7: Reaction of roGFP mutant proteins to singlet oxygen produced by molybdate and hydrogen peroxide *in vitro*. The proteins were incubated with 20mM hydrogen peroxide and 20 mM sodium molybdate in PBS buffer (pH 7.4) for 10 minutes. Data are expressed as excitation ratio (490/400) after treatment divided by excitation ratio before treatment.

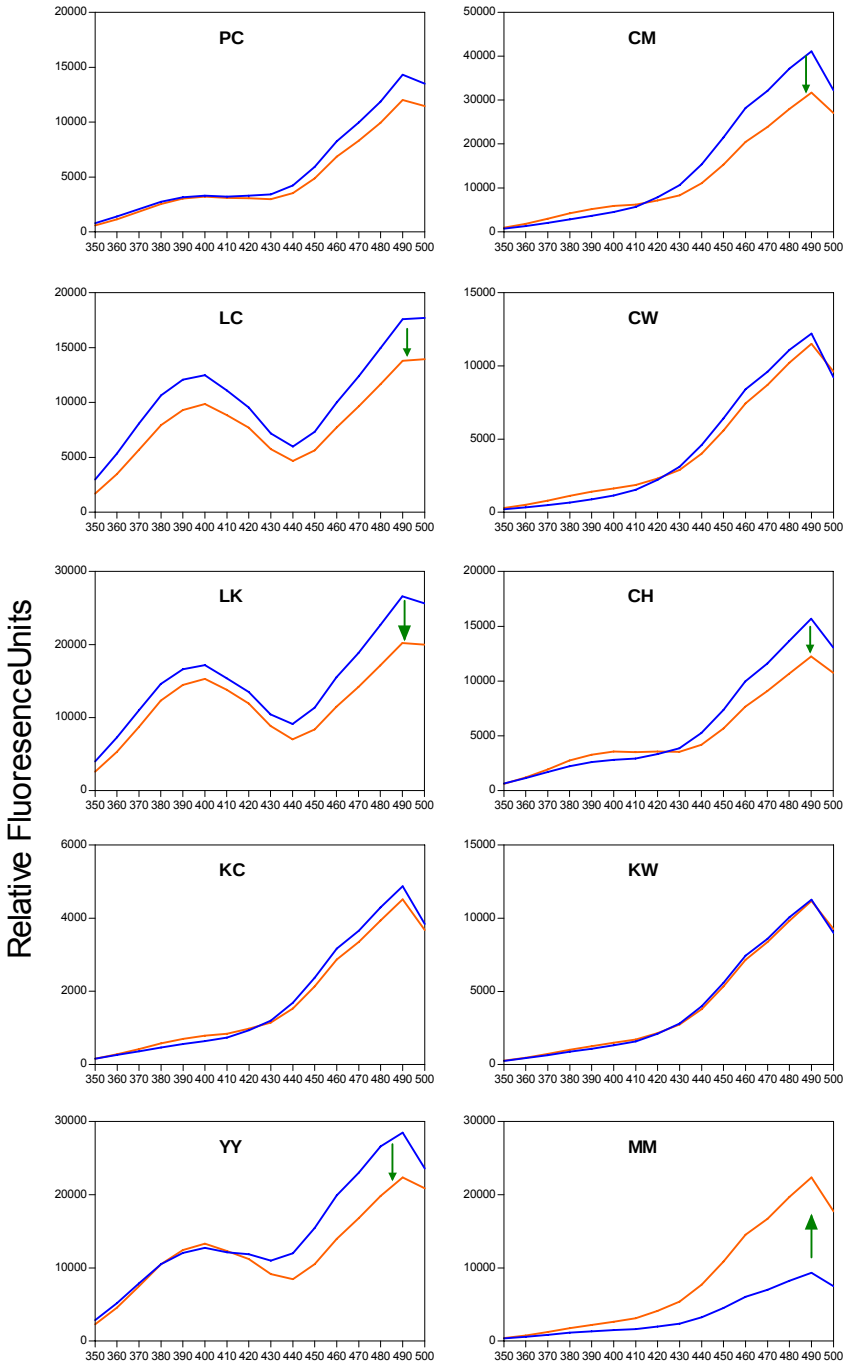

Figure 4.8: Excitation spectra for roGFP mutants *in vitro* before and after singlet oxygen exposure generated by the disproportionation of hydrogen peroxide. Proteins were incubated with hydrogen peroxide and sodium molybdate (both 20mM) in PBS buffer for 10 minutes.

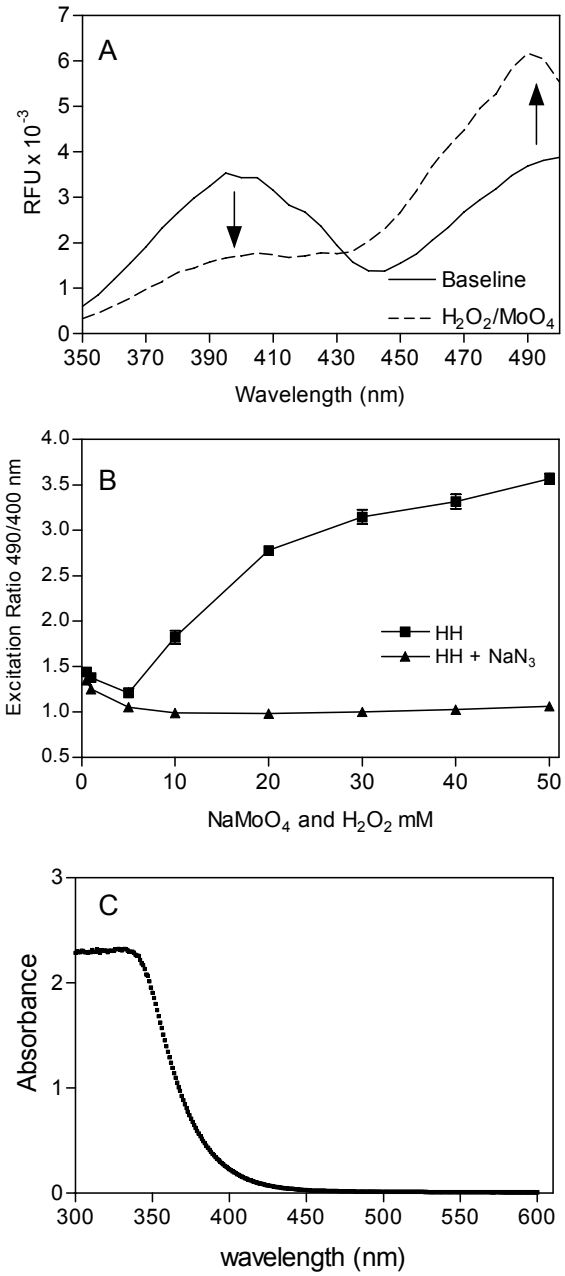

Figure 4.9. Exposure of SOS-HH to singlet oxygen production, by disproportionation of hydrogen peroxide. A: Excitation spectra for SOS-HH before (solid line) and after (dashed line) exposure to Hydrogen peroxide and sodium molybdate (50 mM). B: Excitation ratio changes for SOS-HH are dependant on concentration of singlet oxygen, Sodium azide (50mM) efficiently quenches the reaction. C: Absorbance spectra solutions following reaction of 30mM H_2O_2 and 30mM Sodium molybdate.

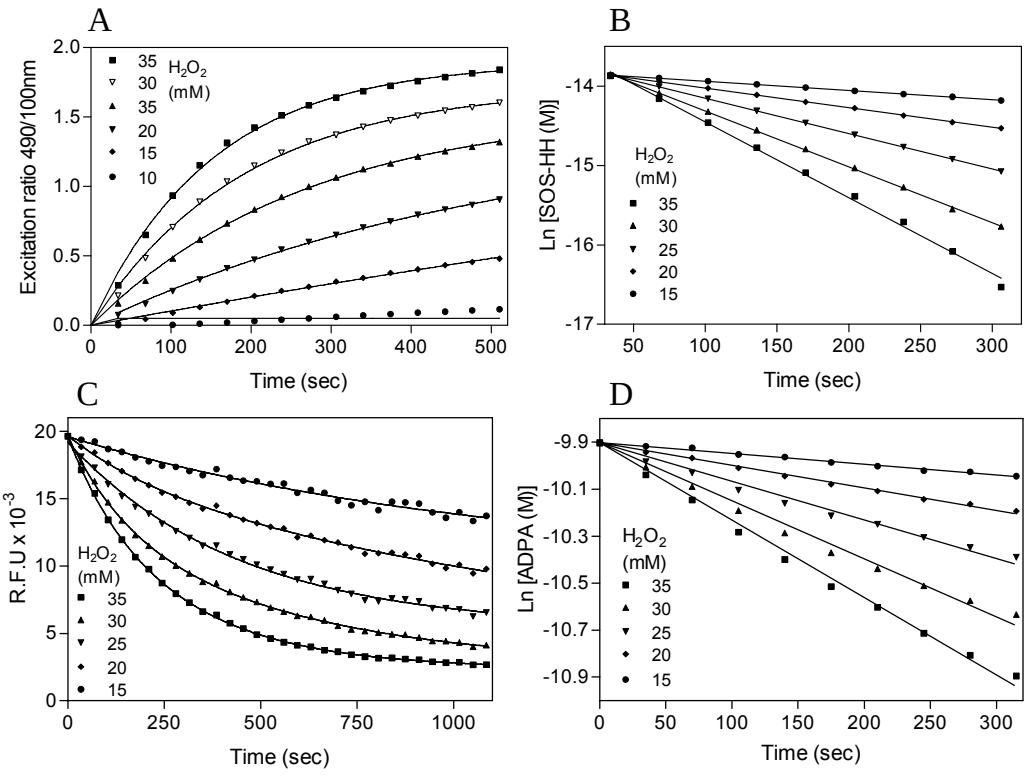

Figure 4.10: Kinetics of singlet oxygen production by the disproportionation of hydrogen peroxide monitored by SOS-HH or ADPA. A: Increased excitation ratios for SOS-HH with increasing H_2O_2 concentrations. B: Plot of natural log of concentration of SOS-HH versus time. C: Inhibition of florescence emission for ADPA with increasing H_2O_2 concentrations. D: Plot of natural log of concentration of ADPA versus time.

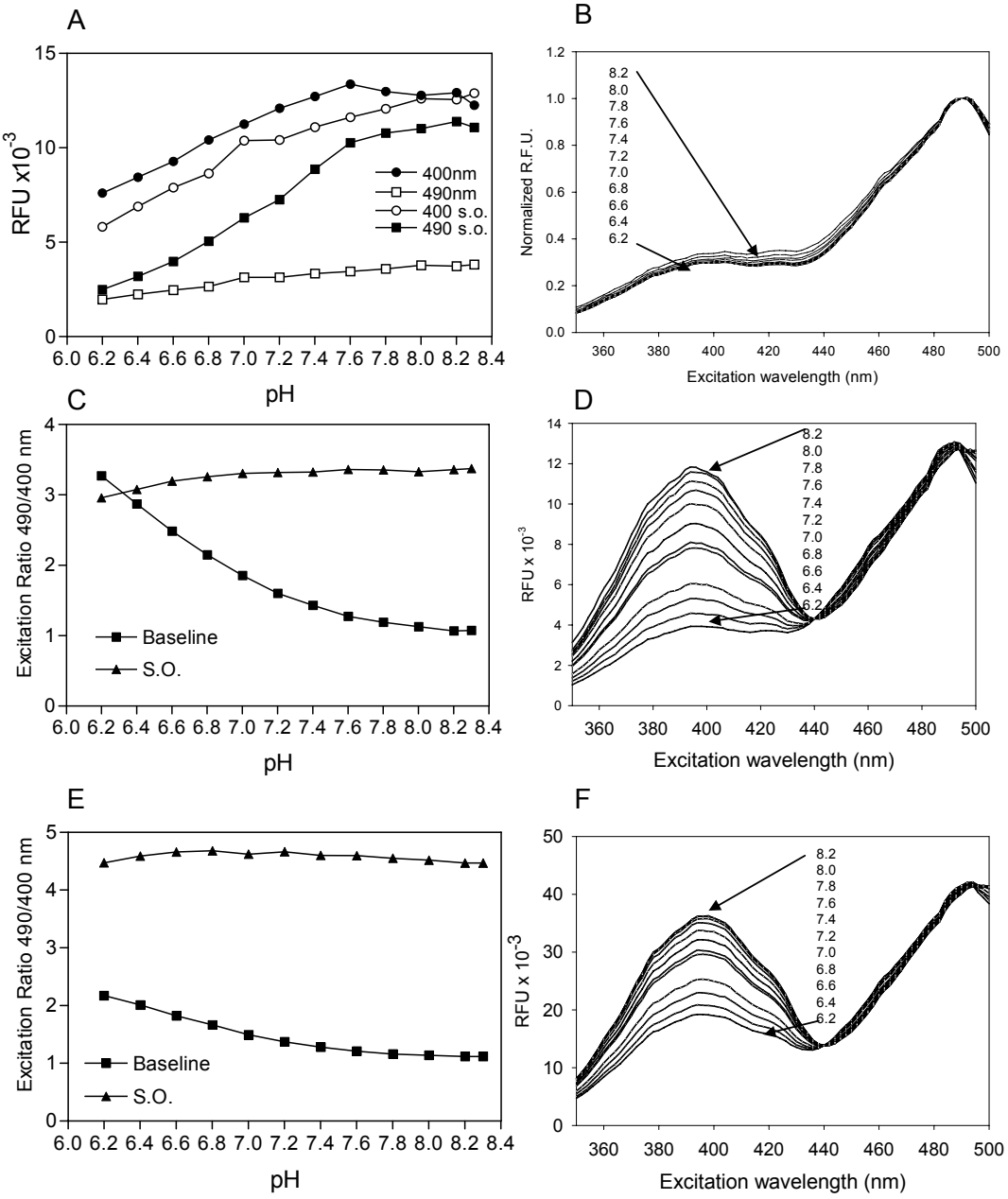

Figure 4.11: Influence of pH on the excitation spectra for SOS-HH before and after singlet oxygen. A) Fluorescence at 400 and 490nm excitation. Normalized excitation spectra for SOS-HH (D) and SOS-HT (F) indicate excitation at 400nm increases fluorescence with increasing pH. (B). Normalized spectra of SOS-HH following exposure to singlet oxygen (30mM H_2O_2/MoO_4^{2-}) the pH sensitivity of SOS-HH at 400nm is abolished. The excitation ratio of SOS-HH (C) and SOS-HT (E) before and after singlet oxygen, pH sensitivity occurs before singlet oxygen exposure but not after.

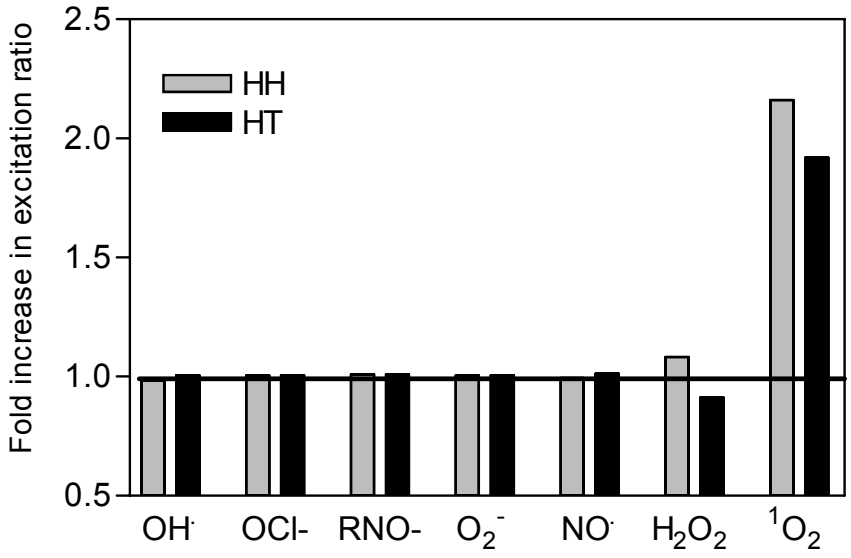

Figure 4.12: Selectivity of SOSGFPs for singlet oxygen. SOS-HH and SOS-HT were exposed to a variety of ROS for 30 min at 37°C. (See methods for details). Bars represent the ratio of excitation ratios before and after exposure.

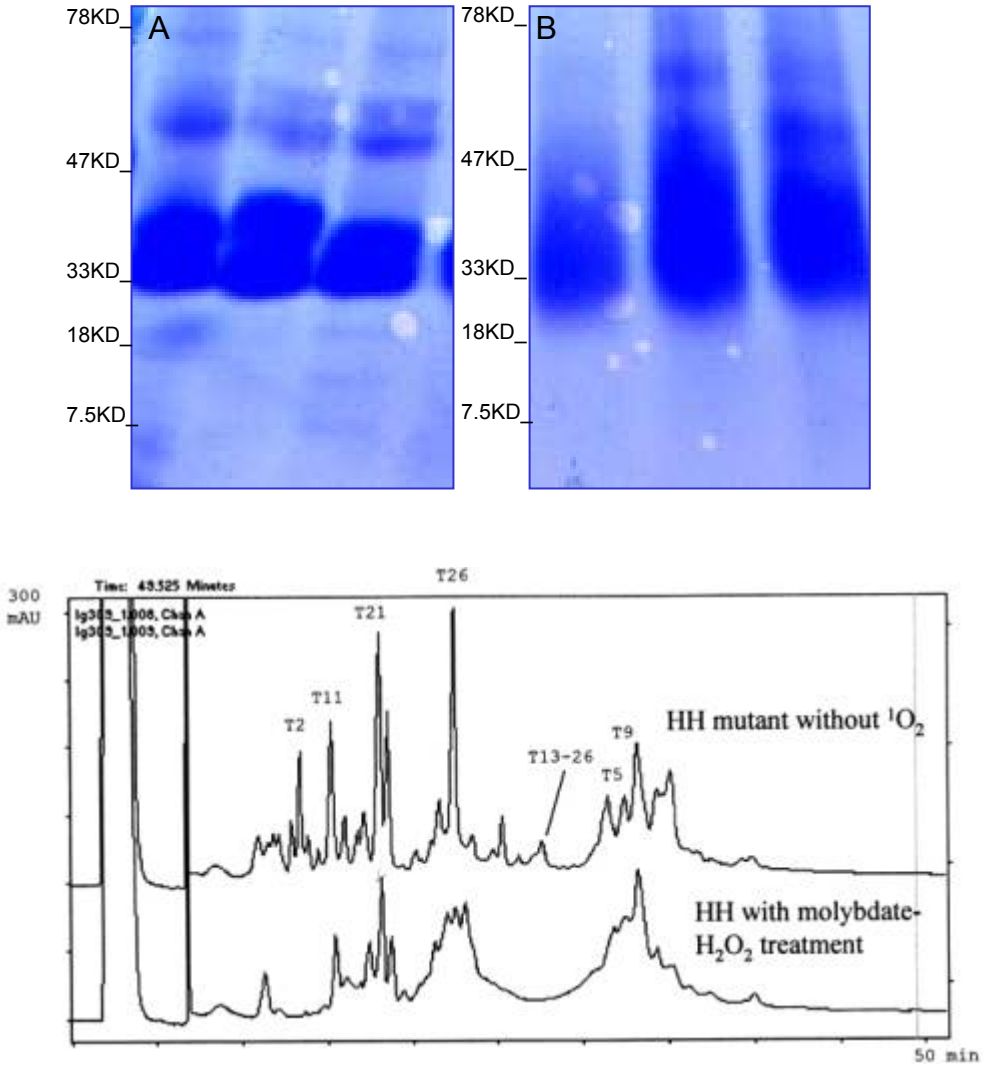

Figure 4.13: SDS-PAGE of SOS-HH, SOS-HV and SOS-HW (left to right) before (A) and after (B) exposure to 30mM H_2O_2/MoO_4^{2-}. Mass spectral analysis of protein digest of SOS-HH before and after treatment with 30mM H_2O_2/MoO_4^{2-} (C).

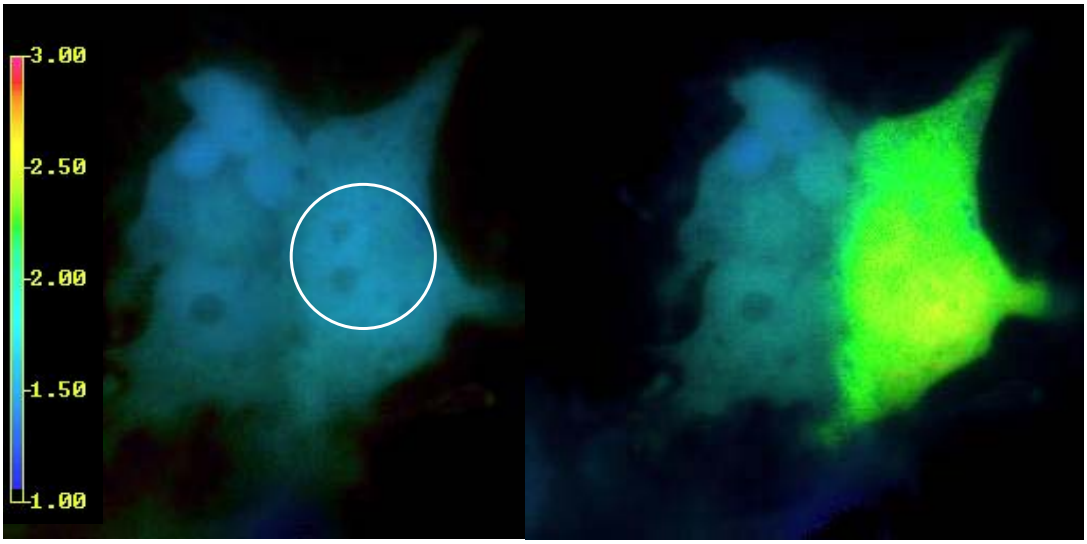

Figure 4.14: Singlet oxygen production in one cell does cross into adjacent cells. COS7 cells expressing SOS-HH were stained with ReASH with 1μM for 2.5 hours washed twice with 1mM BAL. An iris shutter was used to minimize exposure to light to the area indicated in (A). A single cell was exposed to 568nm light for 1 minute.

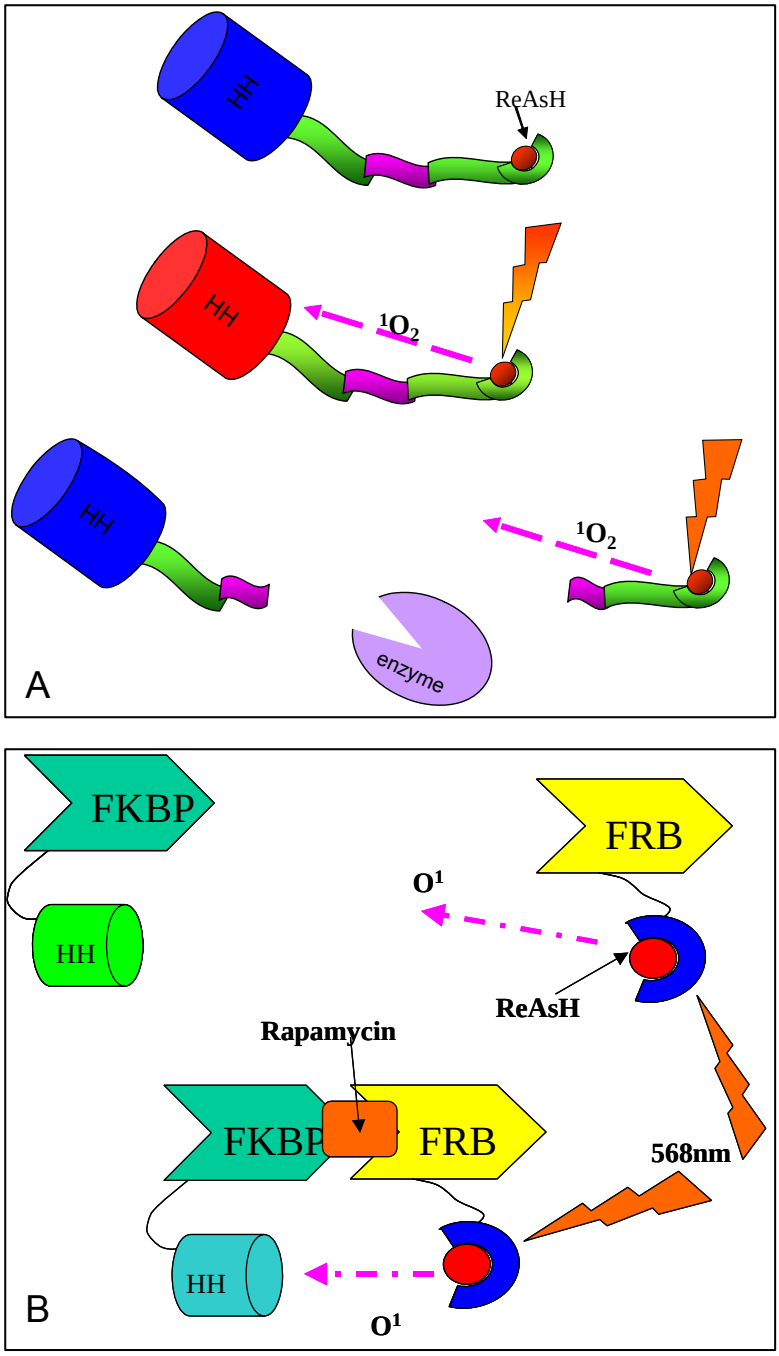

Figure 4.15. Two approaches taken for developing protein proximity assays. A. Singlet oxygen generator and sensor are tethered; following enzymatic cleavage SOS signal is lost. B. Singlet oxygen generator and sensor are induced to associate; SOS signal is only detected when the two proteins are in close proximity.

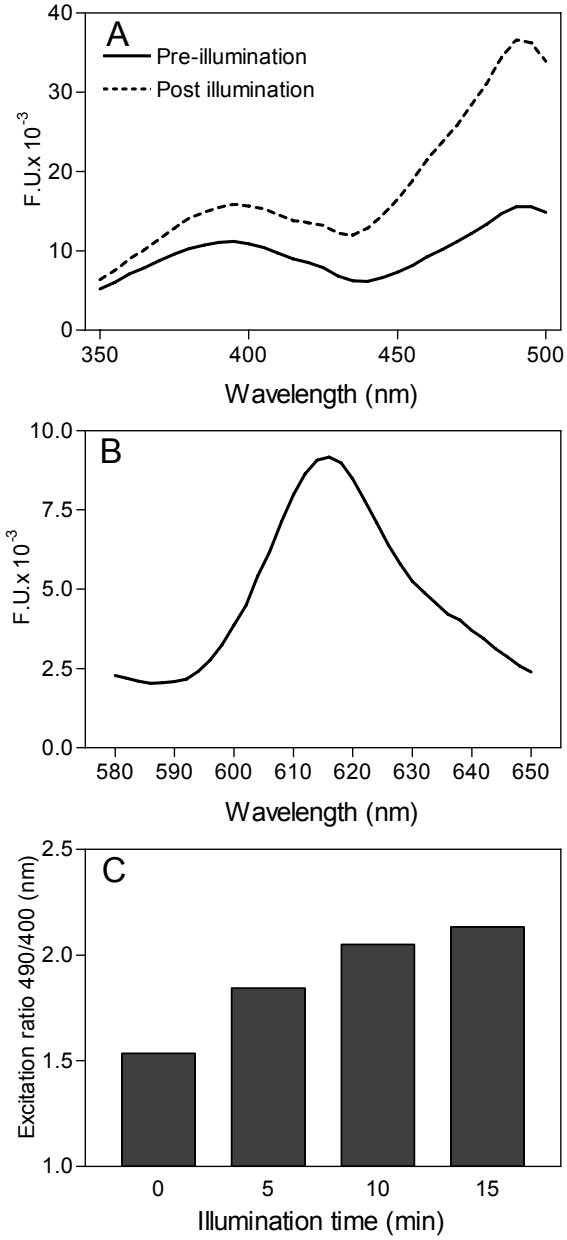

Figure 4.16: The tetracysteine SOS-GFP construct (SOS-HH-4C) stained with the biarsenical dye ReAsH is sensitive to singlet oxygen production by illumination at 568nm. A: Excitation spectra for SOS-HH-4C before (solid line and after (dashed line) exposure to light on solar simulator (568nm). B: Emission spectrum of ReAsH stained SOS-HH-4C following excitation at 490nm, presence of ReAsH is confirmed by FRET emission at 620nm. C: Excitation ratios for the ReAsH stained construct before and after 5,10 and 15 minutes illumination under solar simulator.

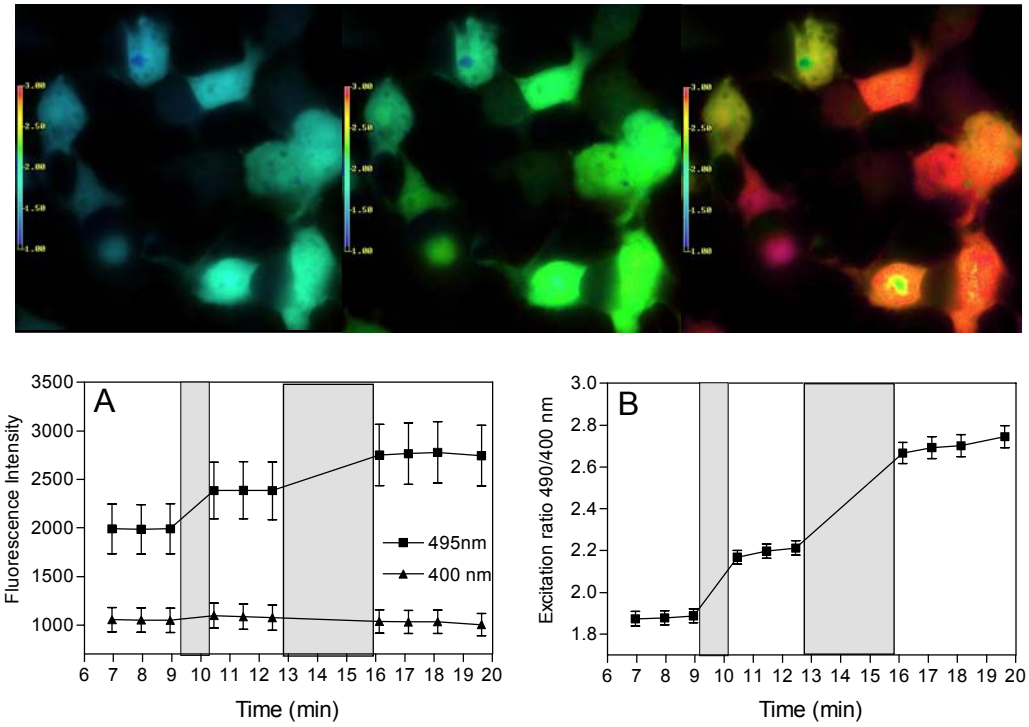

Figure 4.17. Singlet oxygen from a co-targeted source can be sensed by cytoplasmic SOS-GFP. Cells were transfected with SOS-HV-4C. Cells were stained with ReAsH 1 μM for 2.5 hour then washed twice in 10 μM EDT and twice 250 washed μM BAL. A) Individual excitation intensities. B) Excitation ratio 490/400nm. Solid lines indicate 1minute and 3 minute illuminations at 568nm.

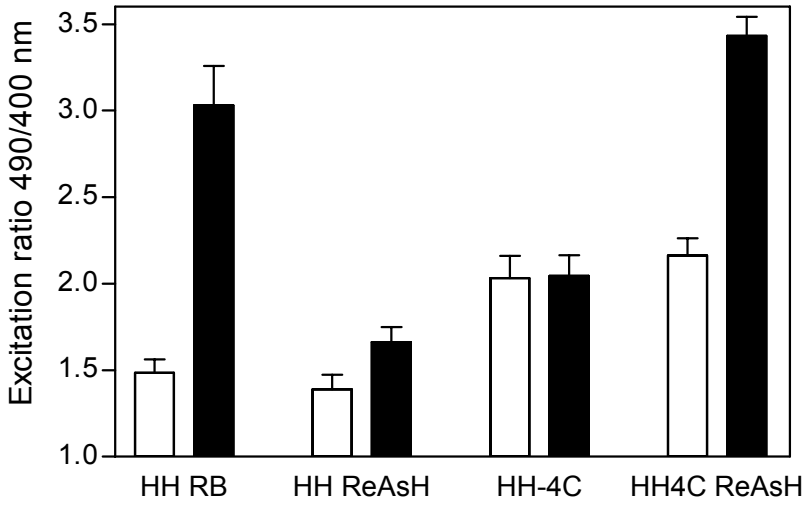

Figure 4.18: Cytoplasmic SOS-HH-4c detects singlet oxygen produced by ReAsH bound to the tetracysteine tag. Two constructs, SOS-HH and SOS-HH-4C were expressed in COS 7 cells. The cells expressing SOS-HH were either stained with 5μM Rose bengal or 1μM ReAsH (see methods), SOS-HH-4C was either stained with 1μM ReAsH or left unstained. Bars represent the excitation ratio observed for the protein before (clear) and after (solid) illumination at 568nm for 1 minute.

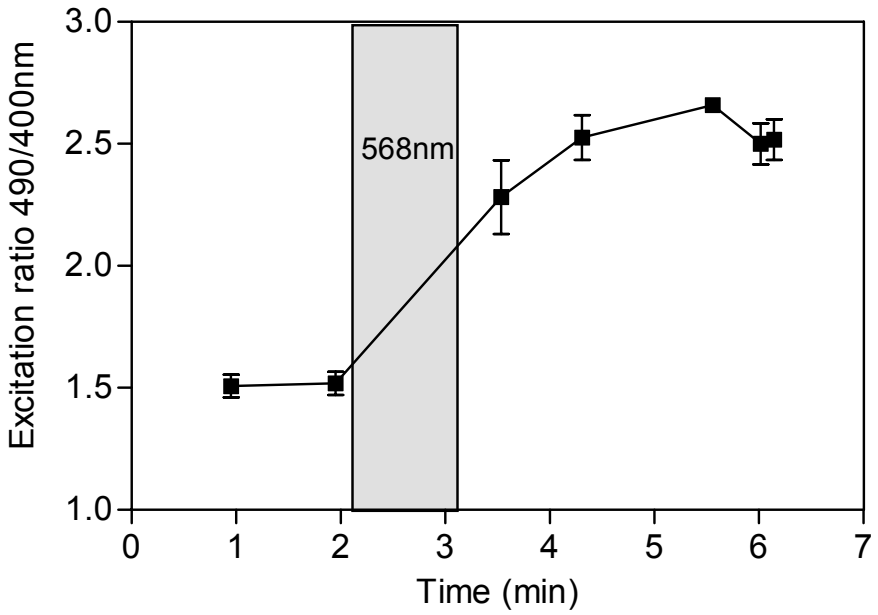

Figure 4.19: Cytoplasmic SOS-HV detects singlet oxygen produced by ReAsH bound to Actin-4C. COS 7 cells co-expressing SOS-HV and Actin-4C were 5μM Rose bengal or 0.5μM ReAsH (see methods) for 1 hour and washed twice with 1mM BAL. Cells were illuminated at 568nm for 1 minute (grey box).

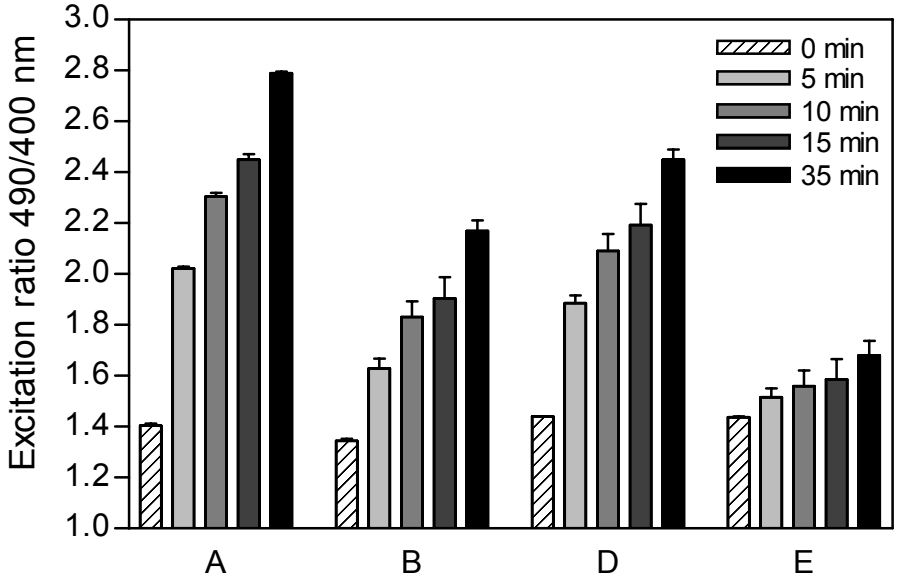

Figure 4.20. When SOS-HH-4C is stained with ReAsH, the light induced singlet oxygen production is detected by SOS-HH-4C in a dose dependant manner. (A). The dynamic range is reduced by washing (buffer exchange) (B). Trypsin cleavage only partially inhibits S.O. detection (D) Physical separation of the tryptic digest is required for full inhibition (E).

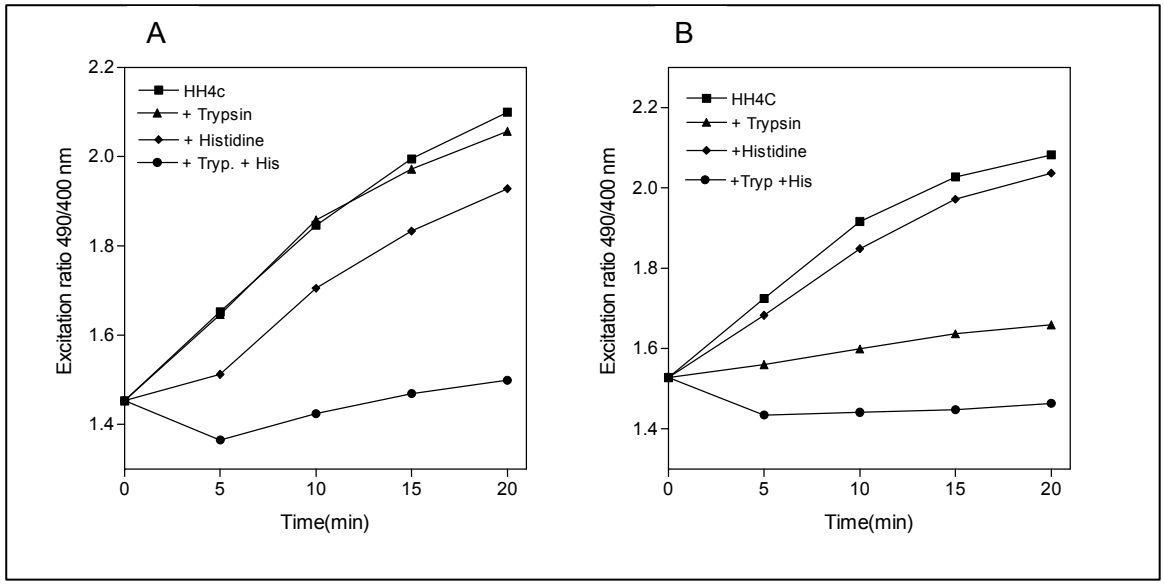

Figure 4.21. Singlet oxygen detection following tryptic digestion is concentration dependant. A: ReAsH stained SOS-HH-4C at 1μM, alone or treated with Trypsin for 3 hours at 37°C, with or without 20mM Histidine. B: ReAsH stained SOS-HH-4C at 0.3 μM alone or treated with Trypsin for 3 hours at 37°C, with or without 20mM Histidine

G. References

1. Kanofsky JR. Singlet oxygen production by biological systems. Chem Biol Interact 1989;70:1-28.

2. Davies MJ. Singlet oxygen-mediated damage to proteins and its consequences. Biochem Biophys Res Commun 2003;305:761-770.

3. Rosen H, Klebanoff SJ. Formation of singlet oxygen by the myeloperoxidase-mediated antimicrobial system. J Biol Chem 1977;252:4803-4810.

4. Pierlot C, Aubry JM, Briviba K, Sies H, Di Mascio P. Naphthalene endoperoxides as generators of singlet oxygen in biological media. Methods Enzymol 2000;319:3-20.

5. Böhme K, Brauer H-D. Generation of singlet oxygen from hydrogen peroxide disproportionation catalyzed by molybdate ions. Inorg Chem 1992;1992:3468-3471.

6. Niu QJ, Foote CS. Singlet molecular oxygen geneeration from the decomposition of sodium peroxotungstate and sodium peroxomolybdate. Inorg Chem 1992;31:3472-3476.

7. Kanofsky JR. Singlet oxygen in biological systems: A comparison of biochemical and photochemical mechanisms for singlet oxygen generation. In Tarr M, Samson F, editors. Oxygen Free Radicals in Tissue Damage. Boston: Birkhäuser, 1993:77-92.

8. Kochevar IE, Redmond RW. Photosensitized production of singlet oxygen. Methods Enzymol 2000;319:20-28.

9. Miller JS. Rose bengal-sensitized photooxidation of 2-chlorophenol in water using solar simulated light. Water Res 2005;39:412-422.

10. Gandin E, Lion Y, Van de Vorst A. Quantum yield of singlet oxygen production by xanthene derivatives. Photochem Photobiol 1983;37:271-278.

11. Redmond RW. Enhancement of the sensitivity of radiative and non-radiative detection techniques in the study of photosensitization by water soluble sensitizers using reveerse micells system. Photochem Photobiol 1991;54:547-556.

12. Lambert CR, Kochevar IE. Electron transfer quenching of the rose bengal triplet state. Photochem Photobiol 1997;66:15-25.

13. Griffin BA, Adams SR, Jones J, Tsien RY. Fluorescent labeling of recombinant proteins in living cells with FlAsH. Methods Enzymol 2000;327:565-578.

14. Adams SR, Campbell RE, Gross LA, Martin BR, Walkup GK, Yao Y, Llopis J, Tsien RY. New biarsenical ligands and tetracysteine motifs for protein labeling in vitro and in vivo: synthesis and biological applications. J Am Chem Soc 2002;124:6063-6076.

15. Umezawa N, Tanaka K, Urano Y, Kikuchi K, Higuchi T, Nagano T. Novel Fluorescent Probes for Singlet Oxygen. Angew Chem Int Ed Engl 1999;38:2899-2901.

16. Tanaka K, Miura T, Umezawa N, Urano Y, Kikuchi K, Higuchi T, Nagano T. Rational design of fluorescein-based fluorescence probes. Mechanism-based design of a maximum fluorescence probe for singlet oxygen. J Am Chem Soc 2001;123:2530-2536.

17. Michaeli A, Feitelson J. Reactivity of singlet oxygen toward large peptides. Photochem Photobiol 1995;61:255-260.

18. Michaeli A, Feitelson J. Reactivity of singlet oxygen toward amino acids and peptides. Photochem Photobiol 1994;59:284-289.

19. Tomita M, Irie M, Ukita T. Sensitized photooxidation of histidine and its derivatives. Products and mechanism of the reaction. Biochemistry 1969;8:5149-5160.

20. Davies MJ, Truscott RJ. Photo-oxidation of proteins and its role in cataractogenesis. J Photochem Photobiol B 2001;63:114-125.

21. Wright A, Bubb WA, Hawkins CL, Davies MJ. Singlet oxygen-mediated protein oxidation: evidence for the formation of reactive side chain peroxides on tyrosine residues. Photochem Photobiol 2002;76:35-46.

22. Shen HR, Spikes JD, Kopecekova P, Kopecek J. Photodynamic crosslinking of proteins. I. Model studies using histidine- and lysine-containing N-(2-hydroxypropyl)methacrylamide copolymers. J Photochem Photobiol B 1996;34:203-210.

23. Guptasarma P, Balasubramanian D, Matsugo S, Saito I. Hydroxyl radical mediated damage to proteins, with special reference to the crystallins. Biochemistry 1992;31:4296-4303.

24. Shen HR, Spikes JD, Kopeckova P, Kopecek J. Photodynamic crosslinking of proteins. II. Photocrosslinking of a model protein-ribonuclease A. J Photochem Photobiol B 1996;35:213-219.

25. Verweij H, Dubbelman TM, Van Steveninck J. Photodynamic protein cross-linking. Biochim Biophys Acta 1981;647:87-94.

26. Shen HR, Spikes JD, Smith CJ, Kapecek J. Photodynamic cross-linking of proteins IV. Nature of His-His bond(s) formed in the rose bengal-photosensitized cross-linking of *N*-benzoyl-L-histidine. J Photochem Photobiol A: Chemistry 2000;130:1-6.

27. Van Steveninck J, Dubbelman TM. Photodynamic intramolecular crosslinking of myoglobin. Biochimica et Biophysica Acta 1984;791:98-101.

28. Guptasarma P, Balasubramanian D. Dityrosine formation in the proteins of the eye lens. Curr Eye Res 1992;11:1121-1125.

29. Stadtman ER, Levine RL. Free radical-mediated oxidation of free amino acids and amino acid residues in proteins. Amino Acids 2003;25:207-218.

30. Balasubramanian D, Du X, Zigler JS, Jr. The reaction of singlet oxygen with proteins, with special reference to crystallins. Photochem Photobiol 1990;52:761-768.

31. Dean RT, Fu S, Stocker R, Davies MJ. Biochemistry and pathology of radical-mediated protein oxidation. Biochem J 1997;324 (Pt 1):1-18.

32. Requena JR, Levine RL, Stadtman ER. Recent advances in the analysis of oxidized proteins. Amino Acids 2003;25:221-226.

33. Parker NR, Jamie JF, Davies MJ, Truscott RJ. Protein-bound kynurenine is a photosensitizer of oxidative damage. Free Radic Biol Med 2004;37:1479-1489.

34. Hanson GT, Aggeler R, Oglesbee D, Capaldi RA, Tsien RY, Remington SJ. Investigating mitochondrial redox potential with redox-sensitive green fluorescent protein indicators. J Biol Chem 2004;279:13044-13053.

35. Dooley CT, Dore TM, Hanson GT, Jackson WC, Remington SJ, Tsien RY. Imaging dynamic redox changes in mammalian cells with green fluorescent protein indicators. J Biol Chem 2004;279:22284-22293.

36. Martin BR, Giepmans BN, Adams SR, Tsien RY. Mammalian cell-based optimization of the biarsenical-binding tetracysteine motif for improved fluorescence and affinity. Nat Biotechnol 2005;23:1308-1314.

37. Shaner NC, Steinbach PA, Tsien RY. A guide to choosing fluorescent proteins. Nat Methods 2005;2:905-909.

38. Taborsky G. Oxidative modification of proteins in the presence of ferrous ion and air. Effect of ionic constituents of the reaction medium on the nature of the oxidation products. Biochemistry 1973;12:1341-1348.

39. Fu SL, Dean RT. Structural characterization of the products of hydroxyl-radical damage to leucine and their detection on proteins. Biochem J 1997;324 (Pt 1):41-48.

40. Moreno MJ, Monson E, Reddy RG, Rehemtulla A, Ross BD, Philbert M, Schneider RJ, Kopelman R. Production of singlet oxygen by $Ru(dpp(SO_3)_2)_3$ inorporated in polyacrylamide PEBBLES. Sensors and Actuators B 2003;90:82-89.

41. Lindig BA, Rodgers MAJ, Schaap AP. Determination of the lifetime of singlet oxygen in D_2O using 9,10-Anthracenedipropionic acid, a water soluble probe. J Am Chem Soc 1980;102:5590-5593.

42. Hoebeke M, Damoiseau X. Determination of the singlet oxygen quantum yield of bacteriochlorin a: a comparative study in phosphate buffer and aqueous dispersion of dimiristoyl-L-alpha-phosphatidylcholine liposomes. Photochem Photobiol Sci 2002;1:283-287.

43. Aubry JM. Search for singlet oxygen in the decomposition of hydrogen peroxide by mineral compounds in aqueous solutions. J Am Chem Soc 1985;107:5844-5849.

44. Wiederrecht G, Brizuela L, Elliston K, Sigal NH, Siekierka JJ. FKB1 encodes a nonessential FK 506-binding protein in Saccharomyces cerevisiae and contains regions suggesting homology to the cyclophilins. Proc Natl Acad Sci U S A 1991;88:1029-1033.

45. Brown EJ, Albers MW, Shin TB, Ichikawa K, Keith CT, Lane WS, Schreiber SL. A mammalian protein targeted by G1-arresting rapamycin-receptor complex. Nature 1994;369:756-758.

46. Sabatini DM, Pierchala BA, Barrow RK, Schell MJ, Snyder SH. The rapamycin and FKBP12 target (RAFT) displays phosphatidylinositol 4-kinase activity. J Biol Chem 1995;270:20875-20878.

47. Aquilina JA, Carver JA, Truscott RJ. Polypeptide modification and cross-linking by oxidized 3-hydroxykynurenine. Biochemistry 2000;39:16176-16184.

48. Verweij H, Christianse K, Van Steveninck J. Ozone-induced formation of O,O'-dityrosine cross-linked in proteins. Biochim Biophys Acta 1982;701:180-184.

49. Davies MJ, Fu S, Wang H, Dean RT. Stable markers of oxidant damage to proteins and their application in the study of human disease. Free Radic Biol Med 1999;27:1151-1163.

50. Alia, Mohanty P, Matysik J. Effect of proline on the production of singlet oxygen. Amino Acids 2001;21:195-200.

51. Johansson L, Chen C, Thorell JO, Fredriksson A, Stone-Elander S, Gafvelin G, Arner ES. Exploiting the 21st amino acid-purifying and labeling proteins by selenolate targeting. Nat Methods 2004;1:61-66.

52. Steinbeck MJ, Khan AU, Karnovsky MJ. Extracellular production of singlet oxygen by stimulated macrophages quantified using 9,10-diphenylanthracene and perylene in a polystyrene film. J Biol Chem 1993;268:15649-15654.

53. Tsien RY. The green fluorescent protein. Annu Rev Biochem 1998;67:509-544.

54. Dickson RM, Cubitt AB, Tsien RY, Moerner WE. On/off blinking and switching behaviour of single molecules of green fluorescent protein. Nature 1997;388:355-358.

55. Bizzarri R, Arcangeli C, Arosio D, Ricci F, Faraci P, Cardarelli F, Beltram F. Development of a Novel GFP-based Ratiometric Excitation and Emission pH Indicator for Intracellular Studies. Biophys J 2006;90:3300-3314.

56. Uchida K, Kawakishi S. 2-Oxo-histidine as a novel biological marker for oxidatively modified proteins. FEBS Lett 1993;332:208-210.

57. Levine RL, Berlett BS, Moskovitz J, Mosoni L, Stadtman ER. Methionine residues may protect proteins from critical oxidative damage. Mech Ageing Dev 1999;107:323-332.

58. Telfer A, Bishop SM, Phillips D, Barber J. Isolated photosynthetic reaction center of photosystem II as a sensitizer for the formation of singlet oxygen. Detection and quantum yield determination using a chemical trapping technique. J Biol Chem 1994;269:13244-13253.

59. Berg K, Selbo PK, Weyergang A, Dietze A, Prasmickaite L, Bonsted A, Engesaeter BO, Angell-Petersen E, Warloe T, Frandsen N, Hogset A. Porphyrin-related photosensitizers for cancer imaging and therapeutic applications. J Microsc 2005;218:133-147.

60. Cao Y, Koo YE, Koo SM, Kopelman R. Ratiometric singlet oxygen nano-optodes and their use for monitoring photodynamic therapy nanoplatforms. Photochem Photobiol 2005;81:1489-1498.

61. Tour O, Meijer RM, Zacharias DA, Adams SR, Tsien RY. Genetically targeted chromophore-assisted light inactivation. Nat Biotechnol 2003;21:1505-1508.

62. Greenbaum L, Rothmann C, Lavie R, Malik Z. Green fluorescent protein photobleaching: a model for protein damage by endogenous and exogenous singlet oxygen. Biol Chem 2000;381:1251-1258.

63. Bulina ME, Chudakov DM, Britanova OV, Yanushevich YG, Staroverov DB, Chepurnykh TV, Merzlyak EM, Shkrob MA, Lukyanov S, Lukyanov KA. A genetically encoded photosensitizer. Nat Biotechnol 2006;24:95-99.

64. Shaner NC, Campbell RE, Steinbach PA, Giepmans BN, Palmer AE, Tsien RY. Improved monomeric red, orange and yellow fluorescent proteins derived from Discosoma sp. red fluorescent protein. Nat Biotechnol 2004;22:1567-1572.

65. Marks AR. Cellular functions of immunophilins. Physiol Rev 1996;76:631-649.

66. Spencer DM, Wandless TJ, Schreiber SL, Crabtree GR. Controlling signal transduction with synthetic ligands. Science 1993;262:1019-1024.

67. Avramut M, Achim CL. Immunophilins and their ligands: insights into survival and growth of human neurons. Physiol Behav 2002;77:463-468.

68. Chen J, Zheng XF, Brown EJ, Schreiber SL. Identification of an 11-kDa FKBP12-rapamycin-binding domain within the 289-kDa FKBP12-rapamycin-associated protein and characterization of a critical serine residue. Proc Natl Acad Sci U S A 1995;92:4947-4951.

69. Chelu MG, Danila CI, Gilman CP, Hamilton SL. Regulation of ryanodine receptors by FK506 binding proteins. Trends Cardiovasc Med 2004;14:227-234.

70. Ho SN, Biggar SR, Spencer DM, Schreiber SL, Crabtree GR. Dimeric ligands define a role for transcriptional activation domains in reinitiation. Nature 1996;382:822-826.

71. Paulmurugan R, Gambhir SS. Novel fusion protein approach for efficient high-throughput screening of small molecule-mediating protein-protein interactions in cells and living animals. Cancer Res 2005;65:7413-7420.

72. Paulmurugan R, Massoud TF, Huang J, Gambhir SS. Molecular imaging of drug-modulated protein-protein interactions in living subjects. Cancer Res 2004;64:2113-2119.